Title
A Physiological Approach to the Ecology and Evolution of Flowers

Author
Roddy, Adam Bryant

Publication Date
2015

Peer reviewed|Thesis/dissertation

A Physiological Approach to the Ecology and Evolution of Flowers

By

Adam Bryant Roddy

A dissertation submitted in partial satisfaction of the

requirements for the degree of

Doctor of Philosophy

in

Integrative Biology

in the

Graduate Division

of the

University of California, Berkeley

Committee in charge:

Professor Todd E. Dawson, Chair
Professor David D. Ackerly
Professor Paul V. A. Fine
Professor Dennis D. Baldocchi

Spring 2015

A Physiological Approach to the Ecology and Evolution of Flowers

Abstract

A Physiological Approach to the Ecology and Evolution of Flowers

by

Adam Bryant Roddy

Doctor of Philosophy in Integrative Biology

University of California, Berkeley

Professor Todd E. Dawson, Chair

Flowers have long been considered one of the hallmarks of angiosperm evolution. They are morphologically complex structures that both promote efficient pollination and protect the developing embryo. When it was championed in 1793 by Christian Konrad Sprengel, this view of the role of flowers in reproduction, however, was highly controversial: how could a form so beautiful and pure as a flower ever be involved in something as vulgar as reproduction? Sprengel and his predecessor, Josef Köhlreuter, are considered the founders of pollination biology, and their work set the stage for that of Charles Darwin nearly a century later. Darwin saw the interaction between flowers and their pollinators as a prime example of the power of natural selection. This approach to studying the evolution of flowers–of focusing on the biotic drivers of floral morphological change–has dominated our understanding and interpretation of floral evolution. Yet, new evidence suggests that extrinsic, abiotic factors and the costs of producing and maintaining flowers may also have influenced the evolution of floral form. These non-pollinator agents of selection could represent another major shift in our understanding of how flowers have evolved.

The series of studies presented in this dissertation takes one important resource, water, and examines how the requirements of providing water to flowers may influence their functioning and evolution. Two complementary approaches are used in these studies: (1) physiological measurements of the dynamics of water use on a few species and (2) comparisons of hydraulic traits for diverse sets of species. Together, these two approaches show the variability of flower water use, the anatomical traits associated with the flux of water through flowers, and how these physiological traits–and, by extension, the water requirements of flowers–vary among extant species. Together, these studies support the conclusion that maintaining flower water balance has been an important factor influencing floral evolution and, more generally, angiosperm ecology.

Three studies are presented that seek to measure, using different approaches, how the water flux to flowers and the hydraulic efficiency of flowers varies among species (Chapters 1-3), within species throughout floral development (Chapters 1 and 2), and diurnally with changing environmental conditions (Chapter 3). Using a new implementation of the heat ratio method for measuring sap flow (Chapter 1), I found that sap flow velocities to flowers and inflorescences vary diurnally, throughout floral development, and among species and microhabitats. Such high variability suggested that a better approach to comparing the hydraulic architecture of flowers would be to measure the maximum efficiency of the floral hydraulic system. In Chapter 2, I quantified for a phylogenetically diverse set of species the maximum hydraulic conductance of whole flowers. This, too, was highly variable among species, as were other hydraulic traits, and the variation in all traits

was driven by just two genera of early-divergent angiosperm lineages. Variation in these traits highlighted the existence of two seemingly discrete hydraulic strategies: one strategy is to maintain a high hydraulic conductance and continuously import water via the xylem while the other strategy is to have a low hydraulic conductance with long water turnover times, slow desiccation rates, and presumably high hydraulic capacitance. Investigating the tradeoffs among these strategies further, Chapter 3 focused on characterizing the water relations of flowers of two *Calycanthus* species, which had among the highest hydraulic conductances measured in Chapter 2. Consistent with my predictions, high hydraulic capacitance in flowers mitigates the reliance on continuous xylem delivery of water. As a result, despite maintaining a high maximum hydraulic conductance (Chapter 2), *Calycanthus* flowers hydraulically underperform most of the time, reaching their maximum hydraulic conductance only when turgor loss is already inevitable. The results from Chapters 2 and 3 together suggest that the monocots and eudicots, compared to the ANITA grade and magnoliids, developed thicker cuticles and reduced their stomatal abundances, which together reduce rates of water loss from flowers and prolonged the time that these flowers can remain turgid without the import of new water.

Having characterized in Chapter 2 some of the anatomical traits that correlate with the hydraulic capacity of flowers, I sought in Chapters 4 and 5 to examine for a large set of species how these traits have evolved and vary among species. Specifically, I asked three questions: (1) Has there been coordinated evolution of water balance traits within flowers, which would suggest that maintaining water balance has been an important component in floral evolution? (2) Is there modularity in hydraulic trait evolution, such that flower and leaf traits have evolved independently? (3) Have hydraulic traits been under natural selection? The results from these two chapters strongly support the conclusions that floral hydraulic traits are under selection, that maintaining water balance has been an important component of floral trait evolution, and that hydraulic traits have evolved independently in flowers and leaves. These results show, for the first time, the importance of water balance in floral evolution and highlight that the physiological demands of and constraints on flowers may provide a strong counterbalance to selection by animal pollinators.

As yet, studies of the physiology of flowers have received little attention and have been ignored in physiological trait databases. As a result, there has been no overarching theory describing or predicting patterns of variance in floral physiological traits. This series of studies is a first attempt at providing such a framework for predicting how floral physiological traits may vary among species and how this may differ between reproductive and vegetative traits. Although it focuses only on traits associated with the movement of water, the results show that there may be consistent trait associations and syndromes among flowers, regardless of morphology. This should be a first step in understanding how flowers function physiologically and how their functioning may vary with a variety of ecological factors and over evolutionary timescales.

Table of Contents

Acknowledgments

I first want to thank my mother, Jill Bryant, for being my first teacher and for always trusting my decisions. Her faith in me is unwavering. My wife, Anna Schürkmann, has been crucial in helping not only with the mundane minutiae of science and fieldwork but also in teaching me there is more to life than just work. Kemmer and Martha Anderson have always provided spiritual support and a poetic balance to my pursuits in science.

My development as a scientist owes a lot to many people. Tony Burgess and Linda Leigh inspired me to study ecology even though they probably do not even know it. Michael Lowry and Pete LaRochelle of the McCallie School had extremely different teaching styles but were both critical influences in my approach to science. Swarthmore College was where I learned most of what I know and how I think, at least some of it from Rachel Merz, José-Luis Machado, Elizabeth Vallen, and Steve Wang. Doing biology there was idyllic, and it is a shame it's not that way in many other places.

More apropos to this dissertation, my attempts at physiology and evolution have been shaped by many mentors, friends, and colleagues. Nelson Edwards first taught me about physiology, and Stan Wullschleger gave me freedom and has, for some reason, always maintained confidence in me. I owe a lot to Tom Kursar, who gave me grounding, a lab in Panama, and a whole lot of freedom and trust. My attitude towards mentorship comes mainly from how Tom mentored me. From my committee, Todd Dawson, David Ackerly, Paul Fine, and Dennis Baldocchi, I have learned an immense amount about many different topics–too many to list here. For better or for worse, their words continue to echo in me. They have also given me a long leash and let me do what I needed to do; for that I am extremely thankful (as is my wife). Two people, Walt Carson and Greg Crutsinger, told me the harsh realities of being successful in science (which may be starkly different from being a successful scientist), and for their advice and willingness to be honest, I am grateful.

My intellectual development is due largely to conversations with my peers and friends–indeed these are the people from whom I have learned the most. My approach to plant water relations is due largely to discussions with Kevin Simonin, whose ability to synthesize material can be overwhelming. Others have pushed me in various directions–for the benefit of my intellect even if to the detriment of my productivity: Matt Guilliams, Sonal Singhal, Chris DiVittorio, Tracy Misiewicz, Rob Skelton, Kaitlin Maguire, Seth Kauppinen, Bier Kraichak, Carolina Gomez-Navarro, Ben Carter, Eve Robinson, Thorsten Grams, Kate McCulloh, Dan Johnson, Adam West, Arthur Gessler, and Zachary Kayler. With my labmates I have shared many a needed drink and camaraderie both in the lab and in the field: Kevin Simonin always invigorated my mind (even if sometimes I found him overwhelming), Kevin Tu remains my go-to reference for anything biophysical, Michal Shuldman and Emily Burns have been unwavering in their calming abilities, Maya deVries always brightened the lab, An Saveyn has been a quiet, unassuming guidance in both science and life, Paul Brooks has always been both a dear friend and one of the most entertaining people I know, and Chris Wong is always entertaining and competent, a much needed personality in any lab. From everyone else in the lab, old and new (Stefania Mambelli, Ansgar Kahmen, Allison Kidder, Cameron Williams, Clarissa Fontes, Claire Willing), I have learned important things about science and teamwork.

I could not have accomplished the research without the help of some stellar undergraduates: Terapan Lilittham, Jessica Farmer, Trang Pham, Vanessa Wormser, and Ray Donheiser. Holly Forbes of the U.C. Botanical Garden, Joe Dahl of the Tilden Botanic Garden, and Nils Köster, Thomas Dürbye, and Albert-Dieter Stevens of the Berlin-Dahlem Botanical Garden all generously

gave me access to their living collections. Without this access, I could not have done this work. To the many years and significant sums of money that have been invested in these gardens, I am overwhelmingly grateful. Joe Wright, Klaus Winter, and Oris Acevedo of the Smithsonian Tropical Research Institute also provided access to plants and equipment. Cindy Looy, Dave Armitage, and Wayne Sousa of U.C. Berkeley and Marion Cubr of the Berlin-Dahlem Botanical Garden provided access to microscopes–a vital tool I almost always overlook in planning.

Funding has been generously provided by the U.S. National Science Foundation, the U.S. Department of Energy, the Heckard Fund of the Jepson Herbarium, the U.C. Berkeley Department of Integrative Biology, the U.C. Berkeley Graduate Division, the U.C. Natural Reserve System, the Deutscher Akademischer Austausch Dienst (German Academic Exchange Service), the Smithsonian Tropical Research Institute, and the American Philosophical Society.

Chapter 1: Determining the water dynamics of flowering using miniature sap flow sensors

A version of this chapter has been previously published and is reproduced here with permission:
Roddy A.B. and Dawson T.E. 2012. Determining the water dynamics of flowering using miniature sap flow sensors. *Acta Horticulturae* 951:47-53.

Introduction

Flowering can require significant amounts of resources, and for many species this can be the single largest reproductive investment (Bazzaz et al. 1987). Many species flower under suboptimal conditions when resources are limiting. For example, many tropical trees flower in the dry season, when water is scarce (van Schaik et al. 1993). Because many flowers and fruits are maintained at higher, less negative water potentials than subtending stems and leaves (Trolinder et al. 1993; Chapotin et al. 2003), the direction of water flow to and from reproductive organs may vary with time of day, plant water status, and reproductive development. In mango, for example, inflorescences exhibit unidirectional sap flux to the developing inflorescences (Higuchi and Sakuratani 2005), whereas the fruits exhibit sap flux toward the developing fruit during the night, and sap flux from the fruit to the stem during the day (Higuchi and Sakuratani 2006). Because the water dynamics of flowering have been so understudied, we know very little about the diurnal patterns of water use by flowers and fruits, which has been exacerbated by a lack of methods for accurately measuring these dynamics.

Here we apply a new implementation (Clearwater et al. 2009) of the heat pulse method (Marshall 1958; Burgess et al. 2001) to measure sap flow dynamics of leaves, flowers, and fruits in four tropical plants common in the moist, lowland forests of central Panama. Our objectives were: (1) to test these miniature, external sap flow sensors under natural field conditions, (2) to determine whether species differ in the temporal dynamics of sap flow to reproductive organs and (3) to use sap flow measurements to estimate the relative water costs of reproduction in wild, tropical plants.

Materials and Methods

Plant material

From January to April 2011, we studied four species growing in the forests and forest edges of Barro Colorado Island, Panama, at the Smithsonian Tropical Research Institute. The liana *Clitoria javitensis* (Fabaceae) flowers towards the beginning of the dry season, in early February. The shrub *Annona acuminata* (Annonaceae) flowers throughout the year and was measured in March and April. The understory tree *Hybanthus prunifolius* (Violaceae) flowers towards the end of the dry season when the first rains appear toward the end of March. The canopy tree *Cordia alliodora* (Boraginaceae) flowers during the dry season, from late January through April. For measurements on flowers, we installed three sensors on C. javitensis, six sensors on A. acuminata, eight sensors on H. prunifolius, and two sensors on C. alliodora. For each sensor installed to measure flowers, we installed an accompanying sensor to measure a leaf. All data shown are representative sap flow traces from one sensor in each group. Petioles, pedicels, peduncles, and branchlets on which we installed sensors ranged in diameter from approximately 1.5 mm to 8 mm.

Sensor design

We modified the design of Clearwater at al. (2009) to use a nonconductive silicone backing instead of cork in order to minimize the effects of gauge material on thermal diffusivity. Sensors

were connected to 10 cm leads with Molex quick-connectors that were then connected to 10 m long leads to an AM16/32 multiplexer and CR23X data logger (Campbell Scientific Inc., Logan, UT). Sensors were held in place with parafilm, and sensors and connections were insulated with multiple layers of bubble wrap and aluminum foil at least 1 cm above and below the sensor.

Our implementation of the heat ratio method was consistent with previous uses (Burgess et al. 2001; Clearwater et al. 2009), except that we used a four second heat pulse, measured thermocouples every 2 seconds for 200 seconds, and made measurements every 15 minutes. These modifications were made in an attempt to reduce the amount of heat dissipated to prevent damage of small, herbaceous pedicels and petioles.

Heat ratio theory

The heat pulse velocity, v_h (cm s^{-1}) is calculated from the temperature ratio based on the following equation by Marshall (1958) and Clearwater (2009):

$$v_h = \frac{k}{x} \ln\left(\frac{\delta T_1}{\delta T_2}\right)$$

where v_h is the heat pulse velocity in cm s^{-1}, k is the thermal diffusivity (cm^2 s^{-1}), x is the distance from the heater to each of the thermocouples (cm), and δT_1 and δT_2 are the temperature rises (°C) above and below the heater, respectively. We estimated the thermal diffusivity as:

$$k = \frac{x^2}{4t_m}$$

where t_m is the time (seconds) between the heat pulse and the maximum temperature rise recorded x cm above or below the heater under conditions of zero sap flow (Clearwater et al. 2009). We measured t_m every morning before dawn when atmospheric vapor pressures are lowest (between 0500 and 0630 hrs). At this time, the vapor pressure deficit was almost always below 0.3 kPa, and therefore we assumed there was no sap flow. Thermal diffusivity, k, was measured every morning at predawn and used to calculate v_h from the heat ratios for the subsequent 24 hours. Measurements of k on nights with vapor pressure deficit (vpd) always above 0.3 kPa were discarded and replaced with the most recently measured k during conditions of vpd < 0.3 kPa. Vapor pressure deficit was estimated from temperature and relative humidity measurements made every 15 minutes with a HOBO U23 data logger (Onset Computer Corp., Bourne, MA).

The calculation of v_h depends on equidistant spacing of thermocouples above and below the heater. To account for misaligned probes, at the end of each series of measurements, we excised the stem above and below the sensor at predawn and greased the cut ends. The sensor and stem segment were then placed in a cooler kept at outside ambient temperatures for 2-6 hours, during which time heat ratio measurements were made. The average of these measurements made at zero flow was subtracted from all calculated heat ratios. This corrected heat ratio was then used to calculate v_h.

Because of the small diameter of stems being measured, sun exposure or ambient temperature gradients could induce artifacts into the measurement of the temperature ratio. After installing sensors, we removed the heat pulse for at least 24 hours and then reconnected the heaters.

All analyses and figures were performed using *R* software (R Core Team 2012). Because of the high level of noise in the measurements, we smoothed the measurements using the 'loess' function in R. A loess smooth creates a locally-weighted polynomial regression for moving windows of points throughout the dataset and plots the midpoint of that window. For each smoothed point, we used less than 1% of all data, which corresponded to less than 25 measurements. The smoothed curve accurately described periods of sap flow traces when there were consistent changes in sap flow (i.e. overnight and during sunrise and and sunset) and essentially creates a moving average of

measurements during midday. Thus the largest deviations of smoothed values from raw measurements were during the daytime when raw measurements were highly variable, and during these times the smoothed values provide an average of these highly variable raw measurements.

Results and Discussion

Sensor design and analysis

All heat-based sap flow measurements are prone to errors caused by thermal gradients that can have significant impacts on measured temperature ratios. We found that with sufficient insulation (at least 1 cm above and below the sensor of multiple layers of bubble wrap), we could eliminate most of the effects of thermal gradients. By unplugging the heaters from the power source, we tested whether background thermal gradients affected temperature ratios. When heaters were unplugged, we saw no obvious trends in the measured temperature ratios (Figure 1). The increased noise of measured temperature ratios is due to the calculation of the ratio of temperature change based on measurements before and after a heat pulse. When the heaters were reattached to the power supply, measured temperature ratios were consistent with expected sap flow dynamics. Because the magnitude of thermal gradients may depend on the microenvironment around the sensor, we performed this test on all sensors a few days after installation. These results from sensors installed in the understory and exposed environments of a seasonal tropical forest suggest that there are no obvious influences of background temperature on measurements of the temperature ratio.

Interpreting sap flow data requires an accurate estimation of zero-flow, which can prove difficult to achieve. We tested three methods for generating zero-flow estimates: (1) zeroing based on low vpd conditions (removing the demand for water), (2) zeroing after excising around the sensor at predawn (severing the pathway for sap flow), and (3) covering the leaf or flower with plastic wrap and aluminum foil (also removing the demand at the leaf or flower level). Zeroing during low vpd conditions assumes that water potential gradients inside the plant equilibrate overnight while vpd is still declining, but this method could be performed on a daily basis allowing for frequent adjustments in the zero-flow temperature ratio throughout a measurement campaign in case the sensor had moved. Excising around the sensor sometimes produced zero-flow estimates higher or lower than the low-vpd method. One possible reason for the discrepancy between these two methods is that excising may have disturbed thermocouple spacing and affected measured temperature ratios. However, it was impossible for us to test whether this is the case. Additionally, we observed that covering the leaf in plastic wrap and foil estimated a zero-flow comparable to the other two methods (Figure 2). In our figures we present zero-flow estimates based on excision and show data only from days in which the zero-flow estimate from excision matched the zero-flow estimate from low vpd conditions.

Despite effective insulation, we still saw substantial noise in measurements made during the middle of the day (Figure 2). The causes for such variation are unclear. There seemed to be no obvious effects of ambient temperature (Figure 1), suggesting that such variable measurements may result from rapid changes in sap flux at the leaf level. We applied loess smoothing to the data to allow easier comparisons, particularly during midday measurements. This smoothing procedure effectively extracted and highlighted the overall pattern in sap velocity without removing the major differences between days and between samples. For example, smoothed values accurately capture day-to-day variation in sap velocity in response to differences in evaporative demand (Figure 2).

Estimating sap flow requires accurate measurements of thermal diffusivity, k. Across all our measurements, k ranged from 0.0014 to 0.0020 $cm^2\ s^{-1}$. There were no differences between species, and within individual samples, k did not vary as a function of duration into the dry season, suggesting that changes in predawn plant water potential had no effect on k. The range of k for the tropical species and structures measured in the present study are consistent with the range of k reported by Clearwater et al. (2009). Our tests of these sensors show that with proper calibration

and measurement protocols, they can be used to measure diurnal changes in sap flow through small diameter stems under naturally varying environmental conditions and across a range of plant structures.

Sap flow dynamics of leaves and flowers

We measured sap flow on four tropical species varying in growth habit and habitat in the forest. Two species, *H. prunifolius* and *A. acuminata,* occur in the shaded understory and produce flowers born on leafing shoots. Sensors were installed basal to both leaves and flowers, and we defoliated these shoots to determine the sap flow due to flowers. In both *H. prunifolius* (Figure 3) and *A. acuminata* (data not shown), sap flow was consistently near zero after defoliation. During fruiting in *H. prunifolius*, there were slight diurnal increases in sap velocity, suggesting that fruit transpiration may influence sap flow dynamics, whether or not transpiration is controlled by stomata. In contrast to previous sap flow measurements on fruits (Higuchi and Sakuratani 2006), we found no substantial sap flow reversals, probably because these fruits store relatively little water.

In contrast to these understory species, we saw clear sap flow patterns driven by flowering in the two species with sun-exposed flowers. In the liana *C. javitensis*, we measured increases in velocity due to flowers as compared to leaves (Figure 4). Interestingly, flowers not only increased daily maximum velocity but also changed the pattern of sap flow. During the day prior to anthesis and on the first day of anthesis, flowers showed no midday depression in sap flow, unlike adjacent leaves. However, after petals had senesced and only the green, photosynthetic sepals remained, flowering shoots showed similar midday depressions to those of leaves. This pattern suggests that petals may require a constant supply of water, the magnitude of which may overwhelm the midday depression in water use by subtending sepals. If water loss from flowers is unregulated by stomata and driven more by cuticular losses (Hew et al. 1980; Chapters 3, 5), then water may need to be constantly supplied to flowers. Whether it is delivered by the xylem or by the phloem, water flow to petals nonetheless influences sap flow dynamics. This further suggests that flowers may, to some extent, still be hydraulically connected to the stem water supply even if they are phloem-hydrated (Chapotin et al. 2003).

The canopy tree *C. alliodora* produces inflorescences throughout its canopy. Each inflorescence has numerous flowers in various stages of development. We installed sensors on individual inflorescences and nearby leaves on a fully sun- and wind-exposed tree in a clearing (Figure 5). Inflorescences underwent similar daily variation in sap flow as leaves, increasing to daily maxima around midday and then declining to zero flow overnight. However, inflorescences had maximum velocities only about 30-50% that of nearby leaves. Furthermore, the day-to-day variation in vpd affected sap velocities to leaves but had little effect on inflorescence sap flow. Bearing flowers in all stages of development could lead to insensitivity to vpd variation among days if the declining water requirements of senescent flowers were replaced by increasing water requirements of newly opened flowers. Thus, this insensitivity may be observed only at the level of the inflorescence and not for each individual flower on that inflorescence.

Here we have reported on the application of miniature, external sap flow sensors in a tropical forest to understand leaf- and flower-level sap flow dynamics. We show that these sap flow sensors work well under field conditions and are minimally influenced by thermal gradients when properly installed and insulated. Our results also indicate that the sap flow dynamics of flowering is highly species- and habitat-specific; flowers of some species show little measurable sap flow, while flowers of other species have substantial sap flow rates. Flowers of understory species (*H. prunifolius* and *A. acuminata*), which rarely experienced vpd above 1 kPa exhibited little measurable sap flow, whereas sun-exposed *C. alliodora* inflorescences and *C. javitensis* flowers exhibited sap flow velocities approximately one-third of adjacent leaves. Maximum sap velocities to an inflorescence can be as high 50% that of leaves, suggesting that for some species the water requirements of flowering may

be substantial. Understanding how these water requirements vary among habitats and species and in relation to floral morphological and physiological traits will provide new insights into reproductive function in angiosperms.

Figure 1. Times series of one sensor during testing for thermal gradients. The heater on the sensor was originally plugged in to a power supply, then it was detached from power, and finally reattached where indicated. Points represent the measured temperature ratios, and the solid line is the loess-smoothed values. Shading represents nighttime.

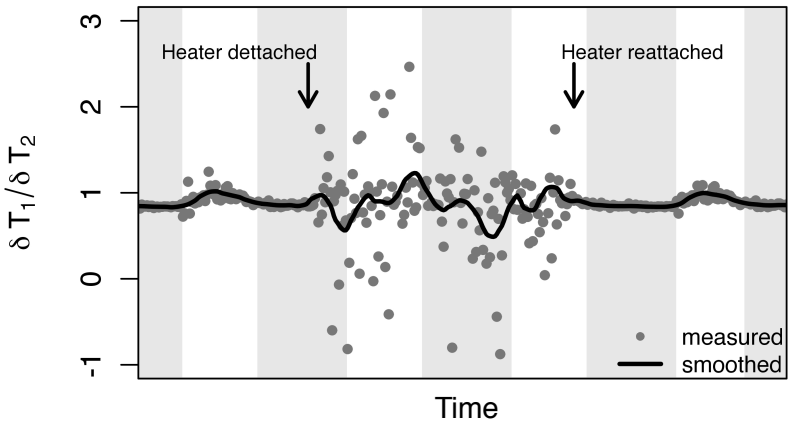

Figure 2. Time series of sap flow velocities recorded on one fully sun-exposed leaf of *C. javitensis* for 23 days during the dry season. The grey line represents the raw velocities calculated from temperature ratios and measurements of thermal diffusivity, *k*. The dashed, black line represents the velocities after loess smoothing. For about 36 hours, the leaf was covered in plastic wrap and aluminum foil to stop transpiration, as indicated in the figure.

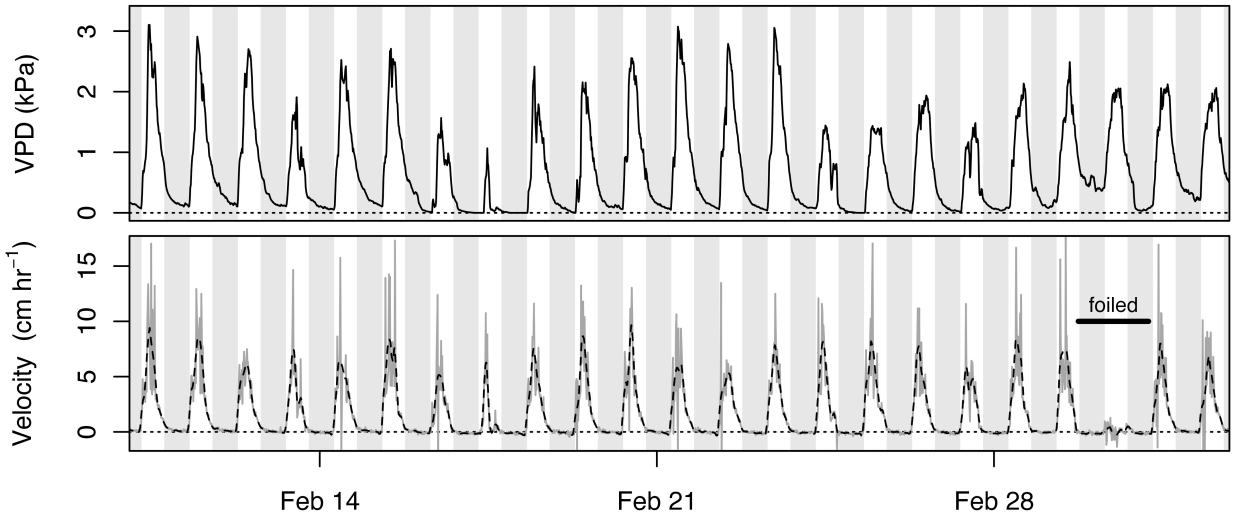

Figure 3. Sap velocities for a flowering shoot of the understory tree *H. prunifolius*. The 95% confidence intervals around the zero-flow estimate are virtually indistinguishable from the zero-flow line shown in the figure and are thus not presented.

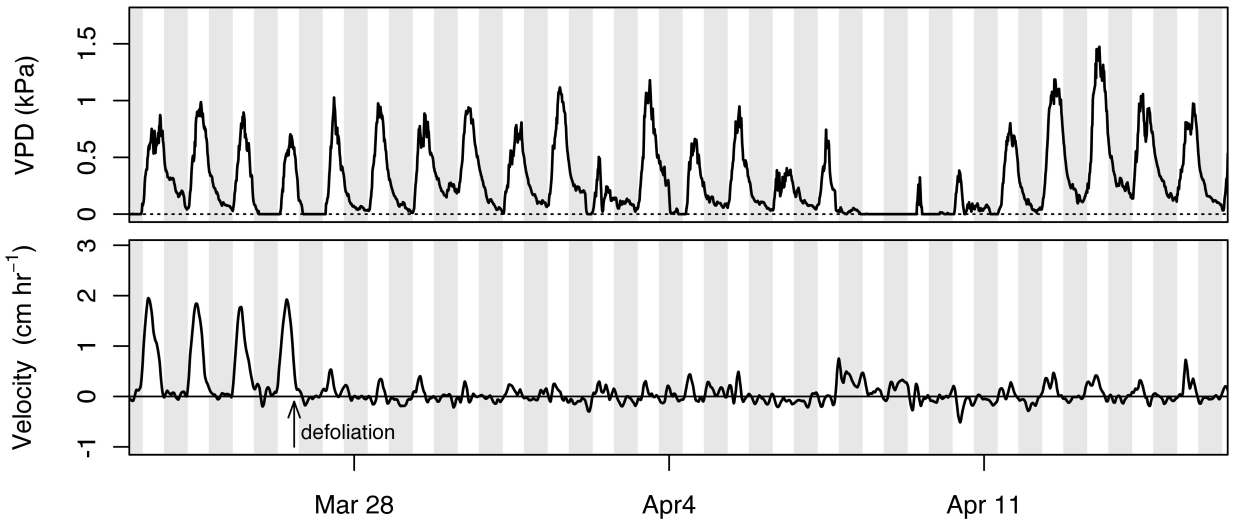

Figure 4. Three days of sap flow on *C. javitensis*. One branchlet (dotted line) bore both leaves and a flower, while another (solid line) bore only leaves. The first day shown was the day just before floral anthesis. Just before predawn on the second day, the flower opened and remained open throughout the day. On the third day shown, only the sepals of the flower remained, while the petals had fully senesced.

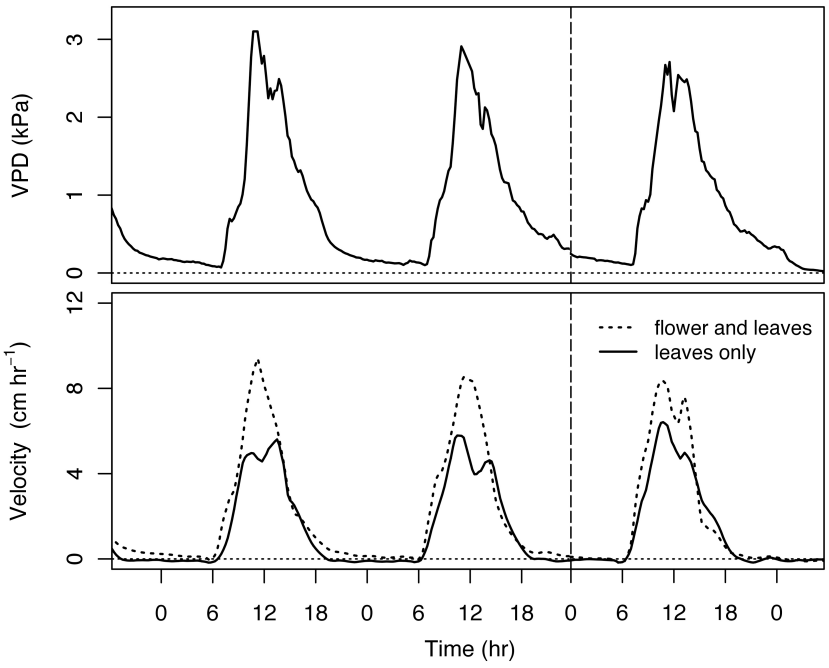

Figure 5. Sap flow velocities for a leaf and an inflorescence of the canopy tree *C. alliodora*. During the six days shown, individual flowers on the inflorescence were in various stages of development.

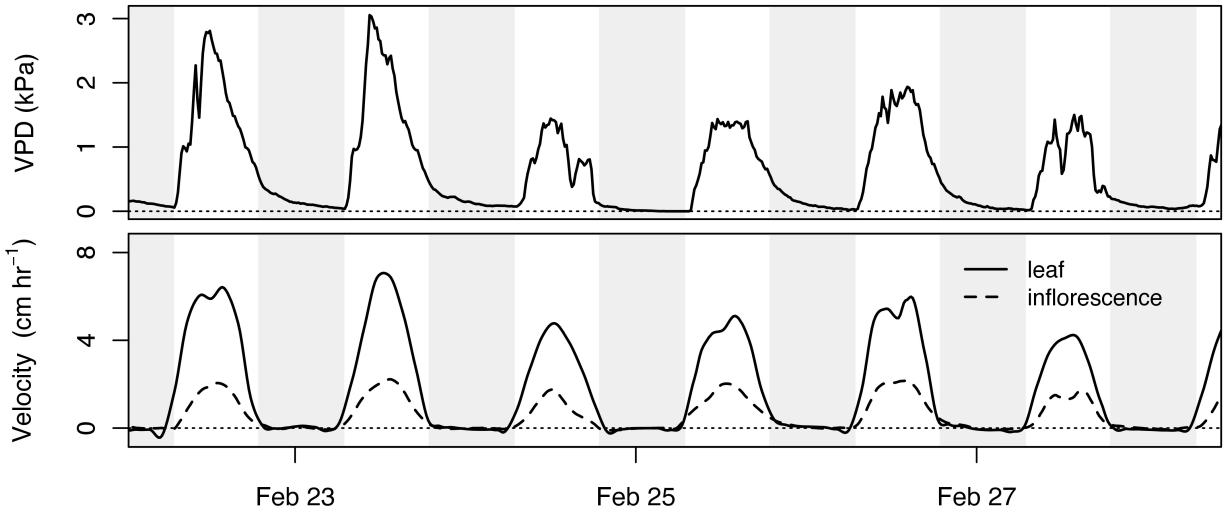

Chapter 2: Structure-function relationships and hydraulic strategies of flowers

Introduction

The primary function of flowers in most angiosperms is to promote sexual reproduction by either attracting animal pollinators or promoting dispersal by wind or water. Animal pollinators have long been thought to be the most important agents of selection on flowers (Sprengel 1793; Darwin 1888), and numerous studies have shown that among narrowly defined groups, pollinator selection can influence a variety of morphological traits, such as color, size, and shape (Galen 2000; Bradshaw and Schemske 2003; Whittall and Hodges 2007; Hopkins and Rausher 2012). However, flowers are subject to the same biophysical constraints of resource supply and demand as other plant organs, such as leaves. These non-pollinator agents of selection, though rarely studied, can also exert selective pressures on floral traits, often in opposition to the preferences of pollinators (Strauss and Whittall, 2006). For example, pollinators generally prefer larger, more showy flowers, but larger flowers have higher water requirements that can exact physiological costs on the rest of the plant (Galen et al. 1999; Lambrecht and Dawson 2007; Lambrecht 2013). Additionally, flowers have extremely variable morphologies, despite the biophysical demands of, for example, being located in the hottest, driest parts of the plant canopy. Knowing how flowers remain turgid and attractive to pollinators under these conditions is fundamental to understanding their structure, function, and evolution.

Despite its importance to the function and evolution of other angiosperm structures, such as leaves and stems (Feild et al. 2009; Pittermann 2010), the hydraulic architecture of flowers has received little attention. In the present study, we quantify for the first time the variability of floral hydraulic conductance among 21 species spanning almost the entire ~140 million year history of the flowering plants and examine the anatomical traits associated with this variation and with the maintenance of water balance in flowers.

The mass balance of flower water can be defined as:

$$\Delta W = J - E \qquad \text{(eqn 1)}$$

where W is the water content, and J and E the rates of water supply and loss, respectively. If mass balance of water is to be maintained, then $\Delta W = 0$, and J must equal E. Water balance may be maintained over a variety of timescales (e.g. diurnally or over the entire lifespan of the structure). At the upper limit, when integrated over a structure's entire lifespan, the water that enters the structure must equal the water that leaves the structure. But plant structures may also be in water balance over shorter timescales as well. For leaves, which have relatively long lifespans and high instantaneous transpiration rates, turnover times of water are very short compared to leaf lifespan. Severed from a continuous source of water, leaves would quickly transpire all their water on the timescale of minutes to hours, particularly if stomata did not close. As a result, water inputs and outputs need to be balanced over much shorter timescales, such as over the course of a day, as the water lost to transpiration throughout the day is replaced by continuous delivery of water during the day and night until water potential gradients from the stem to the leaf equalize. For flowers, which generally have much shorter lifespans than leaves and probably have lower transpiration rates, turnover times of water are probably long such that if they were cut off from a water source they would desiccate slowly, even at their maximum transpiration rate. Using water balance as a framework, in the present study I examine the variability of traits associated with water loss and water supply and whether variation in traits among taxa suggests that there are different hydraulic strategies employed by flowers.

Various factors can influence the instantaneous rates of water loss from and water supply to flowers. Water can be transpired from flowers via stomata or evaporate through the cuticle from epidermal cells. The relative contributions of these two pathways to the total transpirational flux is unknown. In some taxa, flowers seem unable to regulate epidermal conductances to water vapor, probably because species lacking stomata cannot alter their cuticular conductances and those species with stomata may have limited control over stomatal conductance (Hew et al. 1980; Teixido and Valladares 2014), while in other species stomata remain capable of opening and closing (Azad et al. 2007; Feild et al. 2009). Even in flowers that have stomata, reductions in stomatal conductance are unable to curtail the effects of increasing evaporative demand on transpiration rate and prevent significant losses of water content (Chapter 3). If flowers were to be in approximate water balance over short (e.g. diurnal) time courses, then they must have constant, ample supplies of water. The most efficient way of providing large amounts of water to flowers would be via the xylem, the structures predominantly used for transporting water throughout the entire plant. Flowers of some early-diverging, 'basal' angiosperms and magnoliids (the genera *Illicium* (Schisandraceae), *Magnolia* (Magnoliaceae), and *Calycanthus* (Calycanthaceae)) have been shown to have water potential gradients between stems and flowers indicating that they are hydraulically connected to the stem xylem (Feild et al. 2009; Feild et al. 2009; Chapter 3). In contrast, flowers and petals of some eudicot species (*Cochlospermum vitifolium* (Cochlospermaceae), *Luehea speciosa* (Tiliaceae), *Tabebuia rosea* (Bignoniaceae), *Gossypium hirsutum* (Malvaceae)) have higher, less negative water potentials than bracts and leaves, which has been used as evidence to suggest that these flowers are hydrated by the phloem (Trolinder et al. 1993; Chapotin et al. 2003). These 'reverse' water potential gradients imply that for flowers to remain hydrated, then water must be imported against a water potential gradient, which could be performed via the phloem (Chapotin et al. 2003). In contrast to the xylem, the phloem has much higher hydraulic resistance and lower water flux rates, and phloem flow relies on active loading of solutes to create an osmotic gradient (Münch 1930; Nobel 1983; Windt et al. 2009). Relying on phloem-delivered water instead of xylem-delivered water would mean that, on a per flower area basis, J in eqn 1 would be lower, and in order to keep $\Delta W = 0$, then E must also be lower. In other words, to maintain a constant water content, J and E must be coordinated such that reductions in water supply associated with phloem-hydration would be accompanied by reductions in water loss. The presence of reverse water potential gradients–whether or not this is associated with significant hydration by the phloem–suggests that there may be two distinct hydraulic strategies used by flowers. One strategy may be defined by maintaining a high xylem hydraulic conductance to continuously import water throughout anthesis. While phloem water may still be imported throughout anthesis, it would contribute a relatively small proportion of water to the total water budget, as has been shown for developing fruits of grape and tomato (Choat et al. 2009; Windt et al. 2009). The other strategy would be to have a very low xylem hydraulic conductance and discharge stored water (i.e. maintaining a high hydraulic capacitance) that was imported early in development to meet most of the demands of transpiration during anthesis. Phloem-delivered water may be relatively more important in this scenario to the total water budget and may help to recharge hydraulic capacitors and supply transpiration. Flowers employing this second strategy may have very low rates of water loss and, as a result, very low rates of water turnover. While these hydraulic strategies of flowers have been described here as being discrete, there may be variation between these two extremes.

By comparison, leaf hydraulic conductance per unit evaporative surface area (K_{leaf}) is highly variable among species and influenced by both environmental conditions and anatomical traits (Sack et al. 2003; Brodribb and Jordan 2011). Maintaining water balance within thresholds that prevent significant dehydration requires coordination between traits associated with water supply and traits associated with water loss. In leaves, a few important traits have been shown to be critical in maintaining water balance (Boyce et al. 2009; Brodribb et al. 2013). In terms of water supply, vein

length per area (*VLA*, or vein density) is one of the major traits controlling leaf hydraulic conductance (Sack and Frole 2006; Brodribb et al. 2007; Brodribb and Jordan 2011). Leaves with higher *VLA* can deliver liquid water closer to the sites of evaporation in the leaf to prevent desiccation of the photosynthetic tissues during CO_2 exchange with the atmosphere. By increasing the supply of water closer to the sites of evaporation, the leaf can maintain higher stomatal conductances and photosynthetic rates. Furthermore, *VLA* has been shown to be a critical determinant of leaf hydraulic supply capacity across diverse land plant lineages and increased dramatically among angiosperms (Brodribb et al. 2007; Boyce et al. 2009; Brodribb and Feild 2010; Feild et al. 2011; Feild et al. 2011). In terms of water loss, maximum stomatal conductance is tightly coordinated with stomatal size and density and is a major determinant of hydraulic conductance of the leaf lamina (Sack et al. 2003; Brodribb et al. 2013). In addition, there is some evidence that leaves among widely divergent lineages (gymnosperms versus angiosperms) show a similar tradeoff between K_{leaf} and hydraulic capacitance or water residence time (Brodribb et al. 2005).

Here I quantify whole flower hydraulic conductance (K_{flower}) and traits associated with water supply and loss for 21 species from 13 angiosperm families. Because an equivalent amount of floral display area can be distributed among few large flowers or many small flowers, I focus on area-normalized traits to compare hydraulic efficiency regardless of flower size. The complex evolution of floral structures means that comparisons among species are often of non-homologous structures (Irish 2009), but these display structures (tepals, petals, showy bracts) nonetheless perform a similar function. I predicted that among species K_{flower} (per unit area) would correlate with other area-normalized traits associated with liquid and vapor phase fluxes of water. While interspecific comparisons cannot definitively determine functional mechanisms, they are often used to highlight what may be functional relationships. Correlations between K_{flower} and other traits could implicate these traits as being functional determinants of K_{flower}. In addition to *VLA* and stomatal traits, I also measured the Huber ratio of individual flowers (ratio of xylem cross-sectional area to evaporative surface area) and the minimum epidermal conductance to water vapor under non-transpiring conditions (g_{min}), both of which are area-normalized traits. I made four predictions about the hydraulic efficiency and maintenance of water balance in flowers. First, I predicted that there would be positive correlations between water supply traits (*VLA* and Huber ratio) and water loss traits (g_{min} and stomatal traits). Positive correlations between traits in these two suites would suggest that these traits are involved in the transport of water into and through flowers and further support the hypothesis that the constraints of maintaining water balance have require coordinated changes in water supply and water loss traits. Second, I predicted that there would be positive correlations among traits within the two suites of traits. For example, I predicted that Huber ratio and *VLA* would be positively correlated with each other because both are measurements of the abundance of xylem. Stomatal traits and g_{min} were thought to be correlated as well, particularly because floral stomata can be non-functional and may be an open path for transpirational water losses (Hew et al. 1980). Third, I predicted that K_{flower} would correlate with other traits associated with water supply and water loss. Coordination between K_{flower} and water balance traits would indicate that these traits are mechanistically related to the hydraulic capacity of flowers. Fourth, I predicted that there would be a tradeoff between K_{flower} and water residence time. In this case, species with a low K_{flower} are predicted to have low rates of water loss (e.g. g_{min}), which would prolong desiccation.

I made two additional sets of predictions about the variability of K_{flower}. First, I predicted that K_{flower} per unit evaporative surface area would be lower than the hydraulic conductances of both stems and leaves for three reasons: (1) many flowers seem to be hydraulically buffered from variation in plant water status (Trolinder et al. 1993), (2) in contrast to leaves, floral transpiration is considered costly and is expected to have been reduced during floral evolution, and (3) to prevent embolism formation in expensive stems, the points of highest hydraulic resistance (lowest conductance) would be located on more apical regions of the plant (Bucci et al. 2012). We used published and

unpublished data from a variety of ecosystems to examine variability in hydraulic conductance among plant structures. Second, because the hydraulic conductance of fruits can vary throughout development (Choat et al. 2009), we tested whether hydraulic conductance of developing flower buds (K_{bud}) may also vary throughout flower development. We predicted that K_{bud} would increase with bud size if the xylem remains functional throughout bud development. However, if the xylem becomes non-functional, then K_{bud} should plateau or decline with increasing bud size.

Materials and Methods

Plant material

I collected flowering shoots from around the University of California, Berkeley, campus and from the University of California Botanic Garden during the springs of 2013 and 2014. All plants had been kept well-watered. I chose a phylogenetically diverse set of species that differed by two orders of magnitude in floral display size per flower (Table 1). These species also varied morphologically, from flowers with undifferentiated perianths to those with a fully differentiated calyx and corolla and from those with free petals to those with sympetalous connation. Additionally, I included inflorescences of *Cornus florida* (Cornaceae), which have small, inconspicuous flowers but large, white bracts as their showy organs. For each species, I measured K_{flower} on at least three, but generally five or more flowers.

Measurements of hydraulic conductance

I used a low pressure flow meter to measure hydraulic conductance of whole flowers and developing flower buds (Kolb et al. 1996). This method has been shown to be insensitive to variation in irradiance and measures the capacity for water transport into the leaf or flower (Sack et al. 2002). I chose this method rather than the evaporative flux method because the evaporative flux method depends on maximizing boundary layer conductance. Because of the complex morphologies of flowers, I was not confident I could maximize the boundary layer conductance to obtain realistic maximum values of K_{flower}. However, the vacuum pump method has the potential to clear any xylem occlusion. I tested this on a subset of species by (1) comparing flow rates when increasing and decreasing the vacuum pressure and (2) by repeatedly measuring the same flower. I found no differences between flow rates measured while increasing the vacuum or while decreasing the vacuum and no significant increase in K_{flower} with subsequent measurements (data not shown).

Flowering shoots were excised early in the morning (before 9:00 am) when stem water potentials of plants growing in this area are generally higher than -0.25 MPa. Cut shoots were immediately recut under distilled water at least one node apical to the first cut and transported back to the lab. Shoots were kept in water for at least one hour during transport and before any flower was excised, allowing for relaxation of xylem tension. Once in the lab, individual flowers were excised at the pedicel base underwater and connected to hard-walled tubing that led back to an electronic balance (Sartorius CPA225, Sartorius, Goettingen, Germany), on which a vial of dilute electrolyte solution (10 mM KCl, filtered to 0.2 um and partially degassed the morning of measurements) sat. Flowers were placed in a cylindrical plastic chamber that was attached to a vacuum pump and lined with wet paper towels. Flow rates of KCl solution into flower from the balance were measured every 10-60 seconds depending on the absolute flow rate under 5-6 different pressures ranging from 15 to 60 kPa below ambient. At each pressure, flow rates were allowed to stabilize for 3-20 minutes and until the coefficient of variation of the last ten readings was, ideally, less than 5% and the instantaneous measurements converged on the average of the last ten measurements. In practice, low absolute flow rates meant that stable averages could be reached but the coefficient of variation often remained above 5%. To determine K_{flower}, I linearly regressed the flow rates versus pressure and removed, at most, one outlying point from the regression. This regression was not forced through the origin because any deviation in the intercept from zero was

due to differences in height between the level of the flower in the chamber and the water level on the balance. To prevent negative tension due to gravity, flowers were installed to be slightly lower than the water level of the balance, and this slight positive pressure affects flow rates at all vacuum pressure equivalently. Immediately after measurements, we scanned the flowers to determine the one-sided projected surface area of all perianth parts, which we used to normalize hydraulic conductance to calculate K_{flower} in units of mmol s^{-1} m^{-2} MPa^{-1}. For comparison, measurements of K_{flower} of *Magnolia grandiflora* reported by Feild et al. (2009b) using a different method were equivalent to values produced using our method.

Measurements made on developing buds were not normalized by projected surface area. Rather than normalizing for size, we show correlations of bud hydraulic conductance (K_{bud}; mmol s^{-1} MPa^{-1}) plotted against bud length, as measured from the base of the developing petals corolla to the tip. Bud measurements were compared with measurements on whole, open flowers to highlight any developmental changes associated with flower opening. For this analysis, measurements on whole flowers were not normalized by area but were instead plotted against the length between the corolla base and corolla tip, the same points used to determine bud length.

Trait measurements

The Huber ratio is the ratio of the xylem cross-sectional area to the evaporative surface area. In the laboratory, pedicels of the flowers measured for K_{flower} were sliced underwater using a sharp razor blade. The sections were placed in distilled H_2O, while floral structures (tepals, petals, sepals) were individually removed and scanned on a flatbed scanner. The pedicel cross-sections were quickly stained with phloroglucinol and imaged at 5-40x under a compound microscope outfitted with a digital camera. We measured the xylem cross-sectional area and the surface area of flowers using ImageJ (version 1.44o; Rasband 2012). We did not measure the area of individual xylem conduits, but instead quantified the amount of cross-sectional area that was occupied by xylem.

For flowers that had differentiated perianths, we made trait measurements only on the corolla because the petals comprised the largest evaporative surface area. Sampling for vein density (VLA) was identical to Roddy et al. (2013) and briefly summarized here. To account for the high variability in vein density within a petal, we excised multiple 1-cm^2 sections from petals of multiple flowers. These sections were placed in 2% NaOH for clearing. Sections were rinsed briefly in distilled H_2O and then placed into 95% ethanol. Once in ethanol, samples were quickly stained with Safranin O and imaged at 5-20x magnification under a compound microscope outfitted with a digital camera. One or two images per section from each of five to twelve sections per species were captured, and vein densities were measured using Image J (version 1.44o; Rasband 2012).

The minimum epidermal conductance, g_{min}, is the area-normalized conductance to water vapor under non-transpiring conditions when stomata are presumably closed and integrates the permeability to water vapor of the cuticle as well as any leakiness through impartially closed stomata (Kerstiens 1996). We measured g_{min} on individual petals or tepals by sealing the cut edges with a thick layer of petroleum jelly and placing the structures in a dark box into which was placed a fan and a temperature and relative humidity sensor. For connate flowers, we measured the entire tubular structure and sealed the cut base with petroleum jelly. Structures sat on a mesh screen while the fan blew directly onto them and circulated air inside the container. Every 5 to 20 minutes, the container was briefly opened and the structure weighed on a balance with a resolution of 0.1 mg. After approximately 10 measurements, each structure was scanned to measure its area and then placed in a drying oven for later dry mass measurement. Using the temperature, humidity, mass, and area measurements, we calculated g_{min} and the desiccation time (T_{des}), which we define as the time required for the structure to fully desiccate and is calculated as:

$$T_{des} = \frac{H_2O_{area}}{g_{\min}} \quad \text{(eqn 2)}$$

where H_2O_{area} is the fresh water content per area and g_{min} is the minimum epidermal conductance to water vapor per area. The fresh water content was defined as the difference between the initial mass taken immediately after excision during measurements of g_{min} and the final dry mass. T_{des} therefore has units of time. The reciprocal of T_{des} would be equivalent to the proportion of a petal's water that is lost per unit time (in units of time^{-1}). A conservative strategy of limiting water loss would be associated with a long T_{des} and a high proportional rate of water loss. For the present analysis, we have chosen to use T_{des} rather than the rate to highlight the potential tradeoffs that exist between T_{des} and K_{flower}.

To measure stomatal traits (stomatal density and guard cell length) we cleared sections in 2% NaOH, rinsed them briefly in distilled H_2O, and transferred them into 95% EtOH. Images of the epidermis were made using a compound microscope at 5-40x. We imaged 5-20 windows to determine stomatal densities, depending on the abundance of stomata. Guard cell length was determined by measuring the maximum length of at least 10 guard cells for each species with stomata. The stomatal pore area index was calculated as the product of stomatal density and the square of average guard cell length, according to Sack et al. (2003).

We lacked trait data for some species because of limited flower material. Because we prioritized K_{flower} measurements, in some cases there were insufficient flowers to make all accompanying trait measurements, but because there has been so little K_{flower} data previously published we have chosen to include these species in the present analyses when possible.

Comparison of K_{flower} *with other plant structures*

To compare the magnitude of K_{flower} to other plant structures, we compiled values of hydraulic conductance (K) from a variety of published and unpublished sources (Table 2). Leaf hydraulic conductance is commonly measured, but stem hydraulic conductance is less frequently measured because most researchers measure stem hydraulic conductivity instead. As a result, many of the measurements of stem hydraulic conductance are taken from unpublished studies of small-statured plants (seedlings and shrubs) but include species from various habitats, ranging from lowland tropical forests to North American deserts.

Statistical analyses

For correlations between traits, we tested whether there was a significant correlation between variables using both non-parametric (Spearman rank correlation) and parametric tests (Pearson product-moment). If there was a significant correlation for non-parametric and parametric tests, we compared linear, logarithmic, power, and quadratic fits and chose the model with the lowest residual standard error (RSE). Because calculating R^2 values from nonlinear fits is inappropriate, we only report this goodness-of-fit statistic for linear relationships. When a relationship was found to be significant only using non-parametric tests, the Spearman correlation coefficient is reported. All analyses were performed in *R* (v. 3.1.1; R Core Team 2012).

Results

K_{flower} varied widely among all species from a mean of 1.30 mmol s^{-1} m^{-2} MPa^{-1} for *Cornus florida* inflorescences to 40.03 mmol s^{-1} m^{-2} MPa^{-1} for *Illicium mexicanum* flowers. Interestingly, *C. florida* inflorescences, whose showy organs are bracts, had the lowest K_{flower} of any species measured. Differences among species were driven almost entirely by the comparatively high K_{flower} of two genera, *Illicium* and *Calycanthus* ($F = 11.72$; $df = 4$; $P < 0.01$; Figure 8). *Illicium* had significantly higher K_{flower} than the genus *Magnolia*, the monocots, and the eudicots (all pairwise $P < 0.01$), while

Calycanthus was significantly different from only the eudicots (P = 0.04). Interestingly, only two genera of the magnoliids captured most of the variation in K_{flower} of all species measured (averages of 13.84 and 3.12 mmol s^{-1} m^{-2} MPa^{-1}, respectively; P = 0.11). The monocots varied from 1.71 mmol s^{-1} m^{-2} MPa^{-1} for *Iris douglasiana* to 4.03 mmol s^{-1} m^{-2} MPa^{-1} for *Agapanthus africanus*, while the eudicots ranged from 1.30 mmol s^{-1} m^{-2} MPa^{-1} for *Cornus florida* inflorescences to 6.36 mmol s^{-1} m^{-2} MPa^{-1} for *Pyrus pashia*.

I had predicted that if xylem conduits area functional in flowers, then xylem traits should correlate positively with K_{flower}, such that increasing xylem abundance, whether as veins in petals and tepals or as conduits in the cross-sectional area of pedicels, should increase K_{flower}. Suport for this hypothesis was mixed. Among all species, there was a significant relationship between K_{flower} and *VLA*, which was best fit by a linear relationship (R^2 = 0.44, RSE = 4.59; df = 15; P < 0.01; Figure 1), with the equation K_{flower} = 1.42 * *VLA* + 0.77. The relationship between K_{flower} and the Huber ratio was best fit by a power relationship (RSE = 7.77, df = 17, P < 0.01) with the equation K_{flower} = 3.49e5 * $Huber^{2.13}$. However, these significant relationships were driven entirely by the high K_{flower} of *Illicium* and *Calycanthus*. Ignoring these two genera, there were no significant relationships between K_{flower} and xylem traits. Interestingly, the four *Magnolia* species were more similar to the monocots and the eudicots than they were to *Calycanthus*, highlighting that most of the variation in these traits is apparent solely within the magnoliids. There was no significant relationship between the two xylem traits, *VLA* and Huber ratio (Figure 3).

There was mixed support for the hypothesis that water loss traits would correlate with K_{flower}. Consistent with this hypothesis, there was a positive relationship between K_{flower} and g_{min} that was best fit by a quadratic function in which K_{flower} = -0.004 * g_{min}^2 + 0.68 * g_{min} -1.99 (RSE = 6.01; df = 14; P < 0.05; Figure 2a). Species with higher stomatal densities also had higher K_{flower}, which was best described by a linear relationship with K_{flower} = 0.89 * density + 2.78 (F = 12.26; df = 12; P < 0.01). K_{flower} was also significantly correlated with the stomatal pore area index with K_{flower} = 2217.50 * *SPI* + 3.08 (F = 11.11; df = 12, P < 0.01; Figure 2d). There was no relationship between K_{flower} and stomatal size. However, these significant relationships among species in all cases were driven by high trait values for *Illicium* and *Calycanthus* and the almost complete absence of stomata from monocot and eudicot flowers. Although *Magnolia* flowers had stomatal densities and SPI as high as *Illicium* and *Calycanthus*, values of K_{flower} for *Magnolia* species remained low, approximately equivalent to those of the monocots and eudicots. It should be noted that leaves have much higher stomatal densities than I measured on flowers; angiosperm leaves range from 100 to 500 stomata per mm^2 of lamina surface area (Sack et al. 2003), whereas flowers had no more than 15 stomata per mm^2. The range of guard cell lengths I measured on flowers (12-32 μm) was consistent with previous measurements on leaves, but due to low stomatal densities among flowers the calculated SPI was significantly lower for flowers (less than 0.006) than for leaves (0.04-0.20; Sack et al. 2003). These water loss traits were also predicted to correlate with each other. Stomata represent an open path for liquid water to evaporate from substomatal cavities into the atmosphere, so higher abundances or larger stomata should increase the rate at which flowers lose water, particularly if stomata do not close completely. Indeed, there was a significant, positive relationship between g_{min} and stomatal density (RSE = 17.3, df = 11, P < 0.05; g_{min} = 0.001 * $density^{4.32}$; Figure 4b), although this relationship also was driven by a high g_{min} of *Calycanthus occidentalis*. There was no relationship between *SPI* and g_{min} (Figure 4a).

I had predicted that if flowers needed to maintain water balance during anthesis, then water supply traits and water loss traits would correlate positively with each other. While the strongest correlation was between g_{min} and *VLA*, which was best described by a power function with g_{min} = 1.56 x $VLA^{-1.67}$ (RSE = 10.45, df = 12, P < 0.001; Figure 5a), this relationship was also driven primarily by the large variation in both traits among *Illicium* and *Calycanthus*. *VLA* was also significantly correlated with *SPI*, although no parametric model was significant (r = 0.59, df = 12, P

< 0.05). There was no significant relationship between Huber values and either g_{min} or stomatal traits (Figure 5b,d).

I predicted that there would be a tradeoff between maintaining a high K_{flower} and a slow rate of water turnover, as measured by the time to desiccation, T_{des}. Flowers that can efficiently move water may not need to have high water contents, and so H_2O_{area} was predicted to correlate negatively with K_{flower}. Regardless of H_2O_{area}, flowers with high K_{flower} were predicted to turnover water rapidly and have short T_{des}. Contrary to my predictions, species with high K_{flower} also had higher H_2O_{area} (R^2 = 0.31, F = 6.83, df = 15, P < 0.05; $\log(K_{flower}) = 1.07 * \log(H_2O_{area}) - 2.02$; Figure 6a). However, supporting my predictions, there was a tradeoff between K_{flower} and T_{des} (R^2 = 0.37, F = 8.74, df = 15, P < 0.01; $\log(K_{flower}) = -0.61 * \log(T_{des}) + 2.62$; Figure 6b). While both of these relationships were significant among species, they were driven entirely by only two genera, *Illicium* and *Calycanthus*, which had the highest K_{flower}. Among other species, there were no significant relationships between K_{flower} and either H_2O_{area} or T_{des}.

K_{bud} varied throughout floral development for both species and was generally higher for the monocot (*Hemerocallis sp.*) than for the eudicot (*A. buccinatorium*; Figure 7). In both species, K_{bud} generally increased during the first half of development and plateaued by the end of expansion and during anthesis. For *Hemerocallis* buds, there was a marked decline in K_{bud} when buds were between 50-80 mm in length. There was no such decline for *A. buccinatorium* buds, although K_{bud} for this species did plateau during the last stages of bud expansion and slightly decreased open flower opening.

Hydraulic conductance of flowers was much more variable than the hydraulic conductance of stems and leaves (Figure 8). However, most of this variation was driven by two genera, *Illicium* and *Calycanthus*, which had the highest K_{flower} values, even higher than most leaves. In contrast, *Magnolia*, monocot, and eudicot flowers did not differ from each other and had lower hydraulic conductance than most leaves. Surprisingly, flowers did not necessarily have lower conductances on a per unit evaporative surface area basis than stems and K_{flower} was higher than K_{stem} of desert species. These comparisons between structures should be interpreted with caution, however, because the same species were not measured for the different structures.

Discussion

Maintaining water balance in desiccating environments requires the coordination between water supply and water loss. As leaves or flowers transpire water, their water contents and water potentials decline, which drives the movement of water along the soil-plant-atmosphere continuum. In order to maintain turgor and physiological functioning, the capacity to transport liquid phase water should be tightly coordinated with the rates at which water is lost to the atmosphere. In leaves, differences between microenvironments, for example between sun and shade, induce coordinated changes in traits associated with liquid phase and vapor phase conductances to water, lending strong support to the idea that the need to maintain water balance is critical to leaf structure (Brodribb and Jordan 2011). Although they are much more ephemeral than leaves, flowers must remain turgid to attract pollinators and, as a result, may also need to maintain water balance throughout anthesis. How they do this has been a point of controversy, with some suggesting that water is delivered primarily by the phloem against water potential gradients (Trolinder et al. 1993; Chapotin et al. 2003) and others showing that water is imported by the xylem (Feild et al. 2009; Feild et al. 2009; Chapter 3).

In the present study, I took a different approach to examining variability in the hydraulic capacity of flowers among species spanning most of the extant diversity of the angiosperms. I quantified for a phylogenetically diverse species set the maximum hydraulic conductance of whole flowers and related this to other structural and physiological traits predicted to influence hydraulic conductance. The results showed that while there were significant structure-function correlations

among species, in almost all cases these were due to high trait values for just two genera, *Illicium* and *Calycanthus*. Despite large variation in flower size and morphology among the monocots and eudicots, there was remarkable convergence of area-normalized K_{flower} to a very narrow range. While the need to maintain water balance over short timescales has been an important factor influencing the evolution of leaf hydraulic traits (Brodribb and Jordan 2011), for most flowers, there have been no similar repeated, coordinated shifts in hydraulic traits associated with water supply and loss. Although flowers are often located in similar microenvironments as leaves and are thought to have derived from leaves in many lineages, the functional dimensions of their evolution seem to have been drastically different.

Role of stomata in regulating water loss from flowers

The abundance and functioning of floral stomata is highly variable both within individual flowers and among species. In several tropical orchid flowers, for example, stomatal densities are highly variable among different floral organs, and stomatal conductance does not respond to environmental changes (Hew et al. 1980). In both *Calycanthus* and *Cistus* flowers, transpiration rate increases linearly with the vapor pressure gradient driving evaporation, suggesting that stomata are largely incapable of limiting transpiration, although stomatal conductance does vary diurnally in *Calycanthus* flowers (Teixido and Valladares 2014; Chapter 3). Stomatal conductance also varies diurnally in outer whorl *M. grandiflora* tepals but varies little in inner whorl tepals (Feild et al. 2009). Overall, these results from gas exchange measurements suggest that in contrast to leaf stomata, floral stomata, even when present, are mostly incapable of regulating transpiration. Even in cases when floral stomatal conductance varies diurnally, they cannot limit total transpiration rate as efficiently as foliar stomata (Chapter 3).

Unlike foliar stomata (Sack et al. 2003), floral stomata have little influence on the hydraulic conductance of flowers (Figure 2). Surprisingly, stomatal traits had little influence on g_{min} (Figure 4), suggesting that the stomatal pathway for evaporative water loss has little effect on the overall epidermal conductance. Both pathways for water loss–through stomata and through the cuticle–are critical components that influence floral water budgets yet they have little impact on the overall hydraulic conductance of flowers. Compared to leaves, lower stomatal densities in flowers likely increase the relative importance of the cuticular pathway for water loss, particularly among monocot and eudicot flowers, which had few, if any, stomata. Stomata may play a critical role in regulating water loss from flowers, but this role may be different from the role of stomata in controlling leaf transpiration. While angiosperm leaves can actively close their stomata to prevent desiccation, floral stomata, even when they do close, seem incapable of significantly curtailing transpirational water losses (Hew et al. 1980; Brodribb and McAdam 2011; McAdam and Brodribb 2012; Teixido and Valladares 2014; Chapter 3). Stomata represent an open pathway for liquid phase water inside the flower to evaporate into the atmosphere, and the near absence of stomata from many flowers may be an efficient way to prevent transpiration from tissues incapable of assimilating CO_2. Thus, the role of stomata in regulating water loss from most flowers may be not in their capability to close to prevent transpiration but rather in their near absence from many flowers, which forces all transpirational losses to be cuticular. In most plant structures, this cuticular pathway is highly resistant to water loss.

Role of xylem in supplying water to flowers

There is controversy over the relative roles of the xylem and the phloem in delivering water to both flowers and fruits. The water content of reproductive organs results from a balance between water supply by vascular tissues (xylem and phloem) and water losses to transpiration and possible backflow to the stem. There has been substantially more work aimed at understanding these dynamics in fruits. In various agricultural species, water flow to developing fruits early in

development is considered to come predominantly via the xylem, but this contribution diminishes and is surpassed by the phloem contribution later in fruit development (Ho et al. 1987; Lang 1990; Greenspan et al. 1994). However, more recent studies using a variety of methods have called into question the idea that xylem becomes non-functional and that water import later in development is due solely to the phloem (Choat et al. 2009; Windt et al. 2009; Clearwater et al. 2012; Clearwater et al. 2013). Instead, phloem-delivered water may buffer variation in xylem flows.

With comparatively less work done on flowers, the controversy over xylem- and phloem-delivery of water still remains unsolved. While the present study is incapable of determining whether the xylem or the phloem is the predominant source of water to open flowers, our results do suggest that among most species, xylem has little influence on the overall hydraulic conductance of flowers (Figure 1). While increases in K_{flower} associated with increasing *VLA* and Huber ratio strongly suggest that xylem are functional, much of this variation was driven by *Calycanthus* and *Illicium* flowers, which had the highest K_{flower} and among the highest *VLA* and Huber ratios. Flowers of both of these genera have water potentials indicative of xylem hydration (Feild et al. 2009; Chapter 3).

Disregarding *Illicium* and *Calycanthus* flowers, which had the highest trait values, K_{flower} was insensitive to changes in *VLA* among the monocots, eudicots, and the genus *Magnolia*, almost all of which had a *VLA* below about 4 mm mm^{-2} (Figure 1a). In a broader analysis of floral *VLA* variation, the vast majority of flowers had *VLA* below this threshold, although species with floral *VLA* above 4 mm mm^{-2} appear in groups across the angiosperm phylogeny (Chapter 4; Roddy et al. 2013). The insensitivity of K_{flower} to *VLA* among these low *VLA* species implies that veins in these flowers have little influence on hydraulic function and may not conduct water. As *VLA* decreases and the average path length between a mesophyll cell and the nearest xylem vessel increases, hydraulic resistance in this extraxylary path also increases. Reductions in *VLA* decrease hydraulic conductance (and increase resistance) by lengthening the path between veins and the sites of evaporation, a pattern well described in leaves (Brodribb et al. 2007). Flowers that have both low *VLA* (below 4 mm mm^{-2}) and low K_{flower} may rely more heavily on other sources of water to remain turgid. One source of water could be the phloem, and we would expect that flowers with low *VLA* would rely more heavily on phloem flow and on osmotic gradients (rather than hydrostatic tension) to drive water flow. Coincidentally, *Magnolia* species all had *VLA* around this threshold 4 mm mm^{-2}, and inner whorl and outer whorl tepals of *M. grandiflora* vary both in the direction of their water potential gradients and in *VLA*; inner whorl tepals have an average *VLA* of 3.26 mm mm^{-2} and water potential gradients indicative of phloem-hydration and outer whorl tepals have a *VLA* of 5.18 mm mm^{-2} and water potential gradients indicative of xylem hydration (Feild et al. 2009). These results for different *M. grandiflora* tepals within the same flower further suggest that a threshold *VLA* of 4 mm mm^{-2} may be important in determining the mechanisms of water import to flowers.

We also predicted that if the xylem conducts water during floral bud development, then K_{bud} should increase with increasing bud size. K_{bud} increased with bud length for both *Hemerocallis* sp. and *A. buccinatorium*, suggesting that the xylem remain functional throughout most of development (Figure 7). However, in both species measurements made later in development (of K_{bud} for *Hemerocallis* sp. and of K_{flower} for *A. buccinatorium*) indicate that hydraulic conductance either declined or ceased to continue increasing as rapidly. In *Hemerocallis*, K_{bud} dropped dramatically when buds were approximately 50 mm in length and did not recover until they were approximately 80 mm in length, while in *A. buccinatorium* K_{bud} remained constant after about 90 mm in length or even possibly declined after buds opened. In these two species, both of which have low *VLA*, xylem function may be variable throughout floral development and may lose some capabilities of conducting water during the final phase of cellular expansion and anthesis. As developing buds reach their final size and open, the extraxylary resistance may overwhelm the capacity of the xylem to efficiently deliver water to all cells, and, as a result, these flowers may rely less on xylem flows.

Two alternative hydraulic strategies of flowers

Another source of water may be stored water (hydraulic capacitance) that is discharged as water potential declines. Water movement between tissues (e.g. stems and flowers) can be driven by hydrostatic tension or by osmotic gradients. Species with low K_{flower} seem incapable of relying on hydrostatic tension to drive water flux, particularly because of the insensitivity of K_{flower} to VLA variation among these species (Figure 1). Building xylem vasculature capable of withstanding low water potentials may be costly in structures as ephemeral as flowers; relying on osmotic gradients to drive water flux can also be costly, particularly in heterotrophic structures like flowers, because it requires the active loading of solutes to adjust osmotic potential. However, importing water before flower opening into hydraulic capacitors that can then be discharged during anthesis would be an alternative strategy to relying on continuous water import.

Results from the present study suggest that species may use one of these two alternative strategies. While *Illicium* and *Calycanthus* maintain a high K_{flower}, many other flowers may rely predominantly on discharging hydraulic capacitors. Additionally because K_{flower} is low in most species, phloem water may make up a relatively larger proportion of their overall water budget. Discharging hydraulic capacitors can prevent water potential declines and mitigate the need for building structures capable of withstanding high tension in the xylem (Chapter 3; McCulloh et al. 2014). Flowers with a high K_{flower} were predicted to have low water contents because they could rely on newly imported water rather than on stored water to supply transpiration. However, I found the opposite pattern: species with high K_{flower} also had higher water contents (Figure 6a). In contrast, all other species had a low K_{flower}, low water contents, and high T_{des} (Figure 6). Thus, there seem to be two distinct strategies with relatively little variation between these extremes. One strategy is that employed by *Illicium* and *Calycanthus* flowers, which is to maintain a high K_{flower} and turn over water rapidly. The other strategy is that employed by almost all the other species, which is to have a low K_{flower} and very long turnover times. Although maintaining a long T_{des} itself may not normally be considered a strategy, I predict that the alternative strategy to maintaining a high K_{flower} for avoiding water potential declines would be to have a high hydraulic capacitance. The scant available evidence from five species supports this notion that on a whole flower basis, eudicot flowers, which have lower VLA, g_{min}, and K_{flower}, also have higher hydraulic capacitance than *Calycanthus* flowers, which have high VLA, g_{min}, and K_{flower} (Chapotin et al. 2003; Roddy et al. 2013; Chapters 3-5). However, better characterization of hydraulic capacitance and conductance on the same species is desperately needed.

If many flowers receive relatively little new water imported during anthesis, then, unlike leaves, water import and export may not be balanced over the course of a day-night cycle. Low K_{flower} and discharging hydraulic capacitors may lengthen the timescale over which flower water content is balanced. In an experimental drought and rewatering experiment, terahertz time domain spectroscopy, which allows repeated, non-destructive measurements of water content, revealed that the water contents of *Viola* flowers responded to rewatering much more slowly than the water contents of *Viola* leaves (N. Born, pers. comm.). While the water contents of *Viola* leaves immediately increased upon rewatering, water contents of *Viola* flowers continued to decline for twelve hours after rewatering before finally starting to increase again. These results suggest that while flowers can rehydrate, the timescale of rehydration is much slower for flowers than for leaves, consistent with a limited reliance on xylem water potential gradients to drive flow.

Conclusions

Flowers are one of the key innovations of the angiosperms and are incredibly diverse morphologically. Despite differing substantially in morphology and evolutionary origin, many species exhibit very little variation in most hydraulic traits, and most of the variation among all

species is due to only two genera, *Illicium* and *Calycanthus*. As a result, there may be only two distinct, alternative strategies for avoiding water potential declines: maintaining a high hydraulic conductance and maintaining a high hydraulic capacitance. The differences between these strategies are reflected in the relationships between other hydraulic traits. While a high hydraulic conductance could provide significant amounts of water to flowers, reduced hydraulic conductance and greater reliance on stored water may physiologically separate flowers from diurnal variability in the water status of other plant structures. Better understanding the mechanisms and timing of water transport to flowers and the tradeoffs between alternative hydraulic strategies will be an important advancement in our understanding of floral physiology and evolution.

Figure 1. Coordination between whole flower hydraulic conductance (K_{flower}) and water supply traits: (a) vein length per area (VLA; or vein density) and (b) the ratio of xylem cross-sectional area to evaporative surface area (Huber ratio). In both plots, significant relationships are shown by best fit curves.

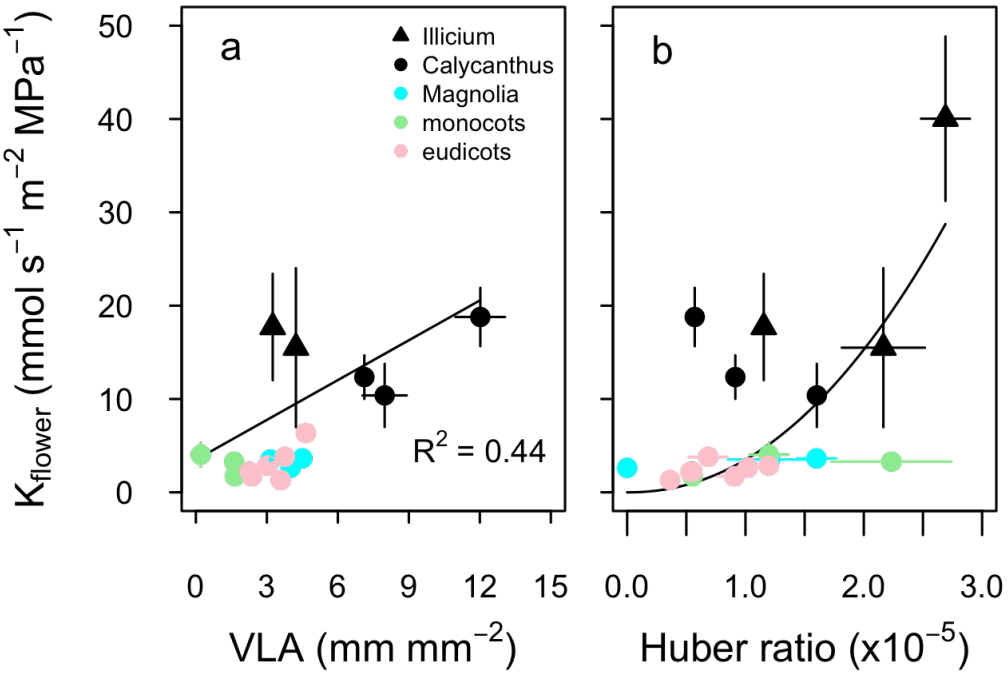

Figure 2. Coordination between K_{flower} and water loss traits: (a) minimim epidermal conductance (g_{min}), (b) stomatal density, (c) stomatal length, (d) stomatal pore area index (SPI). Statistically significant curve fits are shown. Point symbols are the same as in Figure 1.

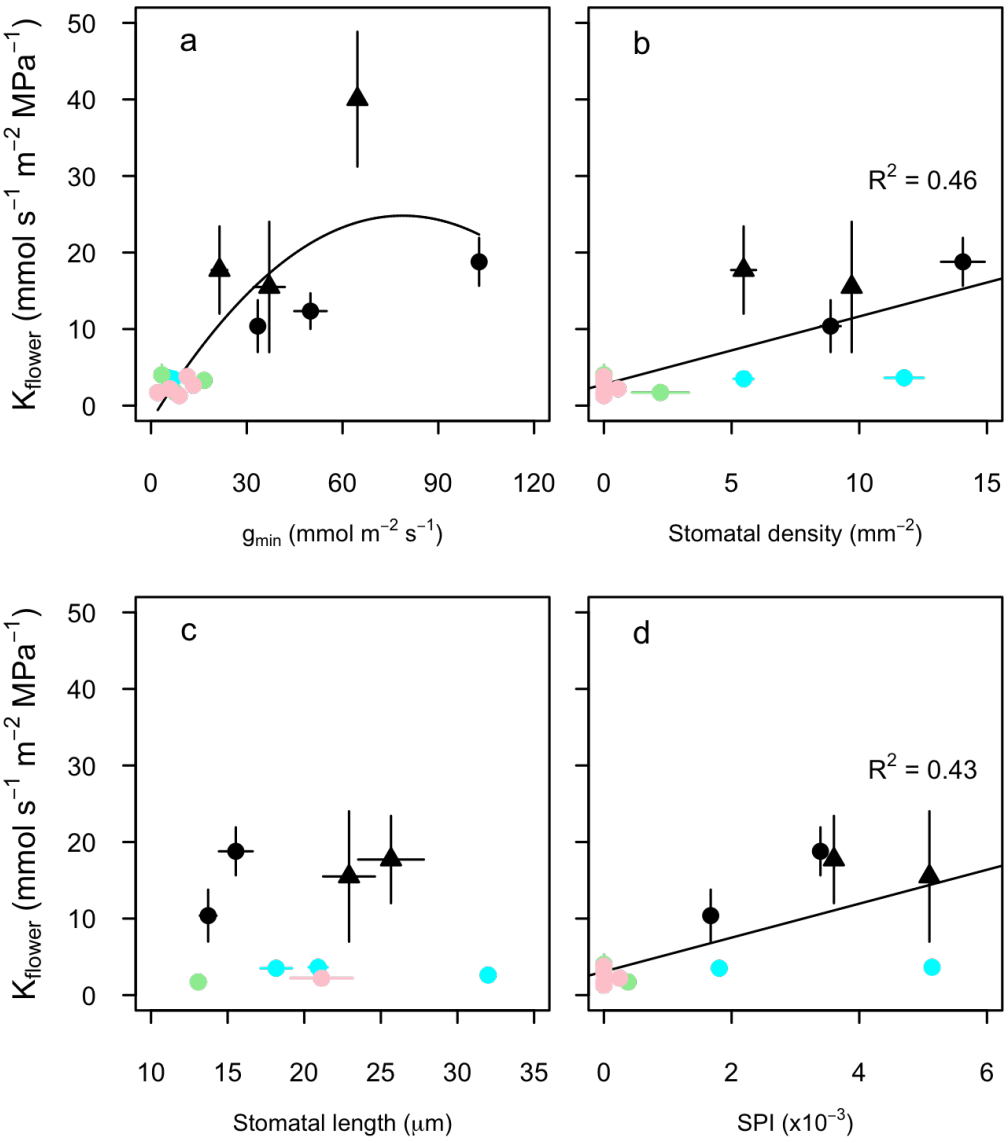

Figure 3. Correlations between the water supply traits, vein length per area (*VLA*) and Huber ratio. Point symbols are the same as in Figure 1.

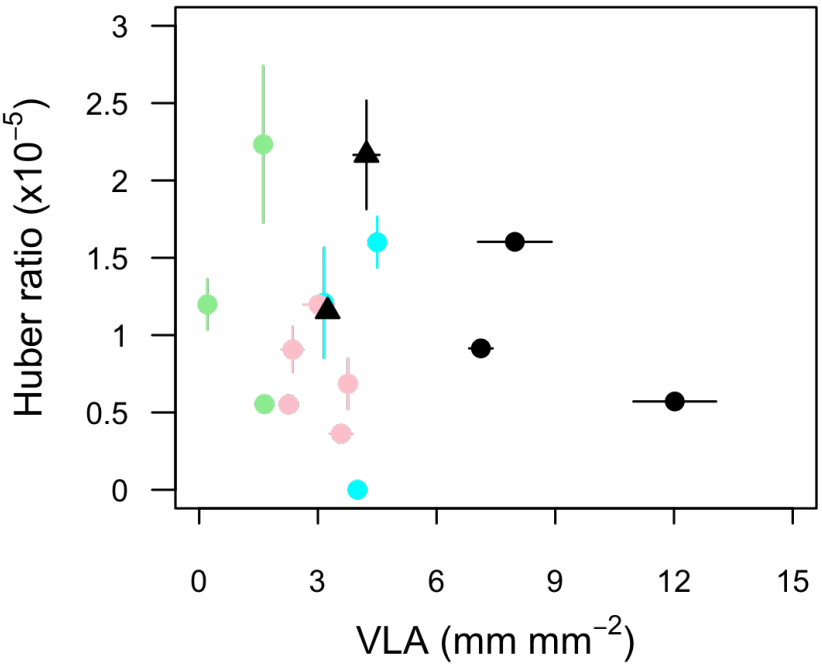

Figure 4. Correlations between g_{min} and (a) stomatal pore area index (SPI) and (b) stomatal density. Statistically significant curve fits are shown. Points symbols are the same as in Figure 1.

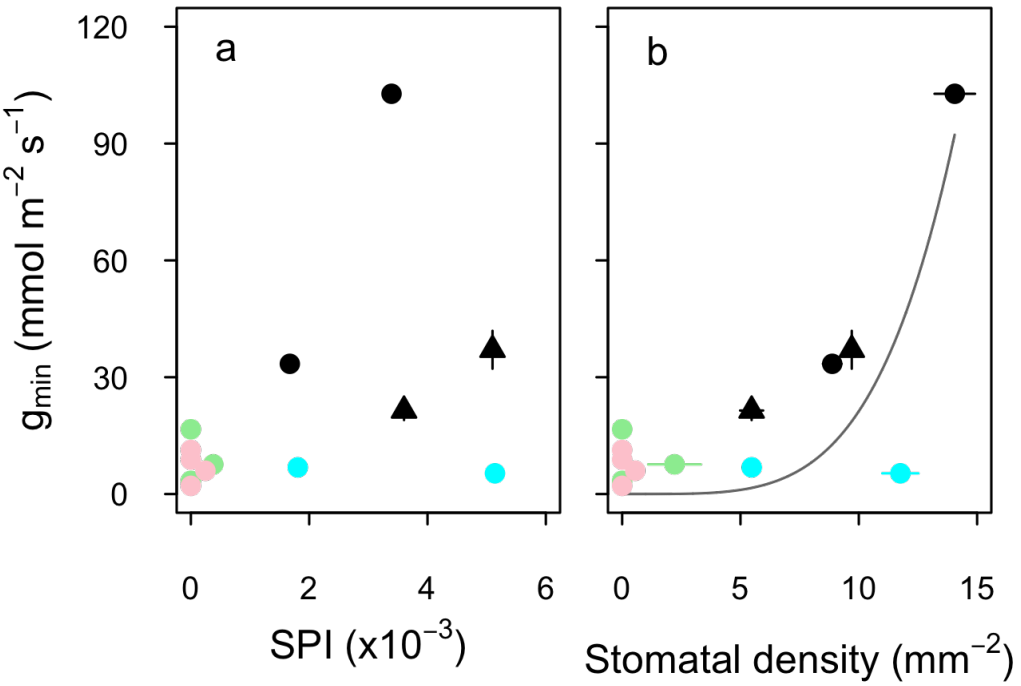

Figure 5. Coordination between water supply traits (*VLA* and Huber ratio) and water loss traits (g_{min} and *SPI*). Statistically significant relationships are shown with curve fits or correlation coefficients. Point symbols are the same as in Figure 1.

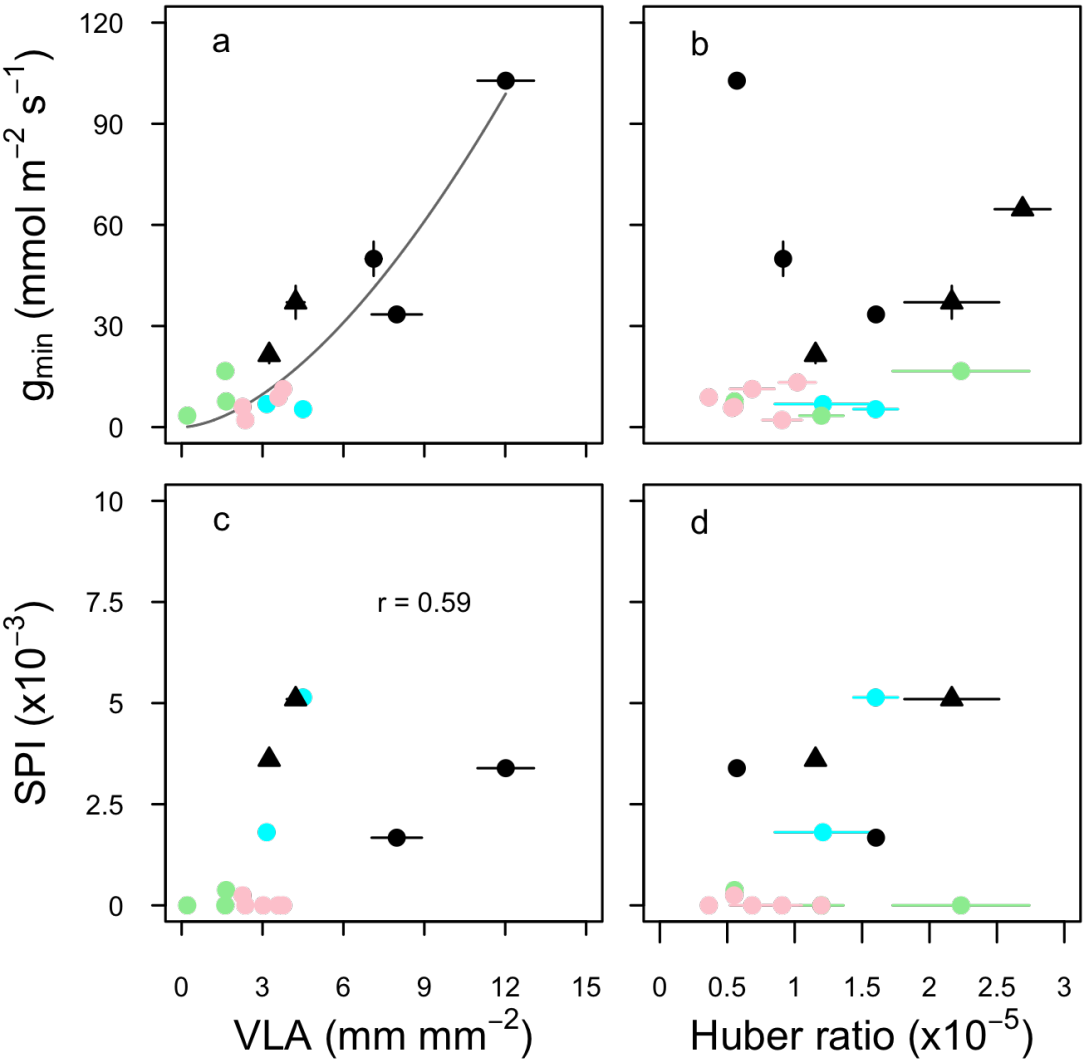

Figure 6. Coordination between (a) water content per area (H_2O_{area}) and K_{flower} and (b) desiccation time (T_{des}) and K_{flower}. Statistically significant relationships are shown with curve fits. Point symbols are the same as in Figure 1.

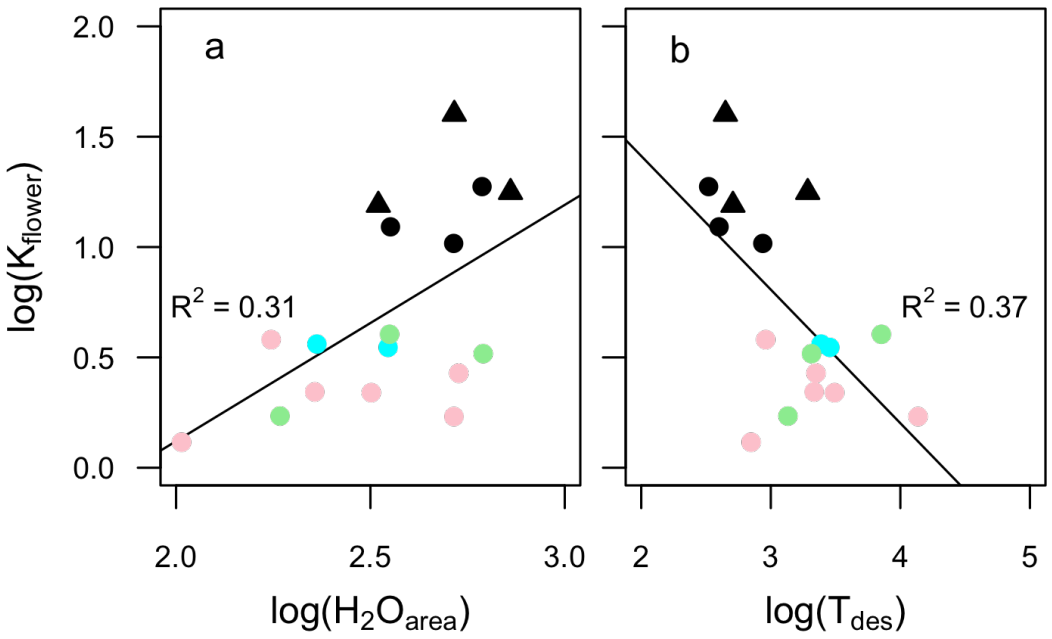

Figure 7. Variation in K_{bud} during bud development for two species, (a) *Hemerocallis sp.* and (b) *Amphilophium buccinatorium*. Closed circles represent measurements on developing buds, and open circles represent measurements on open flowers.

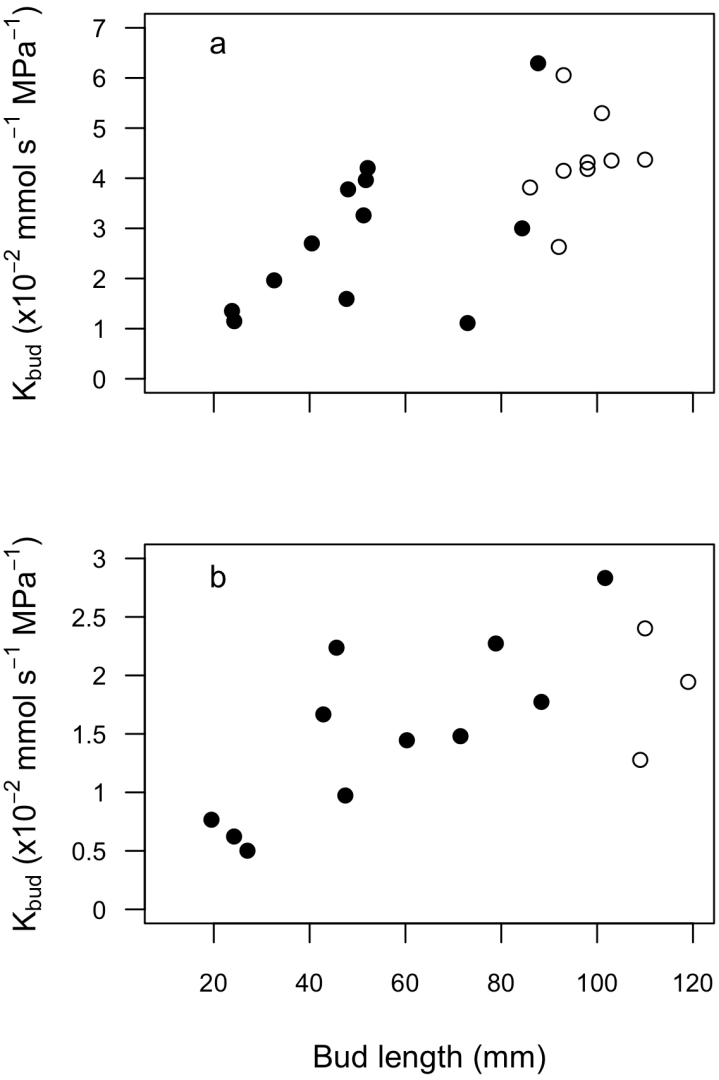

Figure 8. Variation among plant structures in area-normalized hydraulic conductance. Groupings were chosen to highlight the the major differences within structures. Values below the bars indicate the number of species sampled in each group. Data for flowers are from the current study and Feild et al. (2009b); for tropical leaves are from Sack and Frole (2006); for temperate leaves from Nardini and Salleo (2000), Sack et al. (2002), Nardini et al. (2005), Lo Gullo et al. (2005), Scoffoni et al. (2008), Simonin et al. (2012); for desert shrubs from DiVittorio (2014); for tropical seedlings from Brenes et al. (2013).

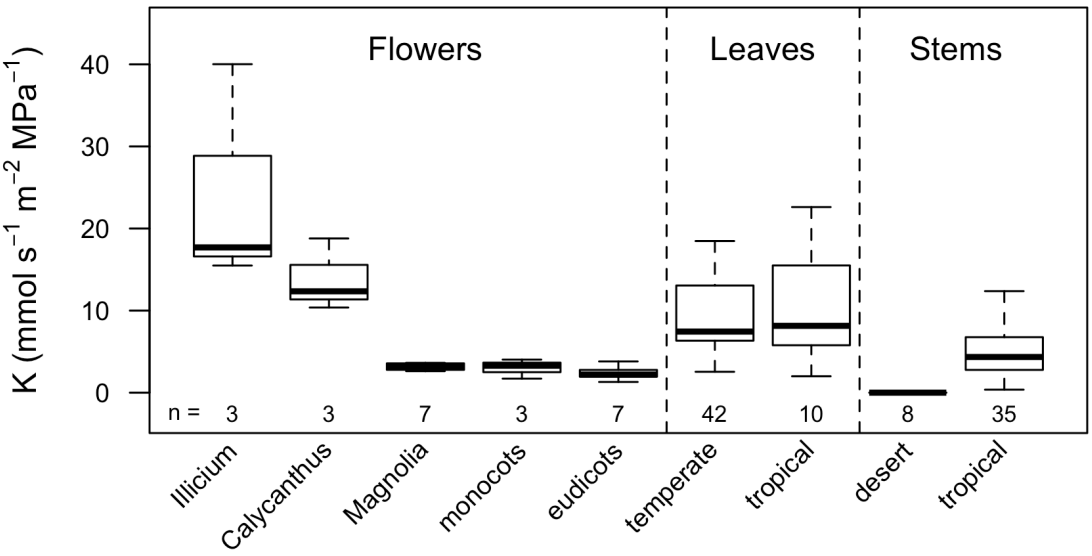

Figure 9. Proposed strategies of maintaining water balance employed by flowers. Associated anatomical traits and their value ranges are shown. Variables measured in the present study are in black and those hypothesized are in grey.

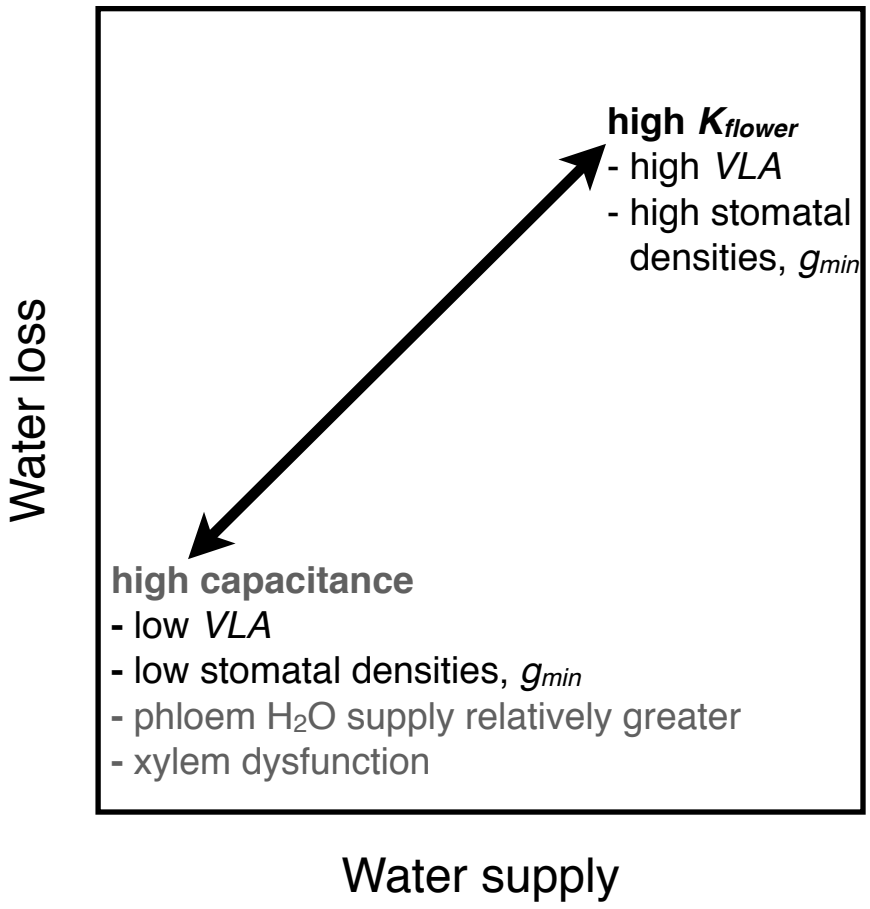

Table 1. List of species used in the current study and some structural and morphological traits.

Species	Family	Area ($x10^{-3}$ m^2)	Mass per area ($x10^{-3}$ g cm^{-2})	Perianth differentiation	Corolla fusion
Agapanthus africanus	Amaryllidaceae	1.07	2.63	monochlamydeous	fused
Amphilophium buccinatorium	Bignoniaceae	6.95	7.73	dichlamydeous	fused
Calycanthus chinensis	Calycanthaceae	9.08	4.86	graded tepals (monochlamydeous)	unfused
Calycanthus floridus	Calycanthaceae	2.53	5.68	graded tepals (monochlamydeous)	unfused
Calycanthus occidentalis	Calycanthaceae	4.91	15.42	graded tepals (monochlamydeous)	unfused
Camellia yunnanensis	Theaceae	4.92	NA	dichlamydeous	unfused
Cornus florida	Cornaceae	4.76	1.87	dichlamydeous	unfused
Hemerocallis sp.	Xanthorrhoeaceae	13.43	4.65	monochlamydeous	unfused
Illicium floridanum	Schisandraceae	2.70	3.88	graded tepals (monochlamydeous)	unfused
Illicium lanceolatum	Schisandraceae	0.96	9.04	graded tepals (monochlamydeous)	unfused
Illicium mexicanum	Schisandraceae	2.10	4.22	graded tepals (monochlamydeous)	unfused
Iris douglasiana	Iridaceae	5.30	1.88	monochlamydeous	unfused
Magnolia doltsopa	Magnoliaceae	22.69	NA	monochlamydeous	unfused
Magnolia grandiflora	Magnoliaceae	45.0	5.3	monochlamydeous	unfused
Magnolia soulangiana	Magnoliaceae	24.44	2.58	monochlamydeous	unfused
Magnolia stellata	Magnoliaceae	11.07	2.00	monochlamydeous	unfused
Paeonia suffruticosa	Paeoniaceae	80.45	3.57	dichlamydeous	unfused
Pyrus pashia	Rosaceae	2.62	NA	dichlamydeous	unfused
Rhododendron johnstoneanum	Ericaceae	4.52	2.20	dichlamydeous	fused
Rhododendron loderi	Ericaceae	16.08	1.96	dichlamydeous	fused

Species	Family	Area ($x10^{-3}$ m^2)	Mass per area ($x10^{-3}$ g cm^{-2})	Perianth differentiation	Corolla fusion
Rhododendron protistum	Ericaceae	8.24	2.92	dichlamydeous	fused

Table 2. Data sources for comparison of hydraulic conductance among plant structures.

Structure	Habitat	Source
Flowers	common garden	Current study
Magnolia grandiflora flowers	temperate	Feild et al. (2009)
Leaves	common garden	Simonin et al. (2012)
Leaves	temperate	Nardini and Salleo (2000); Sack et al. (2002); Nardini et al. (2005); Gullo et al. (2005); Scoffoni et al. (2008)
Leaves	tropical	Sack and Frole (2006)
Stems	desert	Divittorio (2014)
Stems	tropical	Brenes-Arguedas et al. (2011)

Chapter 3: Water relations of *Calycanthus* flowers: the roles of hydraulic conductance and capacitance

Introduction

The most conspicuous character of most angiosperms is the flower, a developmentally and morphologically complex structure whose primary function is to promote sexual reproduction (Specht and Bartlett 2009). Coevolution with animal pollinators has long been considered the primary selective agent responsible for the many, diverse forms apparent among angiosperm flowers (Sprengel 1793; 1996). Indeed, there are notable examples of coevolution between flowers and their animal pollinators (Fenster et al. 2004). Yet, floral adaptations to pollinators may not be as frequent as commonly considered, and non-pollinator agents of selection may also have influenced floral form and function (Herrera, 1996; Strauss and Whittall, 2006). Non-pollinator agents of selection, including the resource costs associated with building and maintaining flowers, can vary substantially among species and may be important factors influencing floral form and function. For example, the water costs of flowers can limit flower size and feedback to affect leaf function (Galen 1999; Galen et al. 1999; Lambrecht and Dawson 2007; Lambrecht 2013). The need to maintain water balance in diverse environments has led to coordinated shifts in hydraulic traits that may have given rise to a variety of hydraulic strategies among flowers (Chapters 2, 5).

The amount of resources required to produce and maintain flowers and how these resources are supplied and provisioned to flowers may be highly variable among species and habitats. There is large variation among species in the amount of water used by flowers during anthesis (Chapter 1; Roddy and Dawson 2012). This variation could be due to a number of causes, including environmental conditions and differences in functions performed by flowers. For example, higher temperatures, increased evaporative demand, and nectar secretion can cause both carbon and water requirements of flowers to increase (Patiño et al. 2002; Patiño and Grace 2002; De la Barrera and Nobel 2004). Similarly, the variability among species in the capacity to efficiently move water is greater for flowers than for stems and leaves, and there may have been important shifts early in angiosperm evolution that have caused such large variation among flowers (Chapter 2). This variation may be linked to the mechanisms of water transport to flowers, with early-divergent *Illicium* and *Magnolia* flowers hydrated predominantly by the xylem (Feild et al. 2009; Feild et al. 2009) and some eudicot flowers hypothesized to be hydrated by the phloem (Trolinder et al. 1993; Chapotin et al. 2003). Such large variation in whole flower hydraulic conductance (K_{flower}) and the mechanisms of water import further suggest that flowers may use a variety of hydraulic strategies to remain turgid during anthesis. Two of these strategies rely on constant water import throughout anthesis driven by water potential gradients. Gradients in water potential are created either by hydrostatic tension in the xylem or by the accumulation of osmolytes. Relying on hydrostatic tension in the xylem to drive water flow can efficiently move large amounts of water, but it depends on having cells and tissues that can withstand the negative tension required to establish the hydrostatic tension (Pittermann et al. 2006). While osmotic loading of cells is useful in driving water flow to maintain turgor, it can be an expensive process because of the energy requirements of actively loading osmolytes into cells. Furthermore, relying on osmotic gradients alone may not be able to drive sufficient amounts of water to offset transpirational losses if these losses are high. The third strategy for maintaining turgor would be to rely on water stored as capacitance that is discharged when cell and tissue water potentials decline. Water stored in a hydraulic capacitor can be imported early in development and slowly depleted during anthesis. This hydraulic capacitor may or may not be recharged by newly imported water, but the presence of a large hydraulic capacitor would nonetheless buffer water potential from changes in water content.

Species probably employ some combination of all three strategies, and the relative reliance on each strategy may vary among species and structures. Some flowers, particularly those of the ANITA grade and magnoliids, can move substantial amounts of water via their xylem networks (Chapter 2). These species tend to have traits associated with higher rates of water supply and loss and display water potential gradients indicative of xylem hydration (Feild et al. 2009; Feild et al. 2009). Other species, particularly those in the monocots and eudicots, have lower K_{flower}, traits associated with lower rates of water supply and loss, and may therefore rely on stored water during anthesis (Chapter 2). Indeed, eudicot flowers have much higher hydraulic capacitance than leaves, and the location of this stored water may be in extracellular mucilage (Chapotin et al. 2003). Importing water to flowers before anthesis and relying on this water to be depleted to maintain turgor could allow flowers to be somewhat uncoupled from stem water status and allow them to have less highly branched venation networks (Chapter 4; Roddy et al. 2013). Thus there may be tradeoffs between relying on hydrostatic tension, osmotic adjustment, and capacitance to maintain turgor. Similar patterns have been shown for stems, for which there is a tradeoff between structural avoidance of tension-induced embolism and reliance on capacitance to buffer xylem pressure declines caused by transpirational water loss (Meinzer et al. 2009; McCulloh et al. 2014).

In other studies of K_{flower} and hydraulic traits (Chapters 2, 4, 5), flowers of the genus *Calycanthus* consistently had traits associated with high rates of water supply (vein length per area), water loss (minimum epidermal conductance), and high hydraulic capacity (K_{flower}). Because *Calycanthus* flowers, particularly those of *C. occidentalis*, had among the highest values for these hydraulic traits, we wanted to better understand their water relations. We focused on two species of the genus *Calycanthus* (Calycanthaceae; Zhou et al. 2006), which differ morphologically and physiologically, with *C. occidentalis* having a significantly higher maximum K_{flower} than *C. chinensis* (Chapter 2). For all analyses we used leaves as a comparison for understanding the water relations of these early-divergent flowers. We quantified the diurnal patterns of water vapor exchange and water potential changes for flowers and, using pressure-volume relations, how this impacts flower drought tolerance. Having a high K_{flower} could help to minimize diurnal water potential declines and would mitigate the need to use stored water to maintain turgor. However, high capacitance would also help to mitigate water potential declines as the capacitor is discharged and may also exhibit a tradeoff with reliance on osmotic gradients to drive water flow.

Materials & Methods

Plant species, study site, and microclimate measurements

Between 5 and 25 May 2014, we studied three individuals of each of the two *Calycanthus* species growing in a common garden at the University of California Botanical Garden. Plants were kept well-watered throughout the study. The three *C. chinensis* individuals were growing in a more shaded microsite than the three *C. occidentalis* individuals. We characterized the microclimates and calculated vapor pressure deficit as (Buck 1981):

$$VPD = \left(0.61121 \times e^{\frac{17.502 * T_a}{T_a + 240.97}}\right)\left(1 - \frac{RH}{100}\right) \qquad \text{(eqn 1)}$$

where T_a and RH are air temperature (°C) and relative humidity (%), respectively. T_a and RH measurements were recorded every 5 minutes with Hobo U23 (Onset Corp., Bourne, MA) that was housed in a covered, white, PVC T-shaped tube and hung 2 m off the ground within 100 m of both species.

In the common garden, both species flower beginning in May. During this time they have flowers in all stages of development, with flowering peaking periodically. Flowers of both species

can last for a few days, during which time those of *C. occidentalis* are entered by and provide shelter for venturous beetles (Grant 1950). *C. occidentalis* tepals wilt and senesce starting at the tip moving towards the tepal base during anthesis. For all measurements, we sampled only newly opened flowers less than a day into anthesis. All analyses were performed using R (v. 3.0.2; R Core Team 2012) unless otherwise stated.

Diurnal measurements of gas exchange and water potential

We measured water vapor flux from entire flowers and parts of leaves of both species using an infrared gas analyzer equipped with a clear chamber (LI 6400 with LI 6400-05 conifer chamber, LI-COR Biosciences, Lincoln, NE). With this cuvette, leaf and flower temperatures were calculated based on energy balance, and the light level was not controlled. All measurements were made under ambient humidity and the reference CO_2 concentration set to 400 ppm. At each time period on each plant, we measured at least one newly opened flower and a subtending leaf. We waited until fluxes had stabilized before recording 5 instantaneous measurements and subsequently averaging these. On 5 May, we measured three *C. occidentalis* at predawn (4:00 to 6:00 am) and every three hours after dawn (8:30 am, 11:30 am, 2:30 pm, 5:30 pm) and *C. chinensis* individuals at predawn and midday (2:30 pm). Based on these data, the lowest daily water potentials and highest gas exchange rates occurred at midday (2:30 pm). Therefore, for measurements on 11 May, we chose to sample only at predawn and midday and to sample multiple flowers per plant at these two time periods. We combined data for the two days of measurements to determine the functional responses of g_s to the calculated vapor pressure gradient (VPG) between leaf or flower saturation vapor pressure and the atmospheric vapor pressure inside the gas exchange cuvette. We compared linear and two nonlinear models (power and logarithmic), and chose the models that best fit the data based on the residual sum of squares and Akaike's An Information Criterion (AIC).

On the evening prior to gas exchange measurements, we covered one leaf subtending each flower in plastic wrap and aluminum foil so that this leaf could be used to estimate stem water potential on the subsequent day. Immediately after gas exchange measurements, we wrapped the unfoiled leaf in plastic wrap, excised the foiled and unfoiled leaf and flower, and placed them into a plastic bag kept in a cool box. Within 5 minutes of excision, the balancing pressure was measured using a Scholander-style pressure bomb (SAPS, Soil Moisture Equipment Corp., Santa Barbara, CA, USA) with a resolution to 0.02 MPa. While inside the pressure chamber, leaves were kept covered by plastic wrap or plastic wrap and foil and flowers were wrapped in a plastic bag to prevent, as best as possible, desiccation inside the chamber during measurement. After water potential measurements, we transported the leaves and flowers to the lab and used a flatbed scanner and ImageJ (v. 1.47v) to estimate the surface area, which was then used to recalculate gas exchange rates. Predawn gas exchange measurements for *C. occidentalis* leaves on 5 May are not included, however, because these leaves were misplaced before their areas could be measured.

From gas exchange and water potential measurements, we calculated flower and leaf hydraulic conductance based on Darcy's law:

$$K = \frac{E}{\Delta\psi} \qquad \text{(eqn 2)}$$

where K is the hydraulic conductance (mmol m^{-2} s^{-1} MPa^{-1}), E is the transpiration rate (mmol m^{-2} s^{-1}) and $\Delta\Psi$ is the difference between stem and leaf or between stem and flower water potentials ($\Delta\Psi_{stem\text{-}leaf}$ or $\Delta\Psi_{stem\text{-}flower}$). This method assumes an approximate mass balance between water flow into the structure (driven by $\Delta\Psi$) and water loss from the structure (E).

Pressure-volume analysis

We determined the relationship between Ψ and relative water content (*RWC*) of 4-5 whole flowers and leaves per species using repeated measures of mass and Ψ (Tyree and Hammel 1972). Flowering shoots were collected early in the morning on cloudy days, as described above. Mass was recorded immediately before and after each water potential measurement and subsequently averaged, and 10-12 measurements were made on each specimen as they slowly desiccated. Specimens were then oven-dried at 60°C for a week to determine dry mass. From the pressure-volume curves, we determined the Ψ and RWC at the turgor loss point (Ψ_{TLP} and RWC_{TLP}) by a regression through at least 5 points of the linear part, the saturated water content per dry weight (SWC; g g^{-1}) from the linear extrapolation to the x-intercept of the Ψ vs. water mass relationship normalized to dry mass, the modulus of elasticity from the slope of the relationship between turgor pressure and RWC above the turgor loss point, capacitance (MPa^{-1}) and absolute capacitance (mol H_2O kg^{-1} dry mass MPa^{-1}) from the slope of the relationship between RWC and Ψ above the turgor loss point and the SWC. Extrapolation of these parameters was done in Microsoft Excel 2011, and differences between structures and species were analyzed using R. To test whether midday water potential declines are linked with hydraulic capacitance, we pooled data for species and structures and used standardized major axis regression to account for variance in both axes (the 'sma' function in the package *smatr*).

Stem hydraulic capacitance was calculated from water release curves of small chunks of small diameter (~1 cm) branches following previously published methods (McCulloh et al. 2014). Three individuals per species were sampled and five samples per species were used in the measurements. Samples were collected in the early morning, wrapped in wet paper towels, and kept refrigerated until analysis. All samples were vacuum infiltrated overnight in water. Excess water was removed from the samples by blotting them with paper towels, after which they were weighed and placed in screen cage thermocouple psychrometer chambers (83 series; JRD Merrill Specialty Equipment, Logan, UT, USA). Chambers were then triple-bagged and submerged in a cooler of water for 2-3 hours to allow equilibration between the sample and the chamber air. After equilibration, millivolt readings were recorded using a psychrometer reader (Psypro; Wescor, Logan, UT, USA). Samples were then removed from the chambers, weighed, and allowed to dry on the bench top for approximately 30 minutes before being returned to the chambers to repeat the measurements. The mV readings from the psychrometer reader were converted to MPa based on calibration curves from salt solutions of known water potentials. Samples were measured repeatedly until water potential values reached ~ -4 MPa, below which the psychrometers could not reliably resolve water potentials. Samples were dried in an oven for at least three days before weighing the dry mass. Relative water content (RWC) was calculated for each measurement and converted to relative water deficit (RWD) as 1 - RWC. The product of RWD and the mass of water per unit tissue volume at saturation (M_w) yielded the cumulative mass of the water lost for each measurement interval. M_w was calculated as:

$$M_w = \left(\frac{M_s}{M_d} \times \rho \right) - \rho \qquad \text{(eqn 3)}$$

where ϱ is wood density and M_s and M_d are the saturated and dry masses of the sample, respectively. The initial, linear phase of the plot of cumulative mass of water lost versus sapwood water potential gave the capacitance over the likely in situ physiological operating range of stem water potential (Meinzer et al. 2003; Meinzer et al. 2008). This regression of the initial linear phase was forced through the origin because of the physical impossibility of water being released at 0 MPa. How many of these initial points were used was similar to the method commonly used for analyzing pressure-volume curves of leaves. In this case, $-1/\Psi$ was plotted against the amount of water released, and the number of initial points of this curve determined by adding points until the

coefficient of variation declined. This final point was determined to be the inflection point on the moisture release curve, and capacitance was calculated as the slope of the regression between 0 and this inflection point on the plot of Ψ versus water released. Based on wood volume and density, hydraulic capacitance could be expressed in the same units as it is expressed for leaves and stems (mol H_2O kg^{-1} dry mass MPa^{-1}).

Water loss rates

At 11:45 am on 11 May, we excised three leaves and flowers per species to determine water loss rates. Cut surfaces were covered in petroleum jelly, and samples were weighed approximately every fifteen minutes on an electronic balance. Between measurements, samples were kept out of direct sunlight but not protected from ambient wind. Afterwards, specimens were scanned to determine surface area, and water loss rates were expressed as mmol m^{-2} s^{-1}. Water loss rates measured in this way are a combination of stomatal and cuticular conductances. After excision and as tissue water potential declines, stomatal closure would reduce the relative contribution of stomatal conductance to overall water loss rates. To determine the effects of species and structure (flower vs. leaf) on water loss rates, we used a repeated measures ANOVA with species and structure within time as the error term.

Results

Climate variation

The two measurements days (5 May and 11 May) differed in their atmospheric conditions (Figure 1). On 5 May, temperature peaked at midday at 21°C, while on 11 May temperature peaked in the early afternoon at 25°C. These differences corresponded to different diurnal courses of VPD. On 5 May, VPD peaked at 1.09 kPa, while on 11 May, VPD peaked at 2.41 kPa.

Water loss rates

Water loss rates of detached flowers and leaves allowed to desiccate under ambient conditions followed similar time courses but different absolute rates (Figure 2). At about 45 minutes after excision, water loss rates increased for flowers and leaves of both species, although the change was much larger for flowers. The average water loss rate of *C. occidentalis* leaves (0.23 mmol m^{-2} s^{-1}) was about 80% less than that of *C. occidentalis* flowers (1.14 mmol m^{-2} s^{-1}). Similarly, the average water loss rate of *C. chinensis* leaves (0.10 mmol m^{-2} s^{-1}) was about 86% less than that of *C. chinensis* flowers (0.71 mmol m^{-2} s^{-1}). Flowers of both species had higher water loss rates than leaves of both species (structure: $F = 62.69$, $P < 0.001$), and *C. occidentalis* leaves and flowers had higher water loss rates than leaves and flowers of *C. chinensis* (species: $F = 10.48$, $P < 0.01$). As a result, there was a significant interaction between species and structure ($F = 7.87$, $P < 0.01$). Flowers of both species had visibly wilted within 1 hour of excision.

Diurnal variation in water status and gas exchange

We measured diurnal variation in gas exchange and water potential on 5 May starting at predawn and continuing every three hours until 17:30 for *C. occidentalis* (Figure 3) and at predawn and midday for *C. chinensis*. Stomatal conductance and transpiration increased for both leaves and flowers throughout the day and peaked for both structures at 14:30. At this time, $g_{s,leaf}$ averaged 0.12 mmol m^{-2} s^{-1} and $g_{s,flower}$ averaged 0.09 mmol m^{-2} s^{-1}. Similarly, transpiration peaked at 14:30, averaging 1.26 and 0.81 mmol m^{-2} s^{-1} for leaves and flowers, respectively. At all time points, area-normalized gas exchange rates were higher for leaves than they were for flowers (Figure 3a,b). Similarly, leaf water potentials were always lower than both stem and flower water potentials (Figure 3c). Midday minimum water potentials were -0.93 and -0.77 MPa for leaves and flowers, respectively. The difference between stem and flower water potentials ($\Delta\Psi$) varied little during the

days, peaking at only 0.10 MPa at 14:30, in contrast to $\Delta\Psi_{stem\text{-}leaf}$ which increased from 0.10 MPa at predawn to 0.25 MPa at midday. As a result of high E relative to the low $\Delta\Psi$, K_{flower} was higher than K_{leaf} at all time points except the last (Figure 3d). In the early afternoon (14:30), when E was highest, K_{flower} averaged 14.45 mmol m^{-2} s^{-1} MPa^{-1} while K_{leaf} averaged 5.04 mmol m^{-2} s^{-1} MPa^{-1}. These measurements of K_{flower} based on the transpiration rate were generally lower than the maximum K_{flower} determined using the vacuum pump method (solid, horizontal line and shading in Figure 3d; Chapter 3). However, in the early afternoon K_{flower} of some *C. occidentalis* flowers equalled and exceeded the average maximum value for this species (18.79 mmol m^{-2} s^{-1} MPa^{-1}). In contrast, K_{leaf} peaked in the early evening (17:30) at 10.24 mmol m^{-2} s^{-1} MPa^{-1} despite lower E, driven mainly by low $\Delta\Psi_{stem\text{-}leaf}$.

Because g_s and E peaked for both leaves and flowers at 14:30, on 11 May, we subsequently measured gas exchange and water potentials at only these times for both *C. occidentalis* and *C. chinensis* (Figure 4). At predawn and midday, $g_{s,flower}$ was higher than $g_{s,leaf}$ for both species. Predawn $g_{s,flower}$ was twice as high as predawn $g_{s,leaf}$ for *C. occidentalis* and more than four times higher than $g_{s,leaf}$ for *C. chinensis*. At midday, $g_{s,flower}$ was more than twice as high as $g_{s,leaf}$ for *C. occidentalis* and six times higher than $g_{s,leaf}$ for *C. chinensis*. Similarly, midday E_{flower} was almost two times higher than midday E_{leaf} for *C. occidentalis* and almost four times higher than midday E_{leaf} for *C. chinensis*. Similar to measurements on 5 May, Ψ_{flower} tracked changes in Ψ_{stem} throughout the day, such that $\Delta\Psi_{stem\text{-}flower}$ only increased slightly for *C. occidentalis*. In contrast, $\Delta\Psi$ increased much more from predawn to midday for *C. occidentalis* leaves and for leaves and flowers of *C. chinensis* (Figure 4c). Interestingly, the change in $\Delta\Psi$ of leaves and flowers was very similar for *C. chinensis*. Consequently, K_{flower} increased more than threefold for *C. occidentalis*, but slightly decreased for *C. chinensis*. On this day, too, K_{flower} sometimes exceeded the average maximum value measured using the vacuum pump method for *C. occidentalis* flowers but not for *C. chinensis* flowers (Figure 4d). K_{leaf} increased throughout the day for *C. occidentalis* but even at midday was less than one-third the value of K_{flower} for this species. K_{leaf} changed little throughout the day for *C. chinensis* (Figure 4d).

Response of stomatal conductance to vapor pressure and light

We characterized the environmental drivers of transpiration from leaves and flowers. Pooling measurements across days, stomatal conductance ranged from 0.041 to 1.724 mmol m^{-2} s^{-1} for *C. occidentalis* leaves and from 0.032 and 0.483 mmol m^{-2} s^{-1} for *C. chinensis* leaves. Transpiration rates from flowers were sometimes higher than for leaves, ranging from 0.175 to 2.32 mmol m^{-2} s^{-1} for *C. occidentalis* flowers and from 0.140 to 0.694 mmol m^{-2} s^{-1} for *C. chinensis* flowers. The responses of leaf g_s to the vapor pressure gradient (VPG) between leaf and air was best modeled by a power function for *C. occidentalis* ($t = 2.0$, $P = 0.05$; Figure 5a). For *C. occidentalis* flowers, the relationship between g_s and VPG was best fit by a linear relationship ($R^2 = 0.36$, $t = 3.63$, $P < 0.05$; Figure 5c). No model significantly explained the response of leaf g_s to PAR (Figure 5b). For flowers, g_s was best fit by logarithmic equations (*C. occidentalis*: $t = 7.32$, $P < 0.001$; *C. chinensis*: $t = 9.27$, $P < 0.001$; Figure 5d).

Pressure-volume relations

We used water release curves and pressure-volume relations to characterize the drought responses of stems, leaves, and flowers (Figures 6-7). Based on the regression of water released versus stem water potential, *C. chinensis* stems had a higher capacitance than *C. occidentalis* (100.7 compared to 88.0 mol kg^{-1} MPa^{-1}; Figure 6). For both species, flowers wilted at higher water potentials than leaves, although this difference was significant only for *C. occidentalis* ($t = 4.73$, $df = 5.01$, $P < 0.01$; Figure 7a). However, leaves and flowers of each species did not differ in the relative water content at the turgor loss point, although RWC_{TLP} was higher for *C. chinensis* than for *C. occidentalis* (Figure 7b). Leaves and flowers differed significantly in their saturated water contents

(SWC; Figure 7c). For both species SWC was almost three times higher in flowers than in leaves, and SWC was higher in *C. chinensis* than in *C. occidentalis* (all pairwise $P < 0.001$). In contrast to stems, leaves and flowers of *C. occidentalis* tended to have higher absolute hydraulic capacitance than *C. chinensis* leaves and flowers. Flowers of both species had significantly higher absolute capacitances than their respective leaves ($P < 0.0001$), but there was no significant difference between species (Figure 7d).

We asked whether there were tradeoffs between the three hydraulic strategies among leaves and flowers of both species. Data for leaves and flowers were pooled together. There was no significant relationship between osmotic potential and either midday water potential gradients ($R^2 = 0.77$, $P = 0.13$; Figure 8a) or hydraulic capacitance ($R^2 = 0.70$, $P = 0.16$; Figure 8c). However, maintaining a higher hydraulic capacitance significantly reduced midday $\Delta\Psi$ across structures ($R^2 = 0.99$, $P < 0.01$; Figure 8b).

Discussion

Many species flower under adverse conditions, such as when water is limiting. Maintaining flowers despite these resource demands is critical for sexual reproduction in many species. Even species native to mesic habitats, such as *Calycanthus*, must support their flowers when atmospheric demand for water is high. We found that despite being well-watered and having among the highest K_{flower} of any species measured, *C. occidentalis* flowers visibly wilted by midday when VPD was high. Flowers were incapable of preventing water loss from outpacing water supply and that, given this supply deficit, there was insufficient water stored in flowers to supply their transpirational demands and remain turgid. Furthermore, the transpirational demands of flowers were, under some conditions, higher than those of adjacent leaves (Figure 4b).

Flower gas exchange

There was substantial variation between days in the gas exchange rates of flowers and leaves. During cooler, more humid conditions, leaf gas exchange rates were always higher than those of flowers (Figure 3). During hotter, drier conditions, in contrast, midday gas exchange rates of flowers exceeded those of leaves (Figures 4, 5). The highest midday rates of E_{flower} we measured were higher than E measured on flowers of other species (Blanke and Lovatt 1993; Galen et al. 1999; Patiño and Grace 2002; Feild et al. 2009). Only tepals of avocado (*Persea americana*), another magnoliid, had transpiration rates comparable to those we measured for *Calycanthus* flowers (1.2-1.3 mmol m^{-2} s^{-1}; Blanke and Lovatt 1993). In other species, leaves generally have higher E and higher xylem sap flow rates than flowers and inflorescences (Feild et al. 2009; Roddy and Dawson 2012; Chapter 1), and under cooler conditions *Calycanthus* flowers also have lower E than their subtending leaves.

The functional responses of g_s to VPG and light differed between leaves and flowers (Figure 5). Typical of the stomatal responses to vapor pressure deficit for other species, g_s declined rapidly for *Calycanthus* leaves with increasing VPG (Figure 5a). In contrast, g_s increased with increasing VPG for *C. occidentalis* flowers such that above ~1.5 kPa flower g_s exceed leaf g_s (Figure 5c). Despite increasing evaporative demand, floral stomata do not limit water loss but, rather, accelerate it. Similar linear increases in functional responses to VPG have been shown for Mediterranean *Cistus* species (Teixido and Valladares 2014). Why flower g_s may be so high is unclear but may be related to other physiological constraints. Maintaining a high g_s–and thus also E–would help to maintain floral temperatures below a critical, perhaps damaging, threshold temperature (Patiño et al. 2002; Patiño and Grace 2002). While calculated midday flower temperatures still approached 35°C, elevated transpiration rates were probably important in preventing flower temperature from going even higher. Even under stressful conditions, floral water loss is unregulated, which could help to

maintain reproductive investments under conditions when even vegetative physiology suffers (Galen et al. 1999). Given the relatively short lifespan of flowers and their relatively low surface area compared to leaves, at the whole plant level the water costs of flowers may still be small.

Water balance in Calycanthus *flowers*

Maintaining water balance may have been a critical constraint in floral evolution and diversification. The large variation among species in K_{flower} is coordinated with variation in traits associated with water supply and loss, suggesting that shifts in water balance traits have direct impacts on hydraulic capacity (Chapter 2). The relatively high values of K_{flower} for *Calycanthus* species further imply that these flowers may be capable of transporting enough water during anthesis to meet their transpirational demands. In addition to being able to move substantial amounts of water via the xylem (compared to flowers of other species), *Calycanthus* flowers were predicted to have higher hydraulic capacitance than leaves. As water potential drops, this stored water is discharged, which was thought to prevent further drops in water potential.

Despite having a comparatively high K_{flower} and high hydraulic capacitance, *Calycanthus* species were unable to prevent turgor loss under hot, dry, midday conditions (Figures 3, 4, 7). Declining water contents and potentials that lead to turgor loss result from an imbalance between water supply and water loss. The diurnal variation in g_s and E, and their functional responses to VPG and PAR, suggest that uncontrolled transpiration contributed to declining water content throughout the day. Perhaps even more importantly, hydraulic supply to flowers was limited. Throughout most of the day, K_{flower} was significantly below its potential maximum (Figure 3d). Such hydraulic underperformance was the most likely cause of turgor loss. Although K_{flower} came close to its maximum during midday and early afternoon (Figure 4d), it was already too late in the day to prevent Ψ_{flower} for *C. occidentalis* (-1.13 MPa) from falling below the Ψ_{TLP} (-1.03 MPa; Figure 7a), leading to visible wilting. Similarly, water potentials of *M. grandiflora* tepals also declined to the Ψ_{TLP} during hot, midday conditions (Feild et al. 2009). Despite reaching their lowest water potentials during midday, E and g_s for flowers also peaked at this time point (Figure 3). The resulting positive relationship between E and K is consistent with data from leaves, in which K increases with E to minimize the water potential gradient between stems and leaves (Simonin et al., in press). The present results suggest that diurnally variable K_{flower} may help to minimize $\Delta\Psi_{stem\text{-}flower}$. Indeed, *C. occidentalis*, which has a higher K_{flower} than *C. chinensis*, also experienced lower water potential declines relative to stem water potential (Figure 4c).

In addition to using newly imported water to supply transpiration and maintain water balance, flowers may also discharge stored water as water potential declines. Among both leaves and flowers of *Calycanthus*, increasing hydraulic capacitance minimized the water potential drawdown between stems and either flowers or leaves (Figure 8b). While not statistically significant, the positive relationship between capacitance and osmotic potential also implied that maintaining a high hydraulic capacitance was associated with less reliance on osmotic potential to drive water flux. Despite discharging 3-4 times more stored water per MPa than leaves and increasing K_{flower} throughout the day, *C. occidentalis* flowers could not avoid losing turgor. Flowers may fall at one end along an axis defined by resistance to embolism and reliance on capacitance to buffer water potential declines. Recent work has characterized how stems and, to some extent, leaves may vary along this axis (Meinzer et al. 2009; Johnson et al. 2011; McCulloh et al. 2014), and the current study is, to our knowledge, the first suggesting that flowers may as well.

Given that xylem transport of water to flowers during anthesis is low (Chapter 1; Roddy and Dawson 2012), flowers may recover from drought and rehydrate slowly, if at all. High hydraulic capacitances in flowers could further lengthen rehydration times because this large hydraulic capacitor would need to be recharged. Consistent with this prediction, water contents of *Viola tricolor* flowers, measured by terahertz time domain spectroscopy, increased much more slowly upon

rewatering after drought than did water contents of leaves (N. Born, unpublished data). While this suggests that these flowers are capable of being rehydrated, it also implies that they respond slowly to changes in xylem water potential.

Hydraulic autonomy of flowers

How hydraulically separate are reproductive organs from their subtending stems remains an open question. Having a high hydraulic capacitance may confer upon flowers transpirational autonomy from the stems over the short-term while still keeping them connected to the stem xylem for refilling over the longer term. Our results for *Calycanthus* flowers agrees with those from *I. anisatum* and *M. grandiflora* suggesting that flowers are connected to the stem xylem during anthesis but disagrees with suggestions by others that flowers can remain more well-hydrated than stems leaves (Trolinder et al. 1993; Chapotin et al. 2003; Feild et al. 2009; 2009b). However, data unequivocally supporting reverse Ψ gradients between stems and flowers has been reported only for inner whorl tepals of *M. grandiflora* (Feild et al. 2009). Other implications of phloem hydration of flowers have drawn this conclusion based only on Ψ gradients between leaves and flowers showing flowers to be more well-hydrated than leaves (Trolinder et al. 1993; Chapotin et al. 2003), a result identical to those of the current study and others (Feild et al. 2009; 2009a). Although these authors have argued that if Ψ_{flower} is higher than Ψ_{leaf} then water may flower from flowers to leaves (Chapotin et al. 2003), they have ignored the fact that water would have to flow from flowers to leaves by way of stems, which generally have higher, less negative water potentials than both leaves and flowers. Furthermore, our results show that flowers can have higher, less negative water potentials than leaves and still maintain higher g_s and E than leaves (Figures 3-5). Only in the case of *M. grandiflora* inner whorl tepals were water potentials higher than those of subtending stems (Feild et al. 2009). Hydrating flowers via the phloem would be one strategy for hydraulically isolating flowers from variation in Ψ_{stem}, but there remains little conclusive data supporting this phenomenon. A more likely scenario, as I have described here and elsewhere (Chapter 2), is that flowers maintain a high hydraulic capacitance, which minimizes $\Delta\Psi_{stem\text{-}flower}$. If capacitance is high enough and Ψ_{stem} low enough, it may be possible for Ψ_{flower} to by less negative than Ψ_{stem}, in which case water may flow from flowers back into the stem. While some fruits may serve as hydraulic capacitors that supply water back to the stem under certain conditions (Johnson et al. 1992; Higuchi and Sakuratani 2006), there is no clear evidence that this happens in flowers. Yet, building structures with high hydraulic capacitance would be one way of providing reproductive structures with some autonomy from the water status of the rest of the plant. How and when this water may be delivered to reproductive structures is unclear. While some water undoubtedly is delivered to developing flowers and fruits by the phloem (Choat et al. 2009; Clearwater et al. 2013), more recent measurements using magnetic resonance imaging show that, in contrast to previous studies, most of the water in developing tomatoes is imported via the xylem and not the phloem (Windt et al. 2009). Until similar studies are conducted on flowers, the dynamics of water flow to and, potentially, from flowers will remain a mystery.

Conclusions

The evolution of the flower was one of the hallmarks of angiosperm success. Despite the importance of flowers to reproduction, relatively little is known about their physiology and water relations. Here we show that *Calycanthus* flowers can have significantly higher rates of stomatal conductance and transpiration than their subtending leaves, particularly during hot, dry conditions when water is prioritized to flowers rather than leaves. Despite having among the highest hydraulic conductance of any flowers measured and despite increasing their hydraulic conductance to its maximum throughout the day in response to increasing atmospheric demand for water, *Calycanthus* flowers are sometimes unable to remain turgid and wilt by midday. This suggests that floral

hydraulic architecture is not optimized for the extreme conditions encountered on particularly hot, dry days. Like other species of early-divergent angiosperm lineages with undifferentiated leaf-like tepals, *Calycanthus* flowers remain hydraulically connected to the stem xylem. Yet, these flowers rely heavily on discharging stored water to minimize the water potential gradient from stem to flower, perhaps because their structurally weak vascular system cannot tolerate large water potential gradients. These complex dynamics between different hydraulic strategies could have important implications for our understanding of floral ecology and evolution.

Figure 1. Diurnal variation in air temperature, relative humidity, and VPD during the two days of measurements.

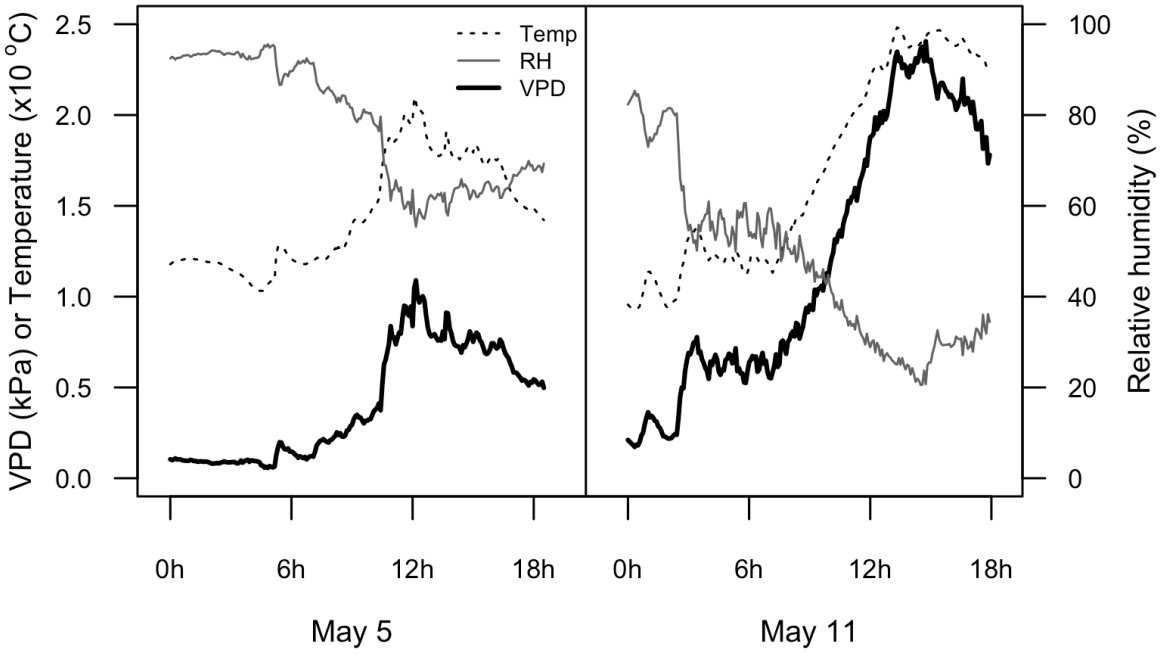

Figure 2. Water loss rates of excised flowers and leaves of the two *Calycanthus* species.

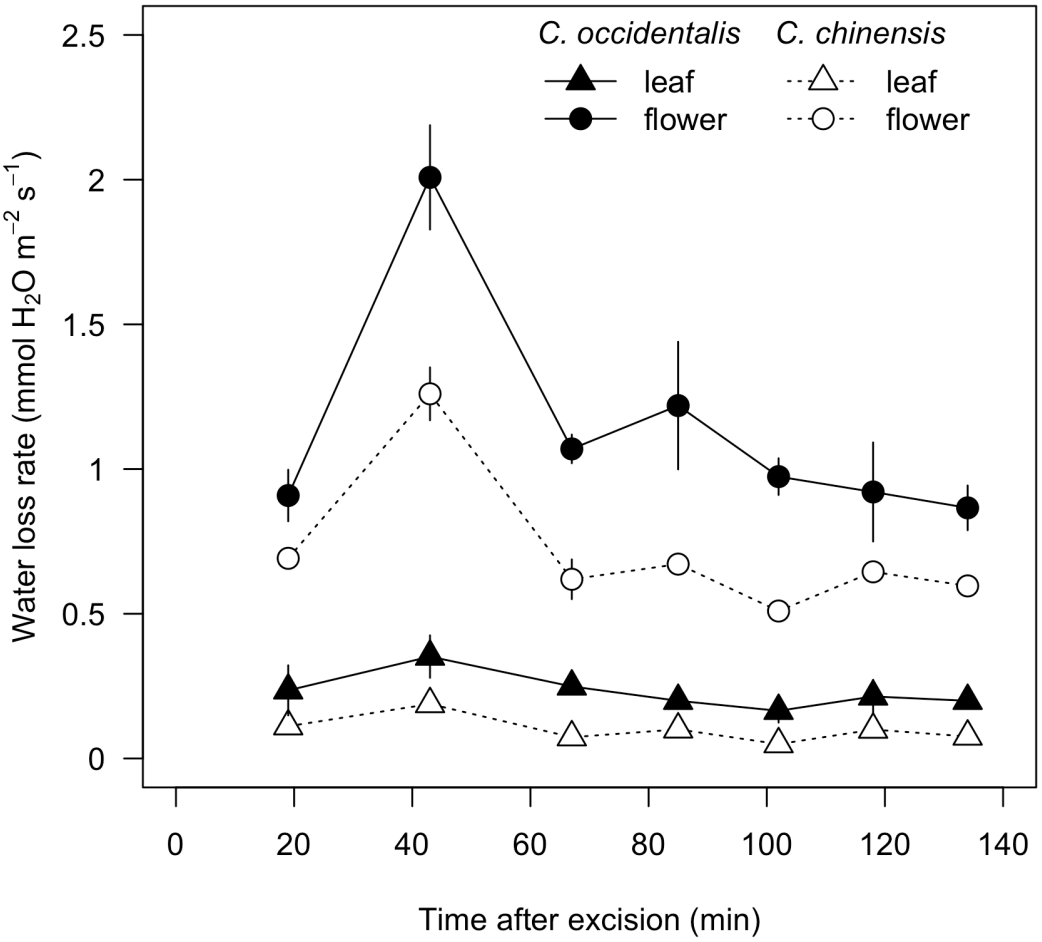

Figure 3. Diurnal measurements of (a) stomatal conductance, (b) transpiration, (c) water potential, and (d) hydraulic conductance on 5 May for *C. occidentalis*. Error bars represent standard error. Slight jitter in the horizontal axis as been added so that points and error bars do not overlap. In (d), the horizontal line and shading represent the average and standard error, respectively, of maximum K_{flower} for *C. occidentalis* as measured in Chapter 3.

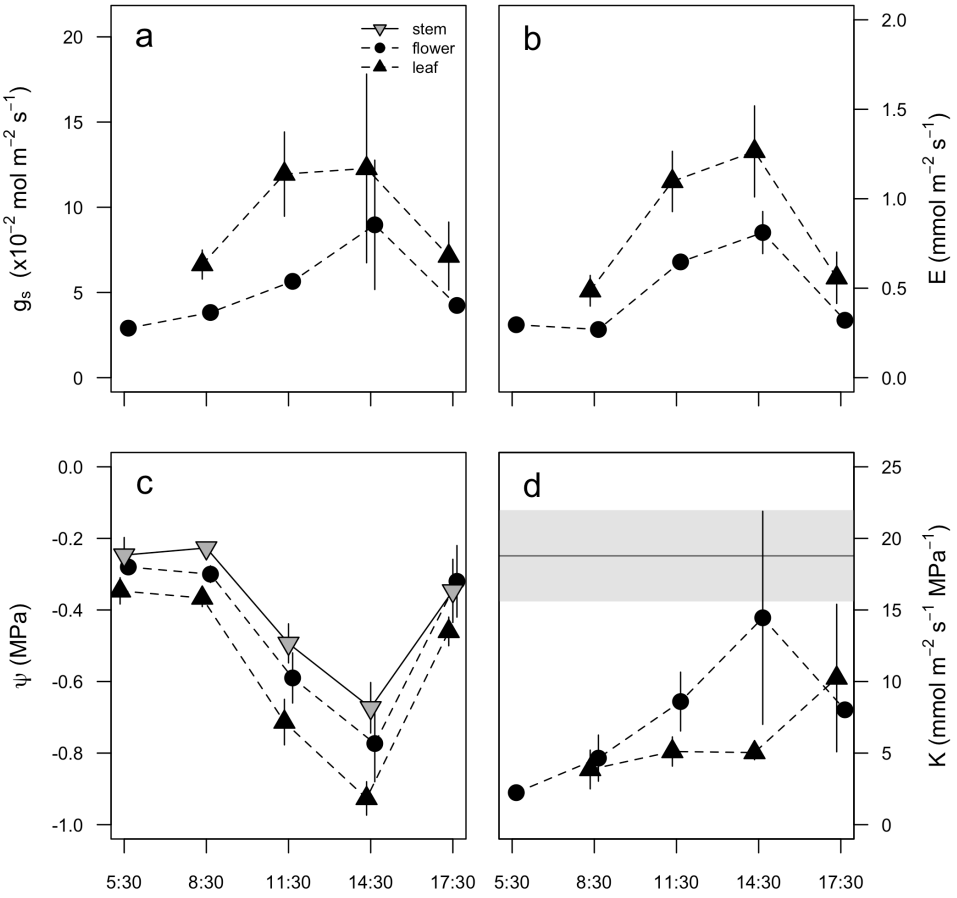

Figure 4. Predawn and midday measurements of (a) stomatal conductance, (b) transpiration, (c) water potential, and (d) hydraulic conductance of leaves and flowers for two *Calycanthus* species on 11 May. In (d), the horizontal lines and shading represent the averages and standard errors, respectively, of maximum K_{flower} for *C. occidentalis* (solid) and *C. chinensis* (dotted) from Chapter 3.

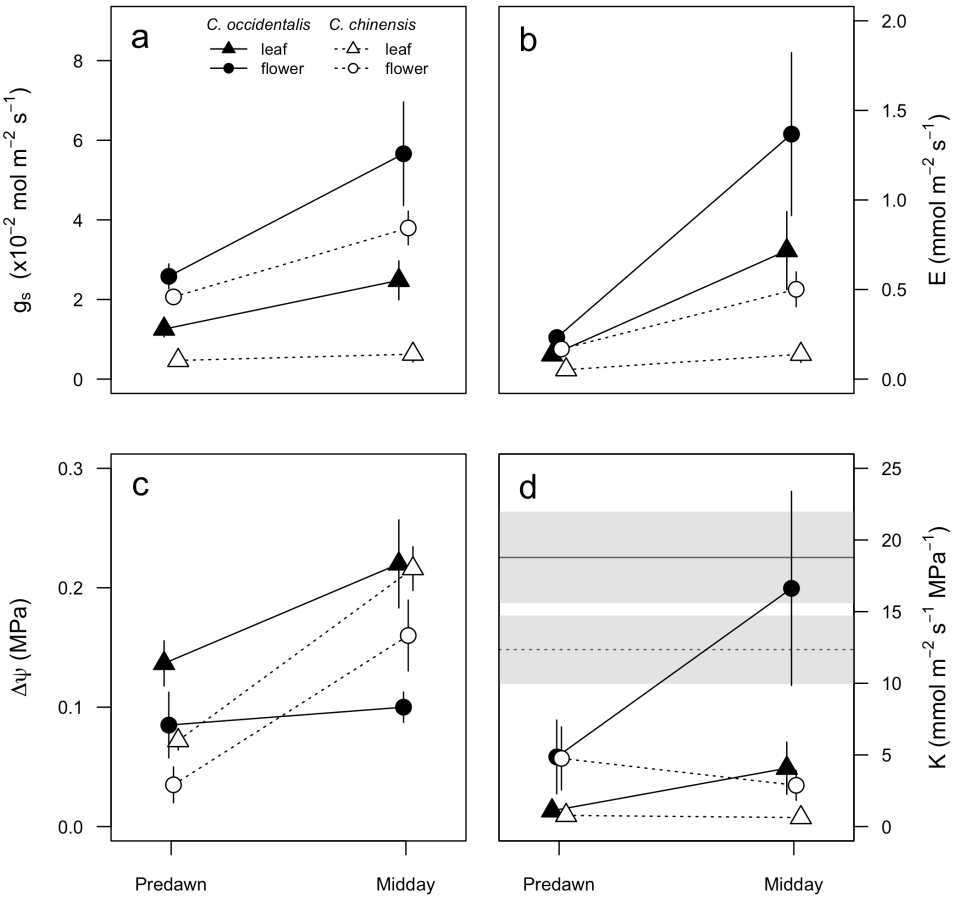

Figure 5. The responses of stomatal conductance for (a,b) leaves and (c,d) flowers to the vapor pressure gradient driving transpiration and to light. Only lines for significant relationships are plotted. Note the different scales of g_s used for leaves and for flowers.

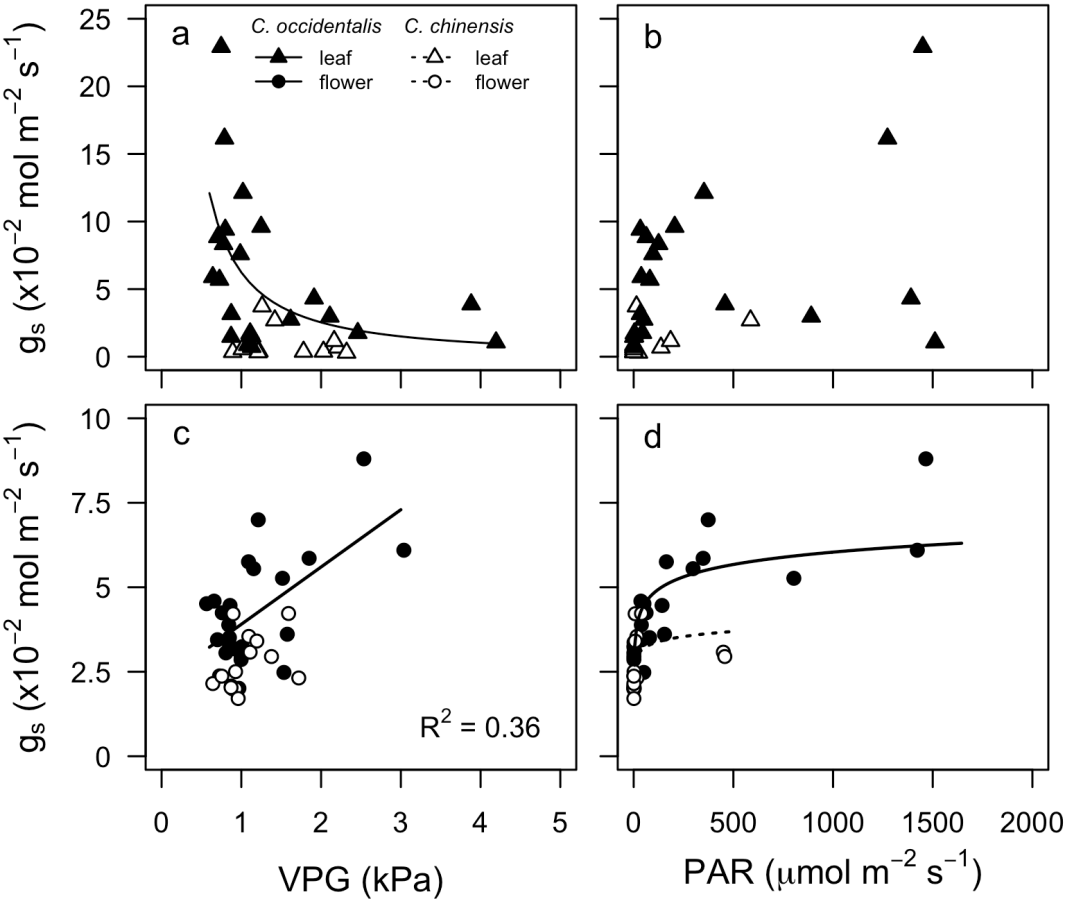

Figure 6. Stem water release curves for (a) *C. occidentalis* and (b) *C. chinensis*. Regression lines for the initial linear phases were forced through the origin because no water can be released at $\Psi = 0$. Values of capacitance (mol H_2O kg^{-1} dry mass MPa^{-1}) are shown in the plot.

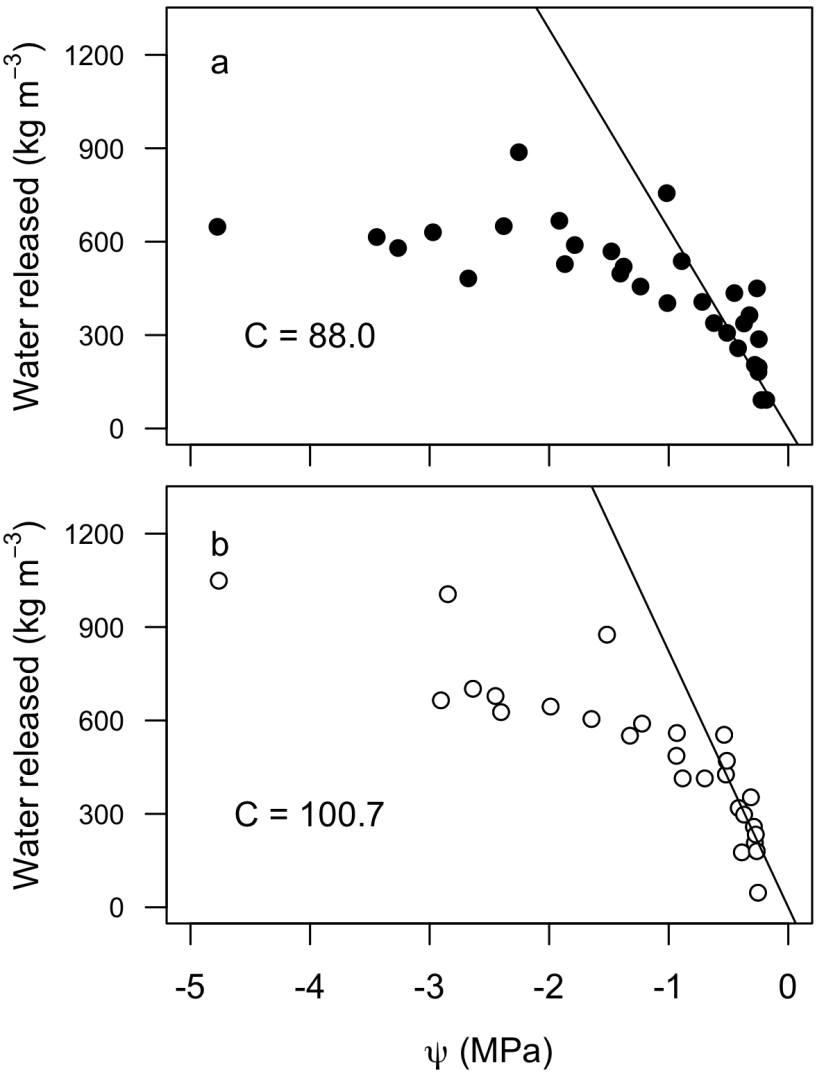

Figure 7. Parameters derived from the pressure-volume relationship for leaves and flowers of the two *Calycanthus* species: (a) water potential at the point of turgor loss, (b) relative water content at the point of turgor loss, (c) saturated water content relative to tissue dry mass, (d) hydraulic capacitance expressed as moles of water per kg dry mass per MPa. For comparison, stem capacitance values calculated in Figure 6 are plotted as filled squares in (d).

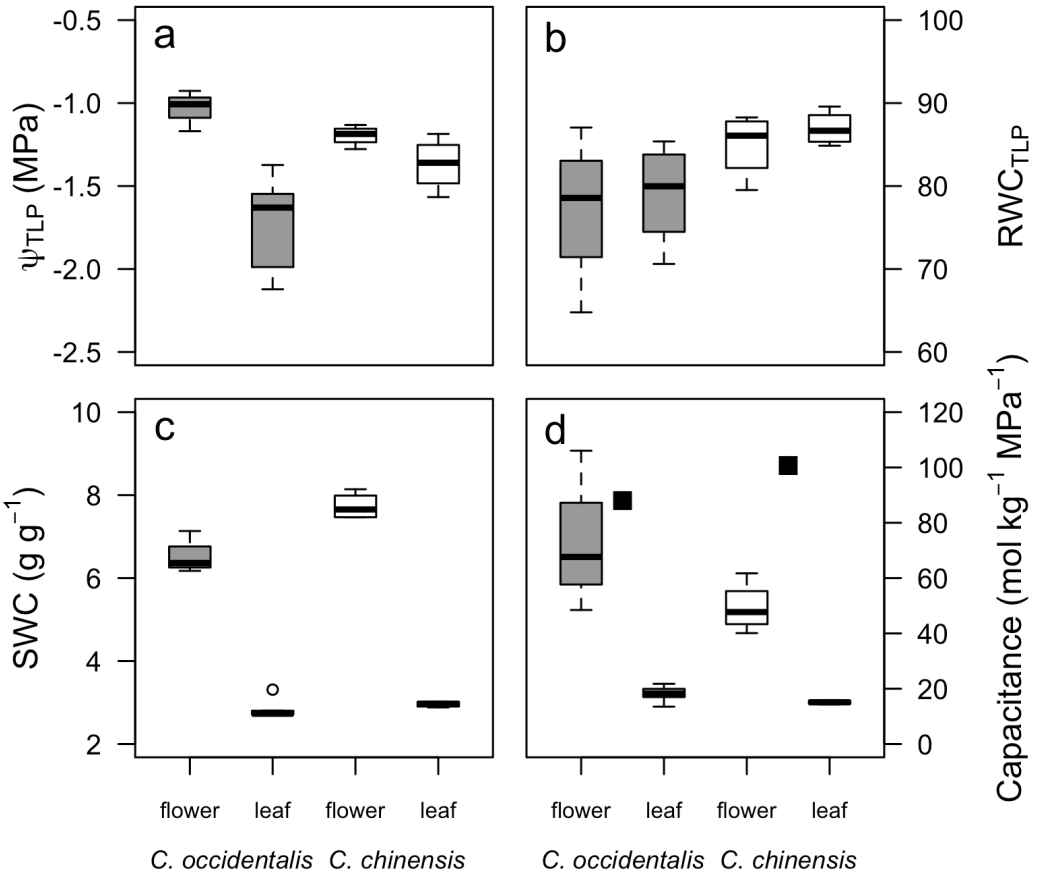

Figure 8. Tradeoffs between the three hydraulic strategies for leaves and flowers. (a) Relationship between midday $\Delta\Psi$ ($\Delta\Psi_{stem\text{-}leaf}$ or $\Delta\Psi_{stem\text{-}flower}$) and Ψ_s. (b) Relationship between midday $\Delta\Psi$ and hydraulic capacitance. (c) Relationship between Ψ_s and hydraulic capacitance. Significant relationships are shown by regression lines and R^2.

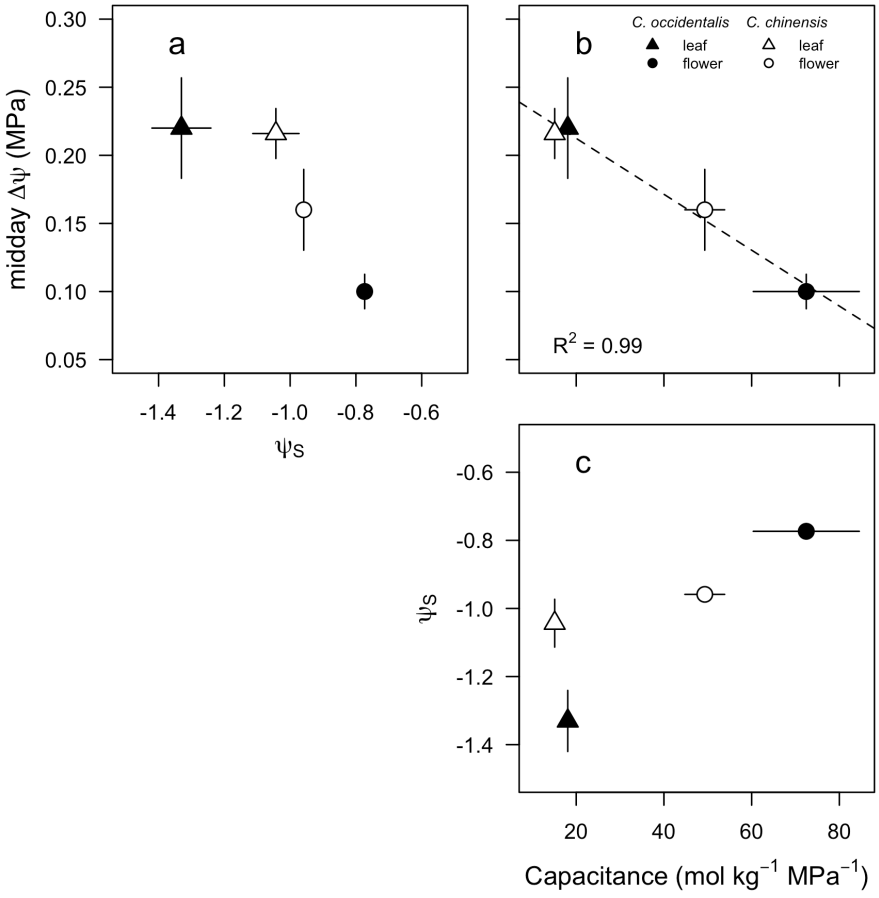

Chapter 4: Uncorrelated evolution of leaf and petal venation patterns across the angiosperm phylogeny

A version of this chapter has been previously published and is reproduced here with permission:

Roddy A.B., Guilliams C.M., Lilittham T., Farmer J., Wormser V., Pham T., Fine P.V.A., and Dawson T.E. 2013. Uncorrelated evolution of leaf and petal venation patterns across the angiosperm phylogeny. *Journal of Experimental Botany* 64:4081-4088.

Introduction

Evolution of the modern angiosperm flower represents an innovation that has reverberated across ecosystems globally. Flowers have coevolved with specialized pollinators, contributing to early angiosperm success and to increases in animal diversification (Thien et al. 2000; Hu et al. 2008; Thien et al. 2009). While major insights about developmental evolution in early angiosperms have focused primarily on flowers (Bowman 1997; Soltis et al. 2007; Endress 2011; Mathews and Kramer 2012; Zhang et al. 2012), understanding floral evolution in the broader context of whole-plant physiology could reveal new sources of selection acting on plant reproduction. For example, constraints on reproductive investment influence vegetative architecture, such as branch ramification (Harris and Pannell 2010) and leaf size (Bond and Midgley 1988).

Despite their unique developmental processes, flowers and leaves are subject to the same environmental and resource limitations, requiring carbon and water to be supplied throughout development. As a result, tradeoffs exist between investments in vegetative and reproductive structures (Bazzaz et al. 1987; Reekie and Bazzaz 1987a-c). While some flowers may be able to contribute substantially to the carbon costs of reproduction (Bazzaz and Carlson 1979; Bazzaz et al. 1979; Galen et al. 1993), water must be supplied to flowers and fruits by roots and stems, potentially at the cost of vegetative function (Nobel 1977; Galen et al. 1999; Lambrecht and Dawson 2007; Lambrecht 2013). Thus, understanding the ecophysiological mechanisms of floral water balance may reveal new insights into the ecology and evolution of flowers (Galen 2000; Chapotin et al. 2003; Feild et al. 2009a,b).

Despite the influence of floral water balance on vegetative physiology (Galen et al. 1999; Galen 2000), reproductive development (Patiño and Grace 2002) and pollinator attraction and manipulation (Bertsch 1983; von Arx et al. 2012), surprisingly little work has focused on understanding the water dynamics of flowering. In general, larger flowers within a species require more water (Galen et al. 1999), but xylem sap flow rates through flower-bearing branches are highly variable among species (Chapter 1; Roddy and Dawson 2012). How flowers are plumbed into the vegetative system probably varies among species as well. Some authors assumed that higher, less negative water potentials of flowers compared to leaves means flowers are hydrated by the phloem (Trolinder et al. 1993; Chapotin et al. 2003). In contrast, blooming (anthesis) flowers of extant, early-diverging angiosperm lineages are hydrated by the xylem (Feild et al. 2009a,b), which may be why these flowers wilt and die even under slight droughts. The distinction between phloem and xylem hydration is complicated because in one early-diverging extant lineage, *Magnolia grandiflora*, water potential gradients indicate that the inner whorl of tepals are phloem hydrated while the outer whorls are xylem-hydrated (Feild et al. 2009). Supplying water via the phloem rather than the xylem during anthesis may allow flowers to access a greater level of hydraulic autonomy and release from drought stress occurring in the rest of the plant, potentially facilitating pollinator attraction under otherwise adverse conditions. Phloem-hydration may also indicate low water requirements of flowers because flux rates through the phloem are much lower than those through the xylem.

In leaves and leaf homologues, such as sepals and petals, xylem and phloem are organized into vascular bundles or veins. One of the major advances among early angiosperm lineages compared to non-angiosperms was the development of densely veined leaves, expressed as the amount of vein length per unit of leaf surface area (Feild and Arens 2007; Brodribb and Feild 2010). Increased vein length per area (VLA; also commonly referred to as 'vein density') brings xylem-based liquid water closer to the sites of evaporation and carbon fixation inside the leaf. Such increased hydraulic supply capacity yields a greater capacity for transpiration and photosynthesis (Sack and Frole 2006; Brodribb et al. 2007). Based on Cretaceous fossil angiosperm leaves as well as on phylogenetic reconstructions across extant basal lineages, angiosperm VLA is estimated to have increased nearly threefold during the first 30-40 million years of angiosperm diversification (Brodribb and Feild 2010; Feild et al. 2011). Increasing the upper limit of leaf VLA allowed angiosperms to assimilate carbon and accumulate biomass more rapidly than non-angiosperms, perhaps facilitating their ecological domination beginning in the Cretaceous (Brodribb and Feild 2010).

How floral venation influences floral water balance and evolution, however, remains unexamined. Because flowers generally require less water than leaves (Blanke and Lovatt 1993; Higuchi and Sakuratani 2005; Feild et al. 2009; Lambrecht et al. 2011; Roddy and Dawson 2012), selection may have acted in different directions on petal and leaf venation. In contrast to selection for increased water transport capacity in leaves, selection probably favored reduced water transport in flowers. Alternatively, modular developmental processes could have buffered floral hydraulic traits from the strong selection for increased VLA in leaves. Unlike leaves, most petals do not synthesize substantial amounts of carbon, mitigating the need for high transpiration rates normally requisite for maintaining high rates of photosynthesis. If petals and leaves experienced different constraints on their water balance, then their hydraulic traits may have evolved independently and may be developmentally modular and possibly also functionally modular. Developmental modularity would occur if the underlying developmental processes causing vein branching frequency, and thus VLA, were different for flowers and leaves. Alternatively, correlated evolution of leaf and petal VLA would suggest that a common developmental program underlies VLA throughout the plant bauplan. In this case, the strong selective advantage of high VLA in leaves carried along petal VLA by overwhelming any selection for low petal VLA. Thus, any reduction in the water requirements of flowering may not be reflected in petal VLA, a trait more associated with water supply than water loss. Whether petal VLA decreased while leaf VLA increased depends on the extent to which floral and foliar VLA experienced selection in different directions.

In the present study, we examine VLA evolution in flowers and leaves across the angiosperm tree of life and test three main hypotheses. First, because flowers generally require less water than leaves, we predicted that floral structures possess lower VLA than associated leaves. Second, because flowers of more recently derived angiosperm species may be phloem-hydrated, we hypothesized that flowers of these species would have lower VLA than flowers of basal angiosperm lineages. Third, although patterns of venation in different structures are related in many lineages (Melville 1960; 1969), we hypothesized that if flowers and leaves experienced different selection regimes for water transport capacity, then flower and leaf VLA evolved independently.

Materials and Methods

Sampling

The majority of sampled taxa were collected from living specimens in the University of California Botanical Garden and the Tilden Botanical Garden, both in Berkeley, CA. Collecting primarily from common gardens ensured that species were well-watered and had grown in similar environmental conditions. We targeted plants with large, recently opened flowers on exposed, sunlit branches and collected flowers and fully expanded leaves from one to three individuals per species.

Other early-diverging lineages were sampled from natural populations in the field (see Table 1). Despite the diversity of our sampling, there remain three large phylogenetic gaps in our dataset, the graminoid monocots, the Asteraceae, and the Orchidaceae. Although these groups account for a substantial amount of all angiosperm diversity, their floral morphologies are markedly different from most other clades. Furthermore, species with small, wind-pollinated flowers were largely excluded.

Leaves and flowers were collected simultaneously and transported to the lab for sample processing. Approximately 1-cm^2 sections were taken from midway between the leaf midrib and margin, midway between the base and tip of the leaf and placed in 2-4% NaOH for clearing. Except for the field-collected specimens, we did not remove the leaf epidermis before imaging. Because of the high variability in vein density within a petal, we collected multiple 1-cm^2 sections from all parts of the petals and sepals and placed them in 2-4% NaOH. For structures that were smaller than 1-cm^2, we placed the entire petal or sepal into NaOH for clearing. For all structures, sections were taken from multiple leaves or flowers per species and pooled into one vial for each structure of each species. After 2-4 weeks, leaves were briefly washed in dH_2O, transferred to a 3% bleach solution for a few minutes, washed again in dH_2O, and then placed into 95% EtOH. Sepals, petals, and tepals were similarly transferred to EtOH, except that most of them did not require clearing for as long, nor did they require bleaching to complete the clearing process. Once in EtOH, most samples were quickly stained with Safranin O. Except for the few field-collected samples, we used a Leica DM2500 microscope outfitted with a Nikon DS-Fi1 camera at 5x-20x. We captured 1-2 images per section from each of 5-12 sections per species. Vein densities were measured using ImageJ (v. 1.44o; Rasband 2012) and averaged. Based on our estimates, at least five samples needed to be measured to reduce the variance to within 5% of the mean of 20 fields (data not shown).

Statistical and comparative analyses

To perform analyses of trait evolution, we grouped some structures together based on their presumed function and on their trait values. Sepals, bracts, and outer whorl tepals did not differ significantly in VLA and are collectively referred to here as "sepals." Petals, hypanthia, and inner whorl tepals of basal angiosperms did not differ significantly in their vein densities and were grouped together and are referred to as "petals." Differentiated perianths have evolved as many as six times among the angiosperms (Zanis et al. 2003), and distinct petals may be derived either from stamen-like structures or bract- or leaf-like structures (Irish 2009). These distinctions, like our groupings of structures, are based on morphological characters, such as the number of vascular traces. To determine whether VLA differed between structures, we used a linear mixed-effects model that treated plant structure (leaf, sepal, petal, flower) as a fixed effect and plant structure nested within species as a random effect. We used Bonferroni-adjusted, Tukey post-hoc, pairwise comparisons to compare VLA between plant structures, using the *glht* function in R (v. 2.14.1; R Core Team 2012). To compare differences in vein density between major clades, we used ANOVA with Tukey post-hoc comparisons to estimate pairwise differences in vein density between clades. For all subsequent phylogenetic analyses, we used ln-transformed vein densities.

We obtained a phylogenetic supertree of our sampled taxa using the online version of Phylomatic (Webb and Donoghue 2005). The resulting undated ultrametric tree was imported into Phylocom 4.2 (Webb et al. 2008) so that recent node age estimates could be written into the tree file using the *bladj* function. We obtained node age estimates for as many nodes as possible in our undated supertree from Bell et al. (2010). Note that *bladj* was used primarily to write these node age estimates into our tree file, rather than to anchor a few nodes and evenly distribute the remaining, unanchored nodes. This dated supertree is poorly resolved for recent divergences (e.g. divergences within genera) but represents, we believe, the best approach to analyzing trait evolution on such a phylogenetically broad dataset. Polytomies in this tree were resolved by adding short branches that represented approximately 1 million years.

Because we lacked measurements for some structures of some species, trees were pruned to include only tips with non-missing data in both traits for each pairwise trait comparison. Phylogenetic independent contrasts (PICs; Felsenstein 1985) were calculated using the *pic* function in the package *ape* for R (v. 2.14.1; R Core Team 2012). PICs quantify the amount of trait disparity that occurs at each node in a phylogeny based on the trait values of the descendent taxa or nodes and the branch lengths between the parent and daughter nodes. PICs are a way to control for the non-independence of sampling related lineages. Independent contrast methodology allows one to test whether two traits repeatedly coevolve in a coordinated way. For example, a significant, positive correlation between PICs for two traits would mean that large divergences in one trait repeatedly occur at the same nodes as large divergences in the second trait. Thus, significant correlations between PICs of two traits are commonly used to determine whether two traits have undergone correlated evolution. The conservative, nonparametric Spearman rank test was used to test for pairwise correlations between ln-transformed traits and for pairwise correlations between PICs. All reported P-values have been adjusted for the number of simultaneous comparisons using the Bonferroni correction.

Results

In total, our dataset includes 132 species from 90 genera and 52 families (Table 1). Plant structure was a significant predictor of VLA ($F = 133.79$, $P < 0.0001$), and all pairwise, post-hoc, Bonferroni-adjusted comparisons were also highly significant (all pairwise $P < 0.0001$; Figure 1). Leaf VLA ranged from 1.09 for *Disporopsis pernyi* to 12.68 for *Calycanthus occidentalis* mm mm^{-2}, sepal VLA ranged from 0.50 for *Smilacina stellata* to 12.70 mm mm^{-2} for *Scutellaria californica*, and petal VLA ranged from 1.00 for *Disporopsis pernyi* to 6.65 mm mm^{-2} for *Calystegia stebbinsii*. Despite substantial overlap in the ranges of VLA for these three structures, mean leaf VLA (5.47 mm mm^{-2}; $P < 0.001$) was significantly higher than mean sepal VLA (3.78 mm mm^{-2}; $P < 0.001$), which was higher than mean petal VLA (2.44 mm mm^{-2}; $P < 0.001$).

Some clades differed significantly in their VLA values (Figure 2). Tukey post-hoc analyses showed that monocot leaf VLA was significantly lower than leaf VLA of the Ranunculales, fabids, malvids, and asterids (all pairwise $P < 0.001$). While slightly higher than the monocots, leaf VLA of basal angiosperms fell within the lower tails of the ranges for all the other major clades. Sepal VLA showed similar patterns to leaf VLA. Tukey post-hoc analyses showed fabid, malvid, and asterid sepal VLA to be significantly higher than monocot sepal VLA (all pairwise $P < 0.001$). Malvid sepal VLA was also marginally higher than Ranunculales sepal VLA ($P = 0.088$). However not all of these comparisons of sepals are of homologous structures. Interestingly, there were no significant differences between any pairwise clade comparisons of petal VLA, although the sampled non-graminoid monocots had generally lower petal VLA than the other major clades.

All pairwise correlations between ln-transformed traits were also significant (Figure 3A-C); species with higher leaf VLA generally also had higher sepal and petal VLA. The highest correlation coefficient was between leaves and sepals ($r = 0.57$, $df = 84$, $P < 0.001$). Leaf and petal VLA ($r = 0.34$, $df = 102$, $P < 0.001$) were more strongly correlated than sepal and petal VLA ($r = 0.32$, $df = 90$, $P < 0.01$). However, correlations of independent contrasts showed somewhat different patterns (Figure 3D-F). There was no significant correlation between leaf and petal contrasts ($r = 0.13$, $df = 102$, $P = 0.19$), although there were significant correlations between leaf and sepal VLA contrasts ($r = 0.40$, $df = 84$, $P < 0.001$) and between sepal and petal VLA contrasts ($r = 0.27$, $df = 90$, $P < 0.05$). These patterns of correlations observed between traits and PICs across the entire phylogeny were consistent with cladewise trait and PIC correlations. In particular, no clade showed a significant correlation between leaf and petal VLA contrasts (data not shown).

Discussion

Our results strongly support the idea that VLA has evolved independently in petals and leaves (Figure 3), demonstrating that vegetative and reproductive organs are developmentally modular. Furthermore, because VLA is so critical to water supply in leaves, flowers and leaves may also be physiologically modular. These results support observations that flower and fruit water status can remain relatively unaffected by large variation in plant water status (Trolinder et al. 1993).

Consistent with our first hypothesis, floral structures exhibited significantly lower VLA than leaves (Figure 1). In particular, mean petal VLA was less than half that of leaf VLA. The maximum measured leaf and sepal VLA values were similar, reflecting the functional similarities of many leaves and sepals. However, the maximum petal VLA was approximately half that of either leaves or sepals. In leaves, a high VLA is associated with higher efficiency because it enables higher rates of transpiration and photosynthesis per unit leaf area and because conduits in leaves with high VLA have higher intrinsic hydraulic conductance (Brodribb et al. 2007; Feild and Brodribb 2013). In contrast, a low VLA in non-photosynthetic petals may translate into higher efficiency because less water and carbon are needed for a given floral display area. However, if the intrinsic hydraulic conductance of petals is associated with VLA as it is in leaves, then the carbon costs of a high VLA in petals may not be that large. Recent work on petal development in *Arabidopsis thaliana* suggests that leaf and petal shape may be controlled by variations on the same underlying developmental process. Such commonality may constrain the range of possible forms in both structures while allowing selection to act on each structure independently (Sauret-Güeto et al. 2013), therefore producing often similar venation patterns in different structures (Melville 1960; 1969).

Our second hypothesis that basal angiosperm flowers developed higher VLA than flowers of more recently derived eudicot lineages was not supported (Figure 2). The average and maximum vein densities of basal angiosperm tepals were not any higher than those of petals from the other major clades. Such a result is perhaps not surprising because early-divergent angiosperm lineages (i.e. Austrobaileyales) possess very low leaf VLA (Feild et al. 2009; Boyce et al. 2009). The difference between leaf and tepal VLA among basal lineages (Austrobaileyales and magnoliids) and the monocots was much smaller than the difference between leaf and petal VLA of the more recently derived eudicot clades (Figure 2). Leaf VLA of these more recently derived lineages increased dramatically during the Cretaceous (Boyce et al. 2009; Brodribb and Feild 2010), leading to large differences between leaf and petal VLA. Thus, in contrast to our hypothesis, selection may not necessarily have favored reductions in petal VLA. Rather, petals may not have been exposed to the strong selection for high VLA in leaves if different developmental processes give rise to leaf and petal VLA.

The large range of petal VLA among the eudicots may reflect the greater diversity of ecological contexts in which these species exist compared to the magnoliids and Austrobaileyales (Feild et al. 2009). Among the eudicots there was remarkable variation in petal VLA even within some genera, further supporting the evolutionary lability of this trait. Alternatively, the large range of petal VLA among all eudicot clades may reflect the myriad developmental origins of the petal (Zanis et al. 2003). Petals are derived from stamen-like structures (andropetaloidy) in some lineages or from bract- or leaf-like structures (bracteopetaloidy) in other lineages (Irish 2009). Apart from their often similar gross morphologies, stamen-derived and bract-derived petals may differ in some key anatomical or physiological traits.

Although petals of reportedly phloem-hydrated eudicot flowers (Trolinder et al. 1993; Chapotin et al. 2003) and *Magnolia* tepals have lower VLA than xylem-hydrated *Magnolia* tepals (Feild et al. 2009), there were no significant differences in petal VLA between major clades (Figure 2C), implying that petal VLA may not reliably indicate xylem- versus phloem-hydration. Despite reports that a variety of fruits (Ho et al. 1987; Greenspan et al. 1994; Dichio et al. 2002) and some flowers (Trolinder et al. 1993; Chapotin et al. 2003) are phloem-hydrated, there is no general consensus on the frequency of phloem-hydration of flowers. Furthermore, reports of phloem-hydration of

flowers have been equivocal. Flowers have not been shown to be more well-hydrated than subtending stem xylem nor is it clear whether maintaining higher water potentials of flowers compared to subtending stems requires hydration by the phloem. Interestingly, recent work on grapes (Choat et al. 2009) and tomatoes (Windt et al. 2009), both of which were previously reported as being phloem-hydrated (Ho et al. 1987; Greenspan et al. 1994), has shown that phloem-delivered water may buffer fruit water status from variation in xylem import rather than supplying the predominant amount of water to the fruit. The water supply dynamics of flowers and fruits may be more complicated than the simplistic model of hydration by either the xylem or the phloem, and water may flow bidirectionally to and from reproductive organs (Johnson et al. 1992). For example, while xylem sap flows toward mango (*Mangifera indica*) inflorescences during the day (Higuchi and Sakuratani 2005), xylem sap flows away from developing fruits during the day and toward them at night (Higuchi and Sakuratani 2006).

Our third hypothesis that VLA has evolved independently in flowers and leaves was also mostly supported by our results (Figure 3D-F). Patterns of venation in petals and leaves have been thought to be correlated with venation patterns in leaves (Melville 1960; 1969). Indeed, our results show that when not controlling for phylogeny, all pairwise correlations of VLA traits were highly significant. However, phylogenetic independent contrast correlations were not similarly significant. The stronger correlation between sepal and leaf contrasts than between sepal and petal contrasts suggests that functional constraints may trump developmental constraints. These nuanced results illustrate the interplay between evolution, development, and physiology. We speculate that sepal and bract VLA have evolved with both leaves and petals because sepals and bracts commonly perform vegetative functions, such as photosynthesis and protecting the developing flower, yet develop at the same time as reproductive structures. These results generally support the idea of functional modularity between vegetative and reproductive structures (Figure 3E; Berg 1959; 1960). Despite the expectation under the Berg hypothesis that selection should favor stronger correlations among floral traits than between floral and leaf traits, our results showed that sepal VLA contrasts and leaf VLA contrasts were more strongly correlated than were sepal and petal VLA contrasts (Figure 3D,F). Such a result may be expected if the function of VLA is different in petals than it is in sepals and leaves. For example, phloem-hydration of petals may alleviate the need for veins to function for water transport, as they likely do in sepals and leaves.

Studies of morphological trait variation have shown similar results and have highlighted the genetic basis for reproductive and vegetative modularity. In *Dalechampia scandens*, floral bract length was more coupled to variation in floral traits related to pollination than it was to variation in leaf traits, including leaf size (Pélabon et al. 2011). Quantitative trait loci mapping of leaf and flower size traits in *Arabidopsis thaliana* showed large, positive genetic correlations among either flower or leaf traits, but not between flower and leaf traits (Juenger et al. 2005). The degree to which floral and foliar traits are decoupled may vary unpredictably among species (Armbruster et al. 1999; Hansen et al. 2007) and may depend on the traits in question. Many of these studies, including those of Berg (1959; 1960), have focused on variation in the size and shape of flowers with little regard for physiological traits. Though they may share developmental motifs that define the ranges of possible variation, physiological traits of leaves and petals may arise from uncorrelated selection pressures.

Conclusions

New insights into the water relations of reproduction are transforming our understanding of angiosperm evolution and plant water transport (Higuchi and Sakuratani 2005; 2006; Feild et al. 2009; Feild et al. 2009). In the present study, we used a novel dataset to address long-standing questions about the comparative evolution of flower and leaf traits, focusing on vein length per area, a trait functionally important to leaves and that evolved rapidly among angiosperm lineages

(Brodribb and Feild 2010; Feild et al. 2011). Despite increased leaf VLA among recently derived angiosperm lineages, petal VLA has evolved independently and has remained relatively low. These results suggest that vegetative and reproductive structures may be developmentally modular. Future studies characterizing the linkages between floral physiological traits, such as VLA or stomatal density, and hydraulic functioning throughout a flower's lifespan would further refine our understanding of the evolution and ecophysiology of flowers.

Figure 1. Boxplot of VLA for leaves, sepals, and petals. All pairwise differences are highly significant ($P < 0.001$). Median values are indicated by the heavy line in the middle of the boxes.

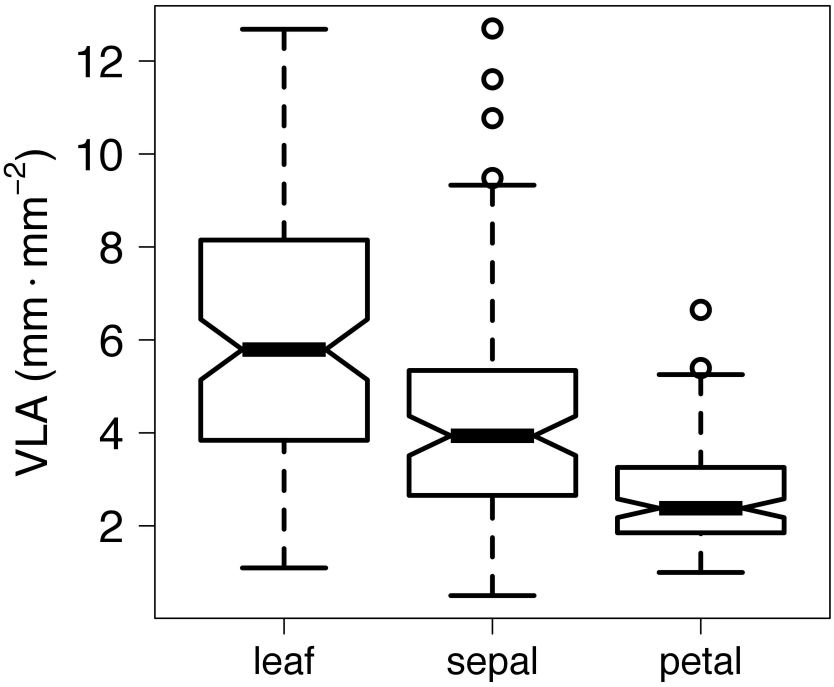

Figure 2. Boxplots of VLA for (A) leaves, (B) sepals, and (C) petals for each major clade included in this study ('basal' = magnoliids and Austrobaileyales, 'mono' = monocots, 'Ran' = Ranunculales, 'malv' = malvids, 'ast' = asterids). See Table 1 for list of species in each clade.

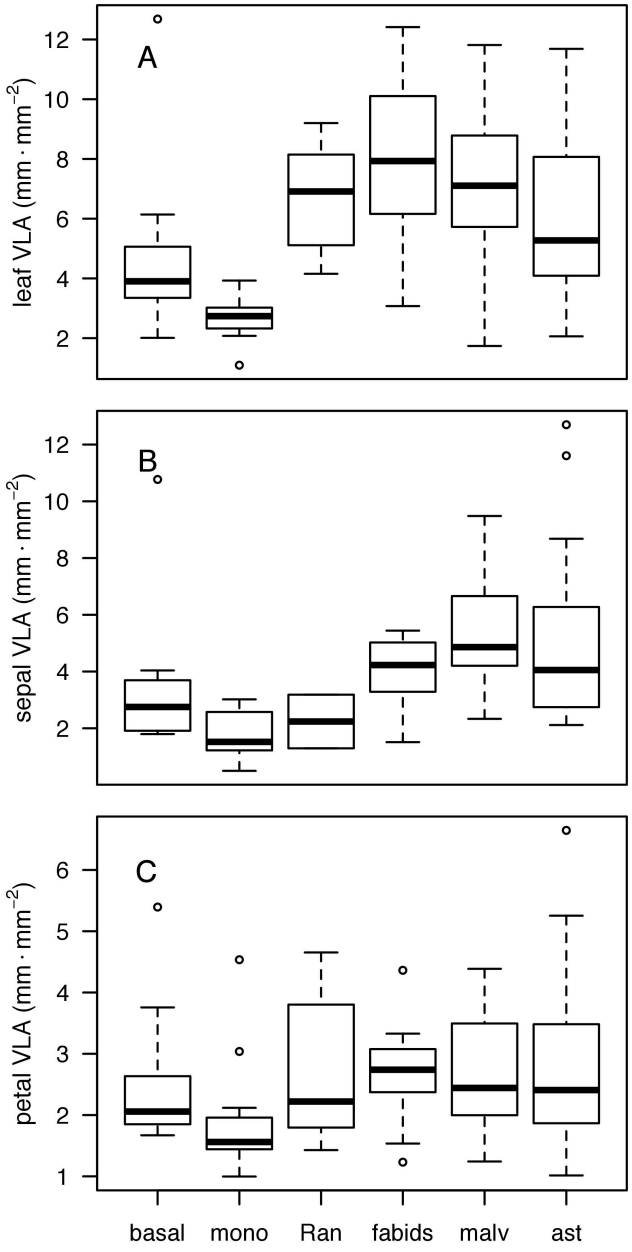

Figure 3. Pairwise (A-C) trait and (D-F) phylogenetically independent contrast correlations. Correlation coefficients and P-values are shown for statistically significant correlations based on Spearman rank tests.

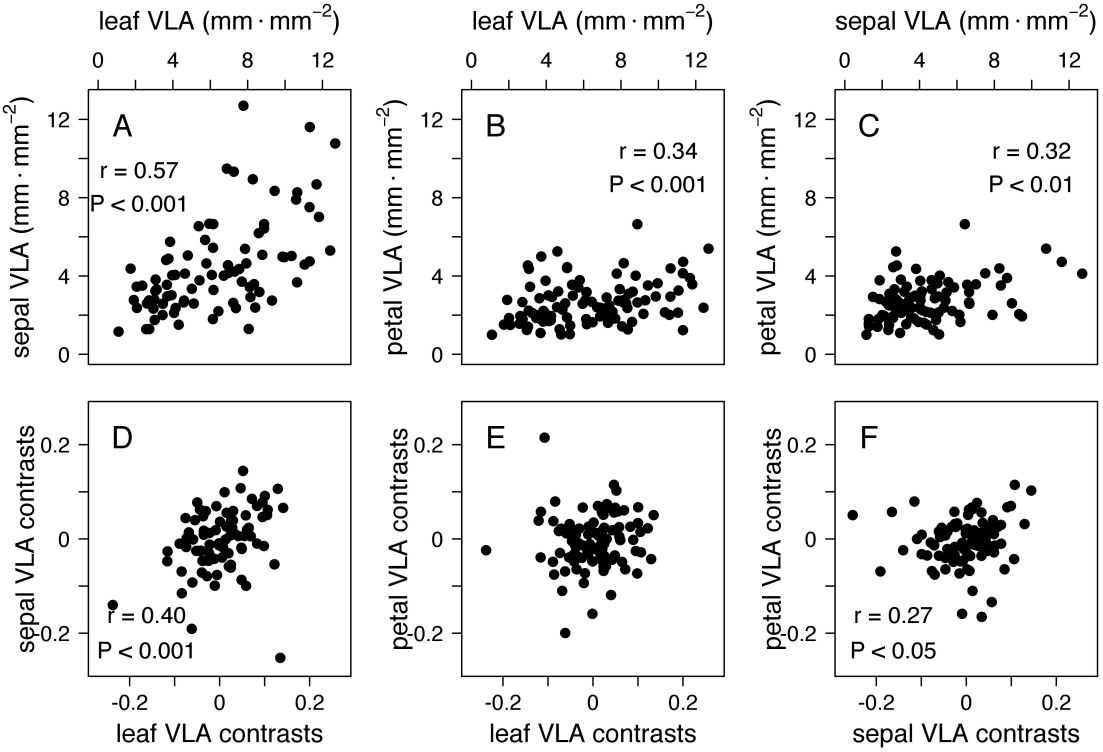

Table 1. List of species, their families, their major clade, and their collection sites analyzed in this study. 'UCBG' = University of California Botanical Garden, 'TBG' = East Bay Regional Parks Botanic Garden at Tilden. Species with no clade listed were not included in the cladewise comparisons

Species	**Family**	**Location**	**Clade**
Adenophora sp.	Campanulaceae	UCBG	asterids
Aesculus californica	Sapindaceae	UCBG	malvids
Anemopsis californica	Saururaceae	TBG	basal
Antirrhinum multiflorum	Plantaginaceae	TBG	asterids
Aquilegia shockleyi	Ranunculaceae	UCBG	Ranunculales
Aristolochia californica	Aristolochiaceae	UCBG	basal
Asarina sp.	Plantaginaceae	UCBG	asterids
Austrobaileya scandens	Austrobaileyaceae	Souita Falls, Queensland, Australia	basal
Baptisia tinctoria	Fabaceae	UCBG	fabids
Berberis darwinii	Berberidaceae	UCBG	Ranunculales
Bergenia crassifolia	Saxifragaceae	UCBG	
Calochortus vestae	Liliaceae	TBG	monocots
Calycanthus occidentalis	Calycanthaceae	UCBG	basal
Calystegia malacophylla	Convolvulaceae	UCBG	asterids
Calystegia stebbinsii	Convolvulaceae	TBG	asterids
Canella winteriana	Canellaceae	Key Largo, FL, USA	basal
Carpenteria californica	Hydrangeaceae	UCBG	asterids
Ceratostigma plumbaginoides	Plumbaginaceae	UCBG	asterids
Chaenomeles speciosa	Roasaceae	UCBG	fabids
Cistus incanus	Cistaceae	UCBG	malvids
Cistus laurifolius	Cistaceae	UCBG	malvids
Clarkia amoena	Onagraceae	TBG	malvids
Clarkia concinna	Onagraceae	UCBG	malvids
Clarkia rubicunda	Onagraceae	TBG	malvids
Clarkia sp.	Onagraceae	UCBG	malvids
Clarkia unguiculata	Onagraceae	UCBG	malvids
Clematis heracleifolia	Ranunculaceae	UCBG	Ranunculales
Clematis hexapetala	Ranunculaceae	UCBG	Ranunculales
Datura wrightii	Solanaceae	TBG	asterids
Dendromecon harfordii	Papaveraceae	UCBG	Ranunculales
Dendromecon rigida	Papaveraceae	TBG	Ranunculales
Deutzia prunifolia	Hydrangeaceae	UCBG	asterids
Dicentra formosa	Papaveraceae	TBG	Ranunculales
Disporopsis pernyi	Convallariaceae	UCBG	monocots
Drimys winteri	Winteraceae	Cultivated, Knoxville, TN, USA	basal
Dudleya attenuata	Crassulaceae	UCBG	
Dudleya caespitosa	Crassulaceae	UCBG	
Dudleya densiflora	Crassulaceae	UCBG	
Dudleya edulis	Crassulaceae	TBG	
Dudleya viscida	Crassulaceae	UCBG	
Epilobium angustifolium	Onagraceae	TBG	malvids

Epilobium canum	Onagraceae	UCBG	malvids
Erica glandulosa	Ericaceae	UCBG	asterids
Erysimum capitatum	Brassicaceae	TBG	malvids
Erythronium multiscapideum	Liliaceae	UCBG	monocots
Eschscholzia californica	Papaveraceae	UCBG	Ranunculales
Fremontodendron californicum	Malvaceae	UCBG	malvids
Fuchsia splendens	Onagraceae	UCBG	malvids
Galvezia speciosa	Plantaginaceae	TBG	asterids
Geranium californicum	Geraniaceae	UCBG	malvids
Geranium goldmanii	Geraniaceae	UCBG	malvids
Geranium himalayense	Geraniaceae	UCBG	malvids
Greyia radlkoferi	Melianthaceae	UCBG	malvids
Hastingsia serpentinicola	Asparagaceae	UCBG	monocots
Hebe macrocarpa	Scrophulareaceae	UCBG	asterids
Heuchera maxima	Saxifragaceae	UCBG	
Hosta hypoleuca	Liliaceae	UCBG	monocots
Houttuynia cordata	Saururaceae	UCBG	basal
Hydrangea macrophylla	Hydrangeaceae	UCBG	asterids
Hydrangea paniculata	Hydrangeaceae	UCBG	asterids
Hydrangea serrata	Hydrangeaceae	UCBG	asterids
Hydrangea villosa	Hydrangeaceae	UCBG	asterids
Hypericum patulum	Hypericaceae	UCBG	fabids
Illicium anisatum	Illiciaceae	Cultivated, Auburn, AL, USA	basal
Illicium lanceolatum	Schisandraceae	UCBG	basal
Incarvillea arguta	Bignoniaceae	UCBG	asterids
Iris douglasiana	Iridaceae	UCBG	monocots
Kadsura longipedunculata	Schisandraceae	Cultivated, Auburn, AL, USA	basal
Keckiella cordifolia	Scrophulariaceae	UCBG	asterids
Kirengeshoma palmata	Hydrangeaceae	UCBG	asterids
Lavatera assurgentiflora	Malvaceae	UCBG	malvids
Lepechinia fragrans	Lamiaceae	UCBG	asterids
Lilium formosanum	Liliaceae	UCBG	monocots
Lilium humboldtii	Liliaceae	TBG	monocots
Lilium pardalinum	Liliaceae	UCBG	monocots
Limnanthes vinculans	Limnanthaceae	UCBG	malvids
Lobelia laxiflora	Campanulaceae	UCBG	asterids
Lupinus arboreus	Fabaceae	UCBG	fabids
Lupinus propinquus	Fabaceae	TBG	fabids
Lupinus sp.	Fabaceae	UCBG	fabids
Magnolia sp.	Magnoliaceae	UCBG	basal
Malacothamnus palmeri	Malvaceae	TBG	malvids
Mimulus aurantiacus	Phrymaceae	UCBG	asterids
Mimulus clevelandii	Phrymaceae	TBG	asterids
Mimulus moschatus	Phrymaceae	TBG	asterids
Monochaetum tenellum	Melastomataceae	UCBG	malvids
Oenothera elata	Onagraceae	UCBG	malvids
Paeonia lactiflora	Paeoniaceae	UCBG	

Pelargonium capitatum	Geraniaceae	UCBG	malvids
Penstemon sp.	Plantaginaceae	UCBG	asterids
Phacelia bolanderi	Boraginaceae	UCBG	asterids
Philadelphus lewisii	Hydrangeaceae	UCBG	asterids
Photinia beauverdiana	Rosaceae	UCBG	fabids
Pickeringia montana	Fabaceae	UCBG	fabids
Polygala virgata	Polygalaceae	UCBG	fabids
Potentilla gracilis	Rosaceae	UCBG	fabids
Rhododendron ciliipes	Ericaceae	UCBG	asterids
Rhododendron cyanocarpum	Ericaceae	UCBG	asterids
Rhododendron davidsonianum	Ericaceae	UCBG	asterids
Rhododendron griersonianum	Ericaceae	UCBG	asterids
Rhododendron lyi	Ericaceae	UCBG	asterids
Rhododendron occidentale	Ericaceae	UCBG	asterids
Rhododendron sp.	Ericaceae	UCBG	asterids
Rhododendron tosaense	Ericaceae	UCBG	asterids
Ribes sanguineum	Grossulariaceae	UCBG	
Ribes speciosum	Grossulariaceae	UCBG	
Romneya coulteri	Papaveraceae	UCBG	Ranunculales
Rosa californica	Rosaceae	TBG	fabids
Rosa nutkana	Rosaceae	UCBG	fabids
Rosa wichuraiana	Roseaceae	UCBG	fabids
Salvia greggii	Lamiaceae	UCBG	asterids
Salvia karwinskii	Lamiaceae	UCBG	asterids
Salvia microphylla	Lamiaceae	UCBG	asterids
Salvia spathacea	Lamiaceae	TBG	asterids
Scutellaria californica	Lamiaceae	UCBG	asterids
Senna sp.	Fabaceae	UCBG	fabids
Sidalcea malviflora	Malvaceae	UCBG	malvids
Sidalcea setosa	Malvaceae	TBG	malvids
Sidalcea sparsifolia	Malvaceae	UCBG	malvids
Sinocalycanthus chinensis	Calycanthaceae	UCBG	basal
Smilacina stellata	Asparagaceae	UCBG	monocots
Solanum hispidum	Solanaceae	UCBG	asterids
Solanum umbelliferum	Solanaceae	UCBG	asterids
Styrax odoratissimus	Styracaceae	UCBG	asterids
Takhtajania perrieri	Winteraceae	Ajanaharibe-Sud, Madagascar	basal
Tecoma stans	Bignoniaceae	UCBG	asterids
Toxicoscordion micranthum	Melanthiaceae	UCBG	monocots
Trillium chloropetalum	Melanthiaceae	UCBG	monocots
Viburnum carlesii	Adoxaceae	UCBG	asterids
Viola glabella	Violaceae	UCBG	fabids

Chapter 5: Hydraulic traits of flowers: the maintenance of water balance, correlated evolution, and natural selection

Introduction

Arguably the greatest innovation of the angiosperms was the flower. Its appearance among early angiosperms provided new dimensions in which angiosperms could both innovate and diversify that had been largely unoccupied by other plants. Present day floral diversity among the angiosperms is remarkable and has long been attributed to the coevolutionary relationships between flowers and their pollinators (Sprengel 1793; Darwin 1859; Stebbins 1970). Close matching between floral structures and pollinator mouth parts and/or body parts has provided strong evidence that plants and their pollinators have undergone coordinated shifts in morphology (e.g. Whittall and Hodges 2007). Moreover, empirical tests of plant-pollinator coevolution have largely supported these observations and have shown that shifts in floral character states are often accompanied by shifts in pollination biology that can lead to character displacement, genetically isolated populations, and diversification (Fenster et al. 2004; Hopkins and Rausher 2011; Hopkins and Rausher 2012). Yet, mounting evidence suggests that non-pollinator agents of selection may also have important effects on floral evolution, either opposing selection by pollinators or reinforcing it (Herrera, 1996; Strauss and Whittall, 2006). Non-pollinator agents of selection incorporate the biophysical and/or physiological axes of selection such as the energy associated with acquiring the resources to produce flowers and the physiological costs of maintaining them throughout the reproductive phase. Understanding how these costs may vary among species could provide new perspectives on floral ecology and evolution and help to explain patterns of diversity.

One resource that is critically important to a plants and their flowers is water. Water is needed for cell and tissue expansion throughout bud development, to produce nectar to attract pollinators, to keep floral structures turgid and on display, and to replace water lost via transpiration throughout the entire lifespan of the flower. Water limitation can impact floral morphology by reducing flower size and display area, effectively opposing pollinator selection (Galen et al. 1999; Galen 2000; Lambrecht and Dawson 2007). Yet, the water requirements of flowers and the mechanisms of water delivery to flowers have been understudied despite their potential impact on floral functional ecology and evolution.

Flowers generally require less water than leaves probably because floral transpiration comes with little benefit (Chapter 1; Roddy and Dawson 2012), even though, in some cases, it can exceed leaf transpiration (Blanke and Lovatt 1993; Chapter 3). Transpiration from flowers can be important in maintaining gynoecium temperatures below thresholds that induce damage (Patiño and Grace 2002) and in attracting pollinators (von Arx et al. 2012). Although the water relations of flowers can have important implications for pollination biology, the physiological processes of water import into flowers are unclear, with some reports suggesting that flowers are hydrated predominantly by the phloem (Trolinder et al. 1993) and others suggesting they are hydrated by the xylem (Feild et al. 2009; Chapter 3). A recent analysis of flower hydraulic efficiency, as measured by whole-flower hydraulic conductance (K_{flower}), showed that there was substantial variation among species but that K_{flower} nonetheless correlated with anatomical and physiological traits associated with water supply and loss (Chapter 2). This suggests that hydraulic traits are critical in determining floral hydraulic capacity and that water balance traits may have undergone coordinated evolution. Here, I build upon this previous work by asking whether traits associated with water supply and water loss are coordinated among a larger set of species and whether they have evolved together. I also used this unique dataset to explore a variety of other questions about floral physiology, ecology, and evolution.

One of the most variable and most well-studied floral traits is flower size, which can vary many orders of magnitude and can evolve rapidly (Davis et al. 2007; Barkman et al. 2008). The potential advantages of increasing flower size could be substantial because larger flowers can better attract pollinators (Galen 2000). Yet, larger flowers require more water to drive cell and tissue expansion and would have larger surface areas from which water could evaporate (Galen 1999). As a result, flower size may vary with water availability among species, as has been documented within species (Clausen et al. 1940; Lambrecht and Dawson 2007). Variation in flower size within species could be due to either direct effects of water availability on flower size or indirect effects of water availability on flower size mediated by leaf physiology and whole-plant water and carbon balance (Lambrecht 2013). Moisture availability can influence flower size directly by limiting the water available for cell and tissue expansion. Moisture availability can influence flower size indirectly by limiting the amount of water available for leaf transpiration, which would suppress leaf photosynthesis and reduce the amount of carbon available to produce and maintain flowers (Lambrecht and Dawson 2007; Lambrecht 2013). However, assuming that species are adapted to their climatic niches, these patterns may not exist among species, and flower size may not vary among species with precipitation. If provisioning water to flowers negatively impacts leaf physiology (Galen et al. 1999; Lambrecht and Dawson 2007; Lambrecht 2013), then selection may have favored reductions in flower water costs, particularly in dry habitats and for large flowers. Thus, flower water use may be lower in drier habitats and among larger flowers to compensate for the additional water needed to produce a large floral display. Alternatively, if there is no relationship between water costs and flower size, then producing flowers would be expensive, and large-flowered species may be restricted to wet habitats. Here I test these alternative predictions using species from the California Floristic Province, for which both hydraulic trait measurements and species distributions are available. Preliminary evidence that K_{flower} correlates negatively with flower size among species suggests that larger flowers are more hydraulically efficient (Chapter 2), which would allow flower size to be invariant along precipitation gradients.

Most previous work examining floral trait evolution has focused on traits in two major realms. First has been the molecular processes involved in floral development (Soltis et al. 2007; Irish 2009; Specht and Bartlett 2009). These studies have shown that for many angiosperms, a relatively simple molecular framework can be easily modified to generate many different floral morphologies (Irish and Litt 2005). For example, some floral traits, such as color, can be controlled by just a single gene with dramatic, cascading effects on pollination and fitness (Bradshaw and Schemske 2003). This molecular framework seems to enable high trait lability and modularity, characteristics that may facilitate maximizing successful pollination in the selective regimes of dynamic, coevolutionary networks. The second type of study has been on the evolution of gross morphological traits by comparing different angiosperm lineages and by studying the fossil record: characters related to reproductive development and function (Stebbins 1951; Crepet and Niklas 2009), morphological traits of narrowly defined groups under selection by pollinators (Whittall and Hodges 2007; Hopkins and Rausher 2012), and traits related to floral organization and structure (Endress and Doyle 2009; Endress 2011). In a classic study, Stebbins (1951) compiled data on eight binary floral traits for almost 300 angiosperm families to determine whether some floral trait combinations may be associated with greater diversity. Other, more recent studies have also sought to link single floral characters, such as symmetry (Sargent 2004) and pollination mode (Dodd et al. 1999), to patterns of diversity. Following upon this previous work, I examined the modularity of floral traits and the linkages between morphology and physiology. In addition to examining how floral traits scale with floral size, an important pollination trait, I also examine whether physiological traits correlate with the set of morphological traits used by Stebbins (1951) that characterize floral organization and reproductive structures. Many of these morphological traits are highly conserved within angiosperm families, which exhibit only a subset of all possible trait combinations. Because

shifts in morphology could change the resource requirements of flowers, I predict that there would be correlations between suites of morphological and physiological traits. I also explored the relationships between physiological traits of flowers and of leaves. Phenotypic integration of developmentally and functionally related structures would cause there to be stronger correlations within structures than between structures, resulting in 'correlation pleiades' (Berg 1959; 1960). Studies of morphological traits in flowers and leaves generally support this idea (Armbruster et al. 1999; Juenger et al. 2005; Hansen et al. 2007). However, for venation traits this is not always the case (Chapter 4; Roddy et al. 2013). In the present study, I expand upon this recent work on flower and leaf venation to include a broader set of physiological traits measured on both leaves and flowers. I predicted that traits would be more strongly correlated within leaves and within flowers than between leaves and flowers, reflecting the different constraints placed on leaves and flowers and the modular developmental pathways that give rise to these different structures.

Materials and Methods

Species sampling

The species selection and sampling protocol was identical to that of Chapter 4 (Roddy et al. 2013) and included the same taxa with some additional ones added, except that in addition to taxa collected at the University of California Botanical Garden, and the Tilden Botanical Garden, both in Berkeley, CA, USA, I also sampled at the Berlin-Dahlem Botanical Garden in Berlin, Germany. Collecting in common gardens ensured that plants were well watered and had similar growth conditions. Our dataset was comprised of a total of 157 species from 89 genera and 51 families. I sampled fully expanded leaves and large, recently opened flowers on exposed, sunlit branches from one to three individuals per species. Despite our diverse sampling, our dataset did not include the graminoid monocots, the Asteraceae, and the Orchidaceae because the floral morphologies of these groups are markedly different from most other clades. Additionally, species with small, wind-pollinated flowers were excluded. Because of some missing samples and trait data, subsequent analyses only contained subsets of all species.

Physiological traits

In most cases, leaves and flowers were sampled simultaneously and transported back to the laboratory for processing. Sampling for vein density was identical to methods in Chapter 4 (Roddy et al. 2013) and briefly summarized here. I excised 1 cm^2 sections from midway between the leaf midrib and margin, midway between the base and tip of the leaf. To account for the high variability in vein density within a petal, I collected multiple 1 cm^2 sections from the petals. Leaf and petal sections were placed in 2-4% NaOH for clearing. After 2-4 weeks, leaves were washed in distilled H_2O, transferred to a 3% bleach solution for a few minutes, washed again in distilled H_2O, and then placed in 95% ethanol. Floral structures were similarly transferred into ethanol, except that most of them did not require clearing for as long, nor did they require bleaching to complete the clearing process. Once in ethanol, samples were quickly stained with Safranin O and imaged at 5-20x magnification under a compound microscope outfitted with a digital camera. One or two images per section from each of five to twelve sections per species were captured. For each image, the total length of veins was measured manually using Image J (version 1.44o; Rasband 2012) and divided by the total area of the image to calculate vein length per area. The mean for each structure of each species was calculated and used for subsequent analyses.

The Huber value, the ratio of the xylem cross-sectional area to the projected surface area, was determined for leaves and all perianth structures. In the laboratory, leaf petioles and flower pedicels were sliced underwater using a sharp razor blade. The sections were placed in dH_2O, while the leaf lamina and floral structures (tepals, petals, hypanthia, sepals) were individually removed and either scanned on a flatbed scanner or flattened with a non-reflective plexiglass and imaged with a

digital camera. For flowers, surface areas of all floral whorls were summed for the total surface area. These measurements for leaves and flowers were used in subsequent analyses of flower and leaf size. The petiole and pedicel cross-sections were quickly stained with Safranin O and imaged at 5-40x under a compound microscope outfitted with a digital camera. I measured the xylem cross-sectional area and the surface area of leaves and flowers using ImageJ (version 1.44o; Rasband 2012), and these whole leaf or whole flower area measurements were used in subsequent analyses. I did not measure the area of individual xylem conduits, but instead quantified the amount of cross-sectional area that was occupied by xylem.

The minimum epidermal conductance, g_{min}, is the area-normalized conductance to water vapor under non-transpiring conditions when stomata are presumably closed. g_{min} integrates the permeability to water vapor of the cuticle as well as any leakiness through impartially closed stomata (Kerstiens 1996). For flowers, I measured g_{min} on individual petals or tepals. For floral structures and leaves, I sealed the cut edges with petroleum jelly and kept the structures in a dark cabinet or box into which was placed a fan and a temperature and relative humidity sensor. Structures sat on a mesh screen while the fan blew directly onto them and circulated air inside the container. Every 5 to 20 minutes, the container was briefly opened and the plant structure weighed on a balance with a resolution of 0.1 mg. After approximately 10 measurements, each structure was either scanned or photographed for subsequent measurement of its area and then placed in a drying oven for later dry mass measurement. Using the temperature, humidity, mass, and area measurements, I calculated g_{min} and the desiccation rate (R_{des}), which is the proportional rate of desiccation and is defined as:

$$R_{des} = \frac{g_{\min}}{H_2O_{area}} \quad \text{(eqn 1)}$$

where g_{min} is the minimum epidermal conductance and H_2O_{area} is the water content per area and R_{des} is in units of time^{-1}. H_2O_{area} was calculated as the difference in fresh mass (the initial measurement during g_{min} measurements) and dry mass divided by surface area. R_{des} is similar to a half-life, or turnover rate, of water and is equivalent to the reciprocal of the total time required to fully desiccate. From measurements of g_{min}, dry mass and mass per area were also calculated. For flowers, these measurements were made only on the corolla because of its importance to pollination biology. Because in most species the calyx probably has physiological traits more similar to leaves than to the corolla (Chapter 4; Roddy et al. 2013), extrapolating measurements based on the corolla alone would undoubtedly bias trait estimates for entire flowers. Nonetheless, the corolla structures constituted the majority of projected surface area for flowers of most species.

Morphological traits

I constructed a morphological data matrix comprising the same floral traits as those used in previous studies of morphological evolution in angiosperms (Stebbins 1951; Chartier et al. 2014). For ease in scoring and for consistency with previous work, I scored all traits as binary (Table 1). Many of the traits are highly conserved within current circumscriptions of angiosperm families, particularly when scored with only two possible character states. I scored these traits using plant taxonomy reference books such as Judd et al. (2007) and Simpson (2010), as well as taxonomic descriptions for families and genera.

Phylogeny

I obtained a phylogenetic supertree of our sampled taxa using Phylomatic (Webb and Donoghue 2005; Webb et al. 2008). The resulting ultrametric tree was imported into Phylocom 4.2 (Webb et al. 2008) so that recent node age estimates could be written into the tree file using the *bladj* function. I obtained node age estimates for as many nodes as possible in our undated supertree

from Bell et al. (2010). I used *bladj* only to write these node age estimates and not to anchor a few nodes and distribute the remaining, unanchored nodes. Unfortunately, this dated supertree is poorly resolved for recent divergences (e.g. within genera) but represents, I believe, the best approach to analyzing trait evolution on such a phylogenetically diverse dataset. Polytomies in the tree were resolved by adding short branches that represented approximately one million years and subsequently subtracting an equivalent amount from the descendant branches to ensure the tree remained ultrametric. Randomly resolving polytomies in this way has little effect on correlations between independent contrasts (Ackerly and Reich 1999). This fully dichotomous supertree was used for all subsequent phylogenetic analyses.

Climate data

Species collection localities were obtained for each species in our dataset that was native to the California Floristic Province (n = 61 species) from the Jepson eFlora (Jepson Flora Project 2014). Using these species localities, I extracted mean annual climate data (temperature and precipitation) from the 30-year normals provided by the PRISM Climate Group (PRISM Climate Group 2014) and calculated mean annual temperature (MAT) and precipitation (MAP) for each species. Using flowering phenology data from the Jepson eFlora, I calculated mean flowering season temperature and precipitation (MFST and MFSP, respectively) for each species. Log-transformed floral trait values were linearly regressed against climate variables. Precipitation data were log-transformed to improve normality.

Trait comparisons within and between leaves and flowers

All data were analyzed using R software (v. 2.15.2; R Core Team 2012). The list of traits I analyzed is summarized in Table 1. For all analyses trait values were log-transformed to improve normality. I also removed the most extreme one or two points for each trait if they deviated substantially from the log-normal distribution. To determine whether trait values differed between leaves and flowers I first rescaled data for each trait so that the mean and standard deviation of each trait were 0 and 1, respectively. To account for the paired sampling of flower and leaves of the same species, I used a linear mixed-effects model for each trait that treated plant structure (leaf or flower) as a fixed effect and plant structure nested within species as a random effect.

I asked how traits were correlated within plant structures (e.g. how two leaf traits are correlated) and between structures (e.g. how the same trait is correlated in leaves and flowers) both ignoring species' shared history (correlations between traits) and incorporating the phylogenetic relationships of species (correlations of phylogenetic independent contrasts, PICs). For each pairwise correlation, the tree was pruned to include only tips with non-missing data in both traits. Phylogenetic independent contrasts (Felsenstein 1985) were calculated using the *pic* function in the package *ape*. Correlations between both traits and PICs were tested using Pearson product-moment correlations. For PICs, these correlations were forced through the origin because PICs have an expected mean of zero. For examination of trait and PIC correlations using correlation networks, I used the Bonferroni correction to correct for the number of simultaneous correlations being tested in each analysis.

Pairwise correlations between sets of traits were performed using standard major axis regression ('*smatr*' package; Warton et al. 2012) because error was expected to be in both variables and I did not want to assume one variable was independent. For individual pairwise correlations between traits and PICs, I did not adjust P values using the Bonferroni correction.

Multivariate analyses

Principal components analysis (PCA) was used to determine which traits influenced the major axes of variation in flower physiological traits, using the '*princomp*' function in R. Misplaced

pedicel cross-sections meant that Huber ratios were lacking for many species, so I removed this trait from the dataset before running the PCA on the remaining species for which I had complete data (n = 127 species). A PCA was also run on the independent contrasts calculated from these 127 species to determine the major axes of floral physiological trait evolution. To ensure that the PICs had a mean of zero, I replicated the negative inverse of the PICs before running the PCA. In both PCAs, results of only the first two principal components are reported because these two axes captured most of the variation in the data.

To determine whether morphological and physiological traits were correlated with each other, I used canonical correlation analysis (CCA; function '*cc*' in the package '*CCA*'). CCA determines the linear combinations of variables in one variable set that maximize the correlation with linear combinations of a second variable set. Thus, CCA can be used to determine how trait sets of different types (e.g. physiological traits and morphological traits) may be correlated, and it makes no assumption about the statistical independence or dependence of the variable sets. I used CCA to determine the linear combinations of morphological traits that best correlate with linear combinations of physiological traits for six canonical dimensions.

Results

Leaves and flowers differed significantly in almost all traits (Figure 1): VLA ($F = 237.34$, $df = 97$, $P < 0.001$), g_{min} ($F = 55.84$, $df = 105$, $P < 0.001$), R_{des} ($F = 47.61$, $df = 105$, $P < 0.001$), area ($F = 5.77$, $df = 105$, $P = 0.02$), dry mass ($F = 150$, $df = 102$, $P < 0.001$), $mass_{area}$ ($F = 54.39$, $df = 107$, $P< 0.001$), and H_2O_{area} ($F = 9.40$, $df = 108$, $P < 0.01$). Flowers had lower trait values than leaves, except for water loss traits (g_{min} and R_{des}) and H_2O_{area} for which flowers tended to have higher trait values. Correlations among traits and independent contrasts showed that there were stronger trait correlations within structures than between structures (Figure 2). The strongest independent contrast correlation between leaves and flowers was for area.

There were significant, positive correlations between water supply and water loss traits for flowers but not for leaves (Figure 3a-d). Species with higher flower g_{min} also had higher flower VLA ($R^2 = 0.0539$, $P = 0.008$) and higher Huber ratios ($R^2 = 0.1183$, $P < 0.001$). However, the correlations between PICs were significant only for flower g_{min} and Huber ratios ($R^2 = 0.26$, $t = 5.96$, $F = 35.53$, $df = 99$, $P < 0.001$). No correlations between water supply and water loss traits and their contrasts were significant for leaves.

There were significant correlations for both traits and PICs between flower size and water loss and investment traits (Figure 4). Larger flowers had higher H_2O_{area} (traits: $R^2 = 0.0454$, $P = 0.01$; contrasts: $R^2 = 0.05$, $t = 2.73$, $F = 7.43$, $df = 143$, $P = 0.007$) but lower g_{min} (traits: $R^2 = 0.115$, $P < 0.001$; contrasts: $R^2 = 0.22$, $t = -6.23$, $F = 38.83$, $df = 141$, $P < 0.001$) and R_{des} (traits: $R^2 = 0.26$, $P < 0.001$; contrasts: $R^2 = 0.35$, $t = -8.65$, $F = 74.89$, $df = 142$, $P < 0.001$). Correlations between PICs were as strong as or stronger than they were between traits. These patterns were similar to those for leaves (data not shown). For leaves, there was no significant relationship between H_2O_{area} and leaf size ($P = 0.76$), although there was a significant, positive relationship between the independent contrasts ($R^2 = 0.06$, $t = 2.68$, $F = 7.16$, $df = 106$, $P = 0.008$). Leaf g_{min} decreased with leaf size ($R^2 = 0.08$, $P = 0.005$), and the independent contrasts were similarly negatively correlated ($R^2 = 0.06$, $t = -2.53$, $F = 6.39$, $df = 102$, $P = 0.013$). Leaf R_{des} also scaled negatively with leaf size (traits: $R^2 = 0.12$, $P < 0.001$; contrasts: $R^2 = 0.24$, $t = -5.58$, $F = 31.1$, $df = 102$, $P < 0.001$).

Using California species, I asked whether floral physiological traits correlated with temperature and climate, both annual means and during the flowering season (Figure 5). There were no significant correlations between water supply traits (VLA and Huber ratio) and any climate variable, nor between $mass_{area}$ and H_2O_{area} and climate variables. However, water loss traits significantly correlated with both temperature and precipitation. For g_{min}, there was a significant positive correlation with MFSP ($R^2 = 0.10$, $F = 6.06$, $df = 52$, $P = 0.017$) and with MFST ($R^2 =$

0.36, F = 7.38, df = 52, P = 0.009), but not with MAP or MAT (Figure 5c,j). The relationship between g_{min} and climate variables had a strong impact on causing there to be significant relationships between R_{des} and climate variables. R_{des} correlated positively with both MAP (R^2 = 0.10, F = 6.54, df = 56, P = 0.013) and MFSP (R^2 = 0.11, F = 6.57, df = 51, P = 0.013), as well as with MAT (R^2 = 0.12, F = 7.49, df = 56, P = 0.0083) and MFST (R^2 = 0.16, F = 9.73, df = 51, P = 0.003; Figure 5d,k). Species in hotter, drier habitats have flowers with lower g_{min} and R_{des}. Species in warmer locations also had larger flowers (MFST: R^2 = 0.09, F = 5.21, df = 52, P = 0.027; MAT: R^2 = 0.07, F = 4.06, df = 58, P = 0.049), although there was no effect of precipitation on flower size (Figure 5e,f). There were fewer significant correlations between leaf traits and climate than between flower traits and climate (data not shown). Leaf Huber ratio was negatively correlated with MFSP (R^2 = 0.16, t = -5.23, F = 5.3, df = 28, P = 0.029), and leaf R_{des} was positively correlated with MAP (R^2 = 0.11, t = 2.50, F = 6.23, df = 52, P = 0.016). No other leaf traits were correlated with precipitation variables. Leaf VLA was positively correlated with MFST (R^2, t = 1.04, F = 6.07, df = 44, P = 0.018), as was the Huber ratio (R^2 = 0.19, t = 2.57, F = 6.61, P = 0.016). Leaf $mass_{area}$ was positively correlated with MAT (R^2 = 0.09, t = 2.32, F = 5.39, df = 52, P = 0.024), as was leaf H_2O_{area} (R^2 = 0.12, t = 2.72, F = 7.44, df = 53, P = 0.009).

The resource costs of producing floral displays are the sum of the costs of building floral structures and the costs of maintaining these structures. Veins used in conducting water are commonly considered expensive in terms of carbon, such that increasing hydraulic capacity would be particularly expensive in terms of carbon. I explored whether investment in venation to transport water increases the biomass costs of leaves and flowers (Figure 6). Consistent with previous studies, there was no significant relationship between VLA and $mass_{area}$ for leaves, but there was a slight positive effect of VLA on $mass_{area}$ for flowers (R^2 = 0.03, P = 0.041), although for neither leaves nor flowers were independent contrast correlations significant.

I asked whether water investment is correlated with g_{min} and whether water investment reflects investment costs in biomass for leaves and flowers (Figure 7). For both structures, species with higher H_2O_{area} also had higher g_{min} (flowers: R^2 = 0.18, P < 0.001; leaves: R^2 = 0.32, P < 0.001). Independent contrast correlations were weaker for correlations between g_{min} and H_2O_{area} than they were for traits correlations (flowers: R^2 = 0.09, t = 3.65, F = 13.34, df = 142, P < 0.001; leaves: R^2 = 0.25, t = 5.90, F = 34.82, df = 106, P < 0.001). Water investment was also significantly correlated with mass investment on an area basis for both leaves and flowers (flowers: R^2 = 0.35, P < 0.001; leaves: R^2 = 0.57, P < 0.001; Figure 7e,g). For both of these relationships, slopes did not differ significantly from unity (flowers: slope = 1.078, df=110, P = 0.23; leaves: slope = 0.988, df = 144, P = 0.85). Correlations between $mass_{area}$ and H_2O_{area} PICs were stronger than the trait correlations (flowers: R^2 = 0.44, F = 111.2, df = 144, P < 0.001; leaves: R^2 = 0.72, t = 16.91, F = 286.1, df = 110, P < 0.001).

Principal components analysis was used to distinguish suites of correlated and coevolving traits (Table 2). The first two PC axes for traits described 36% and 32%, respectively, of the variation in traits, while the first two PC axes for independent contrasts described 39% and 31%, respectively, of the variation in independent contrasts. Traits PC1 was defined largely by area in opposition to all other traits but mainly g_{min}, R_{des}, and $mass_{area}$, while traits PC2 was driven largely by R_{des} in opposition to H_2O_{area} and $mass_{area}$. Contrasts PC1 was driven largely by g_{min} and R_{des} in opposition to area, consistent with previously described relationships between these traits (Figure 4). Contrasts PC2 was defined by area in opposition to $mass_{area}$ and H_2O_{area}.

Canonical correlation analysis was used to determine whether axes of morphological and physiological traits are correlated (Table 3). The first five canonical dimensions of morphological and physiological traits were significantly correlated, with correlation coefficients ranging from 0.31 to 0.71. In the first canonical dimension, the morphological traits with the strongest influence were perianth cycly and corolla fusion in opposition to placentation, while the physiological traits with the

strongest influence were g_{min} and R_{des}. For the first five canonical dimensions, g_{min}, R_{des}, and H_2O_{area} were consistently among the most influential physiological traits.

Discussion

Sampling a phylogenetically diverse set of species, I found that maintaining flower water balance has been an important factor influencing floral evolution. Because of phenotypic integration within structures, the most important physiological traits are likely different for flowers and for leaves. Furthermore, these physiological traits are strongly linked to morphological traits, such as flower size, which suggests that floral form results from an interplay between pollination biology and biophysical constraints associated with producing and maintaining flowers. As additional evidence of the diverse selective forces shaping floral traits, some of these water balance traits were significantly correlated with climate variables. These results show, for a diverse set of species, the many ways in which physiology may be involved in the evolution of flowers.

Leaf and flower trait comparisons and correlated evolution

Because flowers are less persistent than leaves, I expected flowers to have lower resource costs associated with their construction and maintenance. For traits associated with supplying water and with resource investment, this was generally true, but not for traits associated with water loss rates. Flowers had significantly lower VLA than leaves and tended to have lower Huber ratios, suggesting that they have much lower capacity for transporting water than leaves (Chapter 4; Roddy et al. 2013; Figure 1). Flowers were slightly smaller than leaves and had significantly lower dry mass investment. Surprisingly, though, they had higher H_2O_{area}, g_{min}, and R_{des} than leaves. Despite flowers having traits associated with higher hydraulic costs than leaves, the effective costs may be smaller for flowers because the true cost of traits expressed as a rate (e.g. g_{min} and R_{des}) would be a function of floral lifespan. Shorter floral lifespans may compensate for leakier cuticles and faster rates of desiccation. Indeed, there may be a tradeoff between floral lifespan and these flux-based traits, although examining these potential tradeoffs would depend on rigorously measuring lifespans of individual flowers, which is rarely done.

The strongest correlations between both traits and independent contrasts were within structures and not between structures (Figure 2). The overall lack of significant correlations between leaves and flowers highlights the developmental modularity of these structures and points to the tight phenotypic integration and canalized development within structures, at least for the traits measured here (Berg 1960; Armbruster et al. 1999; Juenger et al. 2005; Hansen et al. 2007; Roddy et al. 2013). Many previous studies examining modularity of floral and leaf traits have examined morphological traits such as size and shape. Interestingly, the major exception in our dataset was for flower and leaf size. Historical correlations accounting for phylogeny showed that flower size is strongly correlated to leaf size, probably because of the relationships between stem size, leaf size, and inflorescence size defined by Corner's rules (Corner 1949; Midgley and Bond 1989; Ackerly and Donoghue 1998). Because of the biomechanics of branching, selection for increases in flower size would require increases in branch diameter, which, in turn, would allow leaf size to increase, and vice versa. The relationships between stem size, leaf size, and inflorescence size are thought to be tightly coupled developmentally and physiologically, which would explain why there was such a strong correlation between independent contrasts of area traits. The overall pattern of correlations between traits were similar for flowers and for leaves both for traits and independent contrasts. The functional importance of some of these correlations are discussed later.

Multivariate analyses were used to identify suites of traits that are coordinated or have undergone correlated evolution. Despite describing almost 70% of the variance in its first two axes, the PCA of flower physiological traits and their independent contrasts did little to help describe suites of traits (Table 2). The PC1 for both traits and contrasts was defined largely by flower size in

opposition to g_{min} and R_{des} (further clarified in Figure 4). PC2 was defined primarily by investment costs ($mass_{area}$, H_2O_{area}) in opposition to R_{des} for traits and flower size for independent contrasts. There were significant correlations between morphological traits and physiological traits (Table 3). The morphological traits primarily characterize floral structure and organ positioning, traits that are highly conserved within angiosperm families. While the physiological traits were based solely on corolla display structures (e.g. tepals, petals), the morphological traits described whole flower structure (Stebbins 1951; Chartier et al. 2014). As such, I did not necessarily expect that shifts in floral morphology would be linked to water balance traits of petals. Yet, there were strong correlations between these suites of traits such that shifts in whole-flower architecture are accompanied by shifts in physiological traits of petals. For example, fused corollas have significantly lower g_{min} in the present dataset, and scoring fusion as a continuous trait among congeneric species showed that more fused flowers had lower K_{flower} (Chapter 2, data not shown). Why corolla fusion decreases g_{min} and K_{flower}, regardless of the effects of fusion on boundary layer conductances under natural conditions, is unclear but warrants further investigation. Determining how and why these morphological and physiological traits may be correlated would require either broader sampling across the phylogeny than I have done here or more targeted sampling of key clades that exhibit substantial variation in one of the traits. Nonetheless, these results are promising and showcase the importance of considering physiological traits in studies of floral evolution at any taxonomic scale.

Maintenance of water balance

To maintain physiological function, plants and their constituent parts must prevent desiccation by coordinating water supply with water loss (Brodribb and Jordan 2011). Under conditions of limited water supply, water loss must also be limited. In leaves, water loss can be reduced by active mechanisms, such as hormonally induced stomatal closure, or by a passive process of stomatal closure resulting from the loss of turgor pressure in stomatal guard cells (Brodribb et al. 2014). In flowers that have few stomata, water loss is limited by the ability of the cuticle to prevent evaporation of water to the atmosphere. Because flux rates of water supply and water loss correlate with anatomical and physiological traits (Sack et al. 2003; Feild et al. 2009; Brodribb and Jordan 2011; Chapter 2), traits associated with water supply and loss are predicted to be correlated with each other and provide the mechanistic basis for the hydraulic capacity of plant structures. The need to maintain turgor in both leaves and flowers has driven the coordination of hydraulic conductance with water supply and loss traits, although the traits most important to maintaining water balance may be different in leaves and flowers (Brodribb and Jordan 2011; Chapter 2).

In a previous study of flowers, water supply and loss traits were shown to be tightly coordinated with each other, particularly VLA and g_{min}, and both of these traits were coordinated with whole flower hydraulic conductance (Chapter 2). In the present study, I asked whether these trait correlations hold across a more diverse sampling of species and, if so, whether these traits have undergone coordinated evolution. While g_{min} and VLA were correlated among a diverse sampling of species, the amount of variation in g_{min} that was explained by variation in VLA was substantially less in the present study (5%) than in the previous study (78%), and there was no sign that these two traits have undergone correlated evolution (Figure 3a,b). Floral veins may not conduct water during anthesis, particularly among flowers with low VLA (Chapter 2). Although VLA correlates with g_{min}, if veins are non-functional during anthesis, then there may be no functional connection between VLA and g_{min} that would have caused them to have undergone correlated evolution. However, g_{min} and the Huber ratio were positively correlated, both in the trait correlations and the independent contrast correlations (Figure 3b,f), suggesting that water supply and loss may be coordinated to maintain flower water balance.

While water supply and loss traits were coordinated to some extent in flowers, there was no such coordination of these traits among leaves (Figure 3c-d,g-h). Minimum cuticular conductance is

probably important in determining leaf survival during droughts because it would determine how rapidly stored water would be depleted. In contrast, VLA of leaves is tightly coordinated with maximum rates of stomatal conductance and transpiration (Boyce et al. 2009; Brodribb et al. 2010; Brodribb and Jordan 2011), and the maximum hydraulic capacity of a leaf, as defined by VLA, is unrelated to its ability to limit water loss under stressful conditions (Figure 3c). The differences between leaves and flowers in these traits highlight that the predominant pathways for water loss are different among these two structures. While most of the water transpired from leaves occurs through the stomata, most of the water that evaporates from flowers occurs through the cuticle because flowers have few, if any, stomata (Chapter 2). The importance of these different pathways in the two structures is reflected in the different water loss traits that control their hydraulic capacity, with stomatal traits primarily controlling leaf hydraulic conductance and g_{min} primarily controlling flower hydraulic conductance (Sack et al. 2003; Chapter 2).

Water balance and flower size

One of the most variable and most well-studied floral traits is flower size. Because they are more visible, larger flowers are generally more frequently visited by animal pollinators, which leads selection for increases in flower size (Galen 2000). Among species, flower size can evolve rapidly, as has been the case for the Rafflesiaceae (Davis et al. 2007; Barkman et al. 2008). In contrast, the water costs of maintaining flowers can limit their size and oppose pollinator selection for larger flowers (Galen et al. 1999; Galen 2000; Strauss and Whittall, 2006; Lambrecht and Dawson 2007). Without an efficient network of highly branched veins to supply water throughout anthesis, large flowers may be particularly disadvantaged if area-normalized water loss rates were invariant with flower size because the total water costs of flowers would be much larger for large versus small flowers. However, based solely on the biophysics of size, I would predict that total water loss rates would covary with flower size. Increasing flower size should decrease the conductance of the boundary layer around flowers, especially due to their complex three-dimensional structures, which would reduce the area-normalized transpiration rate. Yet, these reductions in transpiration due to lower boundary layer conductance may not sufficiently reduce water loss rates, especially if the xylem pathway is non-functional. As a result, I predicted that large flowers would have traits associated with greater water conservation both to compensate for the additional water costs of producing a large floral display and because an inefficient vascular system may disproportionately hinder large flowers. These predictions were strongly supported by the data. In addition to requiring more water to produce a large floral display, larger flowers also had more water per unit area (Figure 4a). Furthermore, large flowers have lower cuticular conductances, which, combined with higher water contents, further reduce desiccation rates (Figure 4c,e). Taken together, these results suggest that as flower size increases, flowers limit water losses by reducing g_{min} and rely more heavily on stored water rather than newly imported water throughout anthesis. Adopting a more conservative strategy may limit the overall water costs associated with building and maintaining large flowers thereby facilitating the development of large flowers to better attract pollinators. Because pollinators probably prefer larger flowers regardless of habitat, this size-scaling of g_{min} and R_{des} may explain why average flower size does not vary along precipitation gradients (Figure 5e). Reducing g_{min} as flower size increases and as precipitation declines would allow large flowers to exist in dry habitats, at least at the community level.

Within species, flower size and display area have been shown to correlate with water availability (Clausen et al. 1940; Lambrecht and Dawson 2007), suggesting that traits such as g_{min} are not as labile within species as is flower size. The presence of significant correlations in both the traits and the independent contrasts suggests that evolutionary changes in flower size are tightly coupled to shifts in flower hydraulic architecture, and the strength of the trait and contrast correlations between R_{des} and flower size were among the strongest I found. Correlations between

independent contrasts were stronger than correlations between traits, suggesting that differences in flower size even among closely related species are accompanied by differences in H_2O_{area}, g_{min}, and R_{des}; the significant correlations between these traits is not due to large divergences in traits deep in the phylogeny that have been maintained over time. As flowers increase in size, they also shift toward a strategy of greater water conservation and reliance on stored water. They may adopt this more conservative strategy because many flowers lack a venation network capable of efficiently transporting water, which would disproportionately impact large flowers (Chapter 2). However, while reducing g_{min} with increases in flower size may conserve water, lower g_{min} combined with lower boundary layer conductances could lead to higher flower temperatures because less heat is dissipated by evaporation of water. Transpiration by flowers can be important in maintaining a cool gynoecium needed for proper floral development of tropical flowers (Patiño and Grace 2002), but it is unclear how strong of a constraint becoming too hot may be for temperate flowers. Many flowers rely on volatile chemicals to attract pollinators and higher temperatures would increase their rates of volatilization (Stebbins 1970; Jürgens 2009). Furthermore, temperate flowers, particularly those in cold climates, may use high floral temperatures themselves as a thermal reward for insect pollinators (Kevan 1975).

Water balance and climate

In addition to correlating with each other, water supply and loss traits were predicted to correlate with climate variables. Correlations between phenotypic traits and climate are often taken as strong evidence for natural selection. Of the physiological traits measured, only g_{min} and R_{des} correlated with climate variables (Figure 5). The directions of these correlations indicate that under conditions of resource limitation (low precipitation) or high evaporation (high temperature, low precipitation), flowers have a more conservative water use strategy of preventing water loss due to lower g_{min} and R_{des}. Interestingly, correlations were stronger for flowering season climate than for mean annual climate. In Mediterranean-type climates, most of the precipitation falls in the winter, and summers are typically hot and dry. For species that flower in the spring, summer, and autumn, monthly precipitation during flowering would be low despite their ready access to groundwater. Contrary to these results, I had predicted that plant water availability may be unrelated to precipitation during flowering, and that stronger trait correlations would exist with MAP than with MFSP. Although the results were not consistent with this prediction, the stronger correlations with flowering season climate variables suggest that environmental conditions during flowering are a greater constraint on floral physiology than mean annual conditions. Furthermore, microclimatic conditions experienced by flowers are thought to be even stronger predictors of floral physiological traits than are mean annual or mean flowering season conditions. Consistent with a recent meta-analysis, trait correlations were stronger with temperature than with precipitation, probably because the amount of precipitation may not reflect plant water availability (Moles et al. 2014). With the exception of flower size, neither water supply traits nor investment traits correlated with either temperature or precipitation. I had predicted that both water supply and water loss traits would correlate with climate, but the lack of significant correlation with VLA and Huber ratios is strong evidence that once flowers are open and receptive, xylem veins–and their associated traits–have little impact on flower water balance. Instead, limiting water loss–rather than continuously supply water–is more important in preventing desiccation. Furthermore, floral physiological traits, in addition to physiological traits of leaves and stems, may be an important, but understudied, factor influencing species distributions, and the present study is the first, to our knowledge, showing a correlation between floral physiological traits and climate. While shifts in floral phenology with changing climate have been well characterized, earlier spring flowering may be driven at least partially by constraints on floral water balance. The role of flower physiology in determining phenological patterns and species distributions is currently speculative at best, but these results nonetheless

highlight the need for more studies examining the interactions between floral physiological traits, species distributions, and phenological patterns. The interactions between these factors have important implications for community ecology, particularly because loss of plant species and shifting plant phenology can cause declines in insect pollinators (Scheper et al. 2014).

Flower economics

Over the last twenty-five years, an emerging paradigm in plant functional ecology has been the leaf economics spectrum, which describes correlations between leaf functional traits related to resource allocation and fluxes (Reich et al. 1997; Wright et al. 2004; Westoby and Wright 2006; Reich 2014). Because these trait correlations define tradeoffs between ecological strategies, understanding the causes of variation along these axes and the sources of variation that lead to deviation from the predictions could increase our understanding of these tradeoffs between ecological strategies. More recently, there have been efforts to move beyond quantifying simple correlations between leaf traits towards understanding the underlying mechanisms governing suites of correlated traits (Blonder et al. 2011). One of the most important traits that controls the flux rate of water through a leaf and thus its photosynthetic rate is VLA (Brodribb et al. 2007). By extension, some have argued that VLA is also critical in determining leaf $mass_{area}$ and have asserted that VLA is the predominant factor driving leaf $mass_{area}$ because maximizing photosynthetic rate requires a large carbon investment in veins, which increases leaf $mass_{area}$ (Blonder et al. 2011; Blonder et al. 2013; Blonder et al. 2014). Thus, they predict that VLA and leaf $mass_{area}$ should be mechanistically and positively correlated. However, angiosperm groups that have achieved the highest leaf VLA have done so by developing novel vein cell microstructures that have decreased the size and cost of their higher order veins (Feild and Brodribb 2013). Furthermore, VLA and leaf $mass_{area}$ show no such coordination among diverse sets of species (Sack et al. 2013; Sack et al. 2014). Consistent with these other analyses, I found no significant relationship between leaf VLA and $mass_{area}$, either in trait correlations or independent contrast correlations (Figure 6c,d). However, there was a weak, though statistically significant, positive relationship between VLA and $mass_{area}$ in flowers, but these traits nonetheless have evolved independently (Figure 6a,b). In leaves the carbon costs of building a vascular structure with high hydraulic capacity is unrelated to the overall biomass investment costs of light capture. However, in flowers veins do have a small influence on flower mass. If floral veins do not conduct water during anthesis, they may still serve a biomechanical function, which would explain why VLA remains relatively high among many groups and why $mass_{area}$ is affected by flower VLA. Nonetheless, the costs of building highly branched venation networks may not be as large as has been previously assumed (Feild and Brodribb 2013).

As yet, there has been no such 'flower economics spectrum' that describes the functional traits of flowers related to resource allocation and ecological strategies. Like leaves, stems, and roots (Reich 2014), flowers may also be differentiated among a 'fast-slow' traits continuum. *Calycanthus* flowers with higher K_{flower} also have less negative water potentials at turgor loss, implying that there is a tradeoff between tolerance to desiccation and maintaining a high hydraulic conductance, although data from other species are desperately needed (Chapters 2, 3). A fuller traits economics spectrum for flowers, however, should incorporate traits associated with pollination and reproductive development. Pollination modes and strategies could influence where species fall along traits spectra or may cause there to be different tradeoff axes unique to each pollination mode. For example, among Annonaceae species petal tissues increase in size and thicken with increasing size and voraciousness of their beetle pollinators (Gottsberger 1999). These structural differences, presumably driven by pollinators, likely also influence physiological traits and functioning of these flowers. Similarly, flowers pollinated by insects or animals that land may need to have more structural support than flowers pollinated by hovering insects or birds. Despite these different pollination constraints, our results suggest that there may be unifying constraints among all biotically

pollinated flowers. For example, there were correlations between traits associated with flux rates (e.g. g_{min}) and traits associated with static investment costs, such as water content (H_2O_{area}). Both flowers and leaves exhibited significant, positive trait and independent contrast correlations between H_2O_{area} and g_{min} (Figure 7a-d). As lineages have reduced their investment of water in these structures, they have also reduced the rate at which this water is lost. An extreme exception to this pattern in leaves would be among succulents, which are not included in the current dataset, but which have relatively high water contents and low water loss rates, suggesting that these correlations may not encompass all possible strategies for leaves and maybe also flowers. Another example of such correlations would be between investment costs of different resources, such as water and carbon. Again, both leaves and flowers displayed significant, positive correlations between H_2O_{area} and $mass_{area}$ in both traits and independent contrasts (Figure 7e-h). Furthermore, the slopes of the relationship were not statistically different from unity for both leaves and flowers, highlighting how closely linked are investment costs of different resources (Reekie and Bazzaz 1987). Movement along this axis of increasing water and carbon costs is probably closely linked to the anatomical differences associated with flower or leaf thickness, which I did not measure, but which can be important in pollination biology (e.g. Gottsberger 1999). Species with high area-normalized carbon and water investment costs are probably thicker and may have other correlated traits, such as long lifespans. How thickness also scales with these traits would be critical in determining the tradeoffs of moving along this axis. It should be noted that neither H_2O_{area} nor $mass_{area}$ would fully quantify the carbon and water costs of leaves and flowers because they ignore the fluxes of carbon and water associated with transpiration and respiration. Nonetheless, these two traits quantify the static investments in these structures and may be indicative of these flux costs, just as H_2O_{area} correlates with g_{min}.

Minimum epidermal conductance, g_{min}, is emerging as a key trait both for determining floral hydraulic capacity and for comparing floral hydraulic strategies. In addition to correlating with climate variables (Figure 5), g_{min} is a strong predictor of floral hydraulic conductance and may be the key determinant of water loss rates from flowers (Chapter 2). Its influence on the rate of desiccation, R_{des}, implicates g_{min} in determining tradeoffs between different hydraulic strategies. Flowers with a high g_{min} tend to have high K_{flower}, fast rates of desiccation and rely little on stored water. In contrast, more conservative flowers have low g_{min} which mitigates the need to maintain a high K_{flower} and allows stored water to be held for a long time. Yet, the anatomical and physiological factors determining variation in g_{min} remain unknown. Minimum epidermal conductance is influenced by both the stomatal pathway for water loss and non-stomatal pathways. Flowers tend to have relatively low stomatal densities, but many of these stomata may remain open throughout anthesis or at least until positive turgor pressure is lost (Hew et al. 1980; Chapters 2, 3). Even if floral stomata do close, they may remain partially open and leaky. Epidermal cell structure may also have some influence. In many dicot flowers, epidermal cells are conically shaped, which could influence boundary layer conductances, although there is little evidence that epidermal cell shape influences petal temperature (Whitney et al. 2011). Properties of the cuticle, such as cuticle thickness and hydrophobicity, would undoubtedly influence the non-stomatal pathway for water loss, although, to our knowledge, there has been no work linking cuticular properties to rates of conductance.

Conclusions

The incredible diversity of floral form is often singly attributed to their presumedly close, coevolutionary relationships with insect and animal pollinators. However, other factors associated with costs of constructing and maintaining flowers may have had important influences on a variety of flora traits, both morphological and physiological. The present study shows for a phylogenetically diverse set of species that physiological traits associated with floral water balance

have been under selection and undergo coordinated shifts with morphological traits. Rather than simplifying the story of floral evolution to solely resulting from coevolution with animal pollinators, these results highlight the many diverse factors that interact with each other to generate structures as variable as flowers.

Figure 1. Standardized means plot for the traits used in this study. Significant differences between leaves and flowers based on paired sampling are shown: *P < 0.05, **P < 0.01.

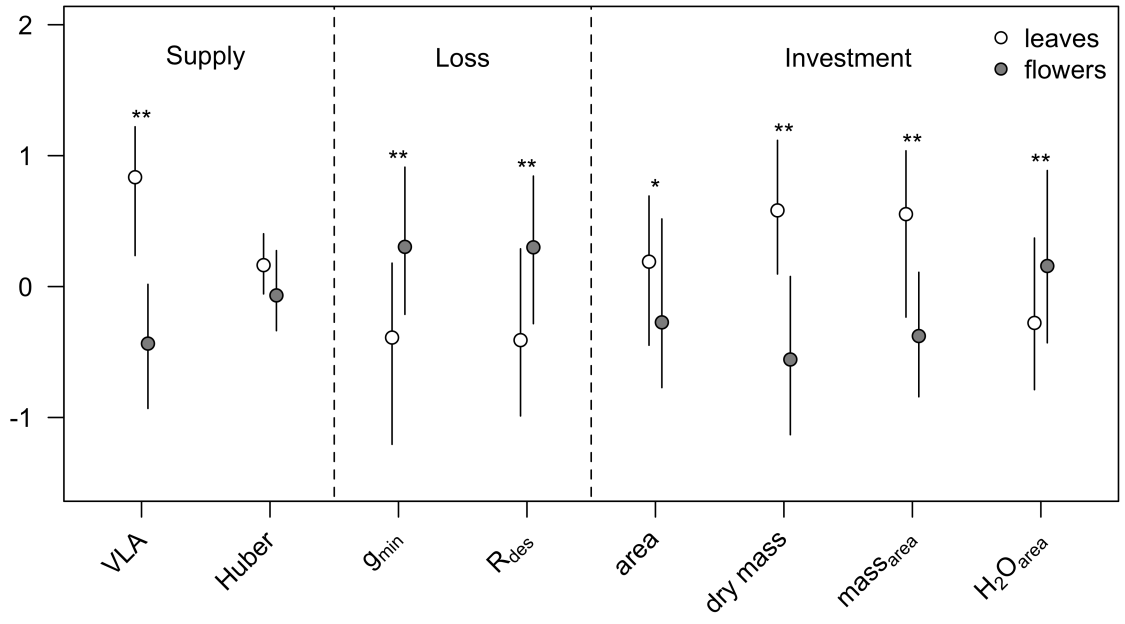

Figure 2. Correlation networks of flower and leaf physiological traits (a) and their phylogenetic independent contrasts (b). In each panel, the left half of the circle refers to flower traits and the right half to leaf traits. Traits are in the same position on each half of each panel as they are labeled on the left half of panel (a). Thickness of lines corresponds to the strength of the correlation, and lines are drawn only for pairwise correlations that are significant at the Bonferonni-corrected P-value of 0.00055.

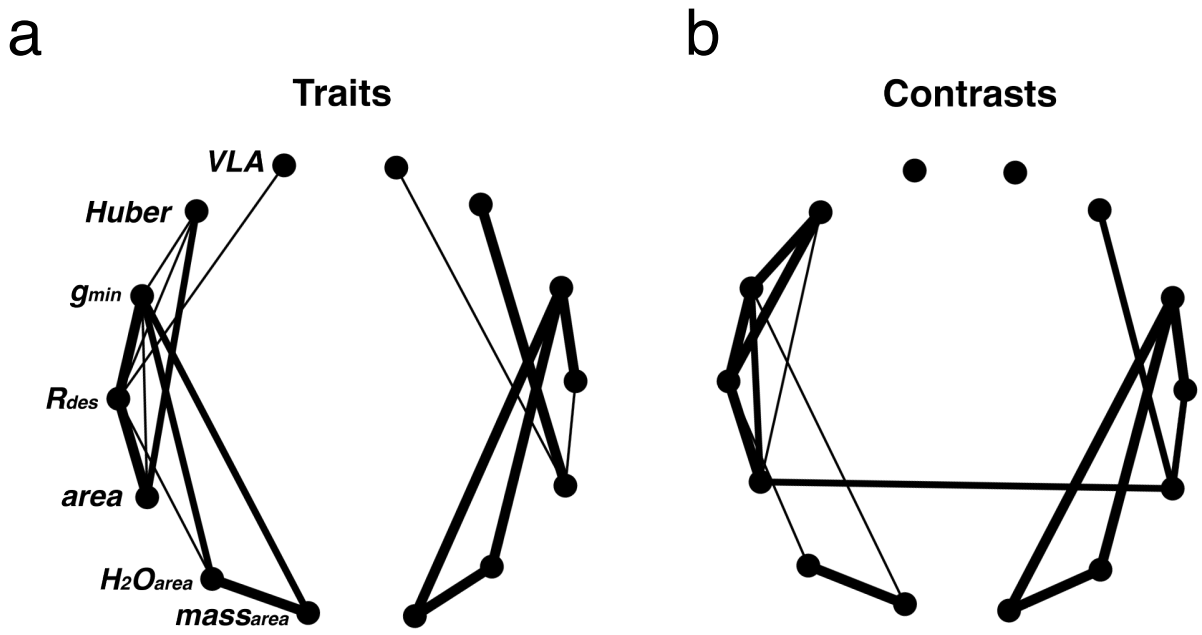

Figure 3. Correlations between water supply traits (VLA, Huber ratio) and g_{min} for flowers (a,b) and leaves (c,d). Correlations between traits are in the top row and between phylogenetic independent contrasts in the bottom row: (e,f) flowers and (g,h) leaves. Best fit curves are shown only for significant regressions. Asterisks after R^2 values indicate the level of significance: *P < 0.05, **P < 0.01.

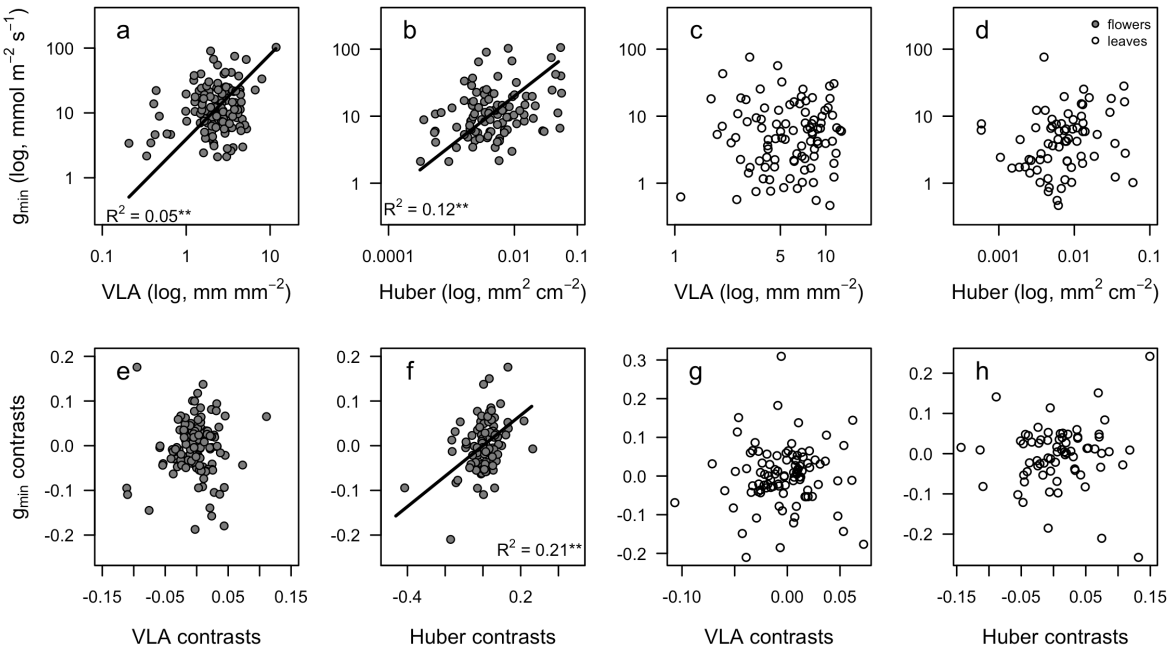

Figure 4. Relationships between flower size and water content (a), minimum epidermal conductance (c), and the rate of desiccation (e), and the phylogenetic independent contrasts of these traits (b,d,f, respectively). Regression lines are shown for statistically significant relationships. Asterisks after R^2 values indicate the level of significance: *P < 0.05, **P < 0.01.

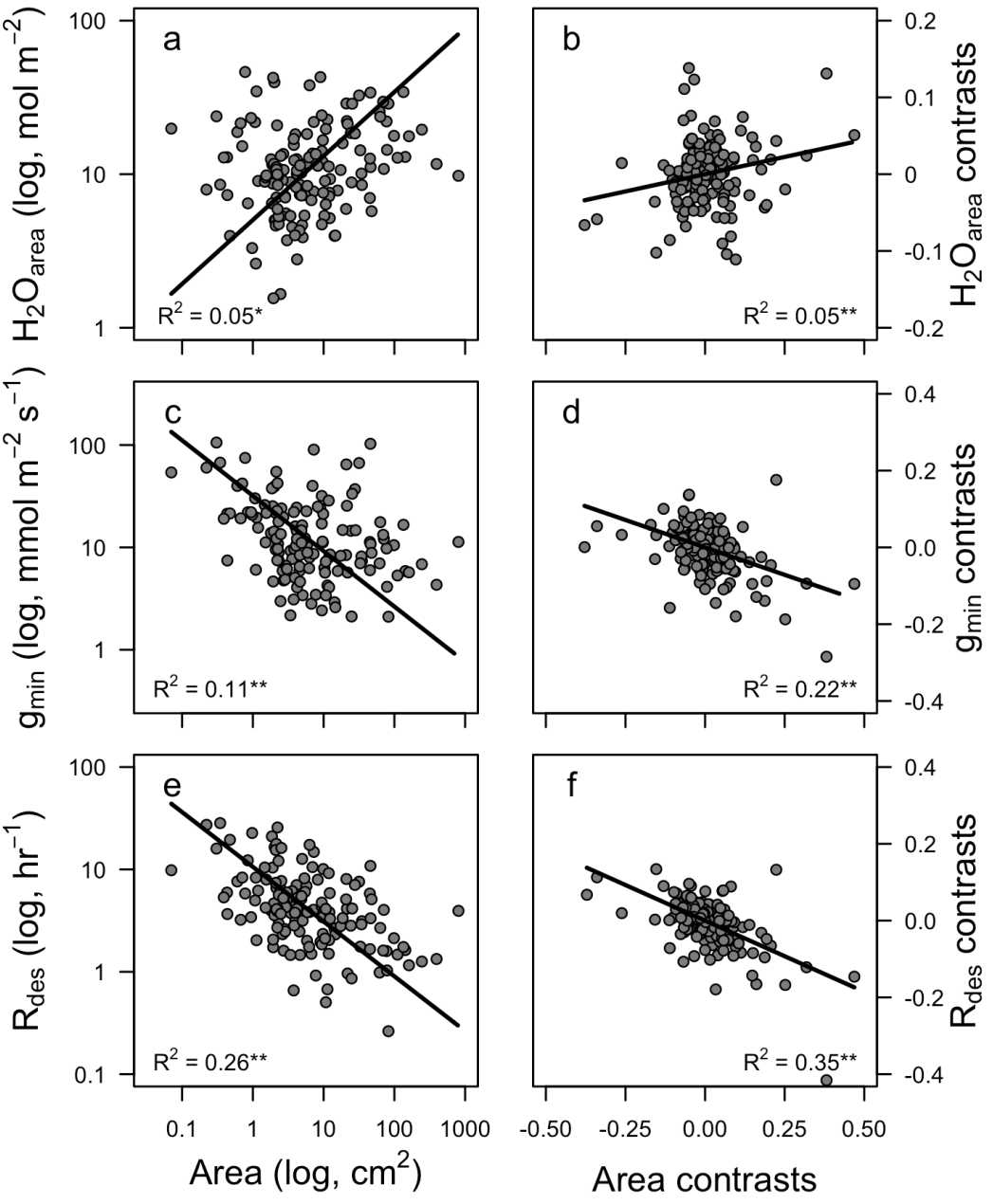

Figure 5. Relationships between flower physiological traits and climate variables. Open circles and grey lines correspond to mean annual climate, and solid circles and black lines correspond to mean flowering season climate. Precipitation was log-transformed to improve normality. Regression lines are shown only for statistically significant relationships. Asterisks after R^2 values indicate the level of significance: *P < 0.05, **P < 0.01.

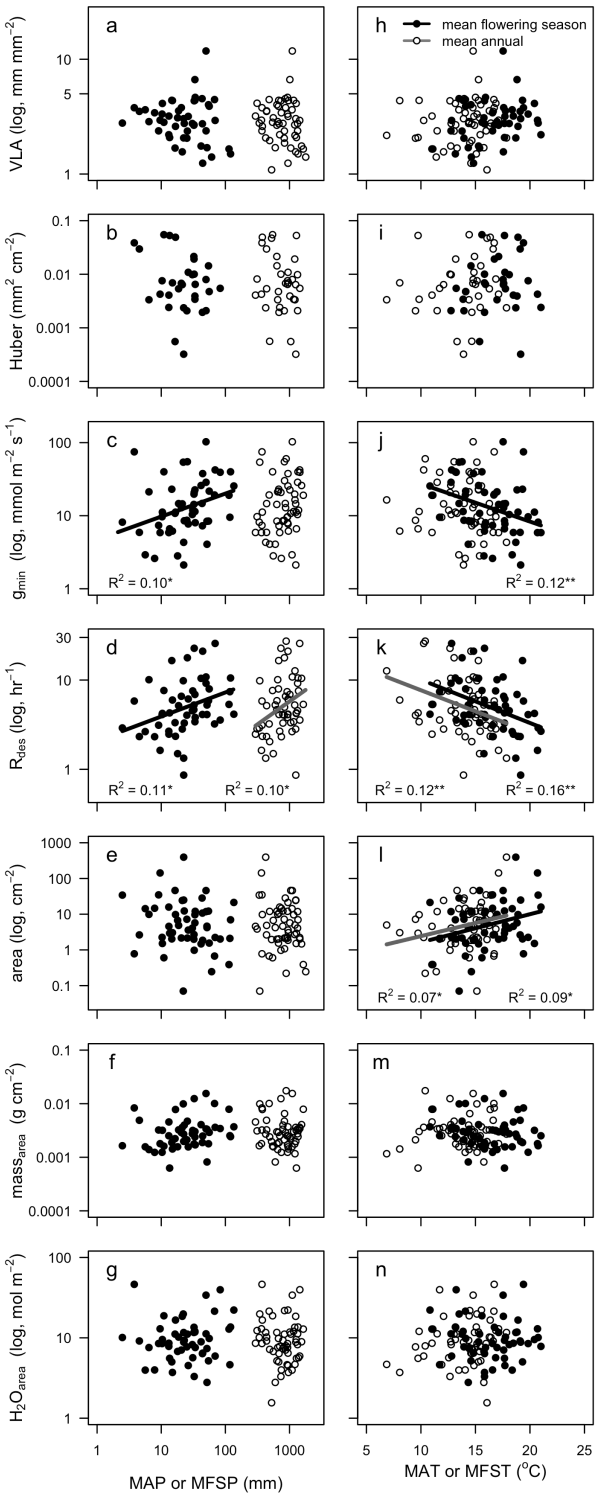

Figure 6. Relationship between VLA and *mass*$_{area}$ for flowers (a) and leaves (c) and their independent contrasts (b, d). Significant correlations are shown by regression lines with accompanying and R^2. *P < 0.05.

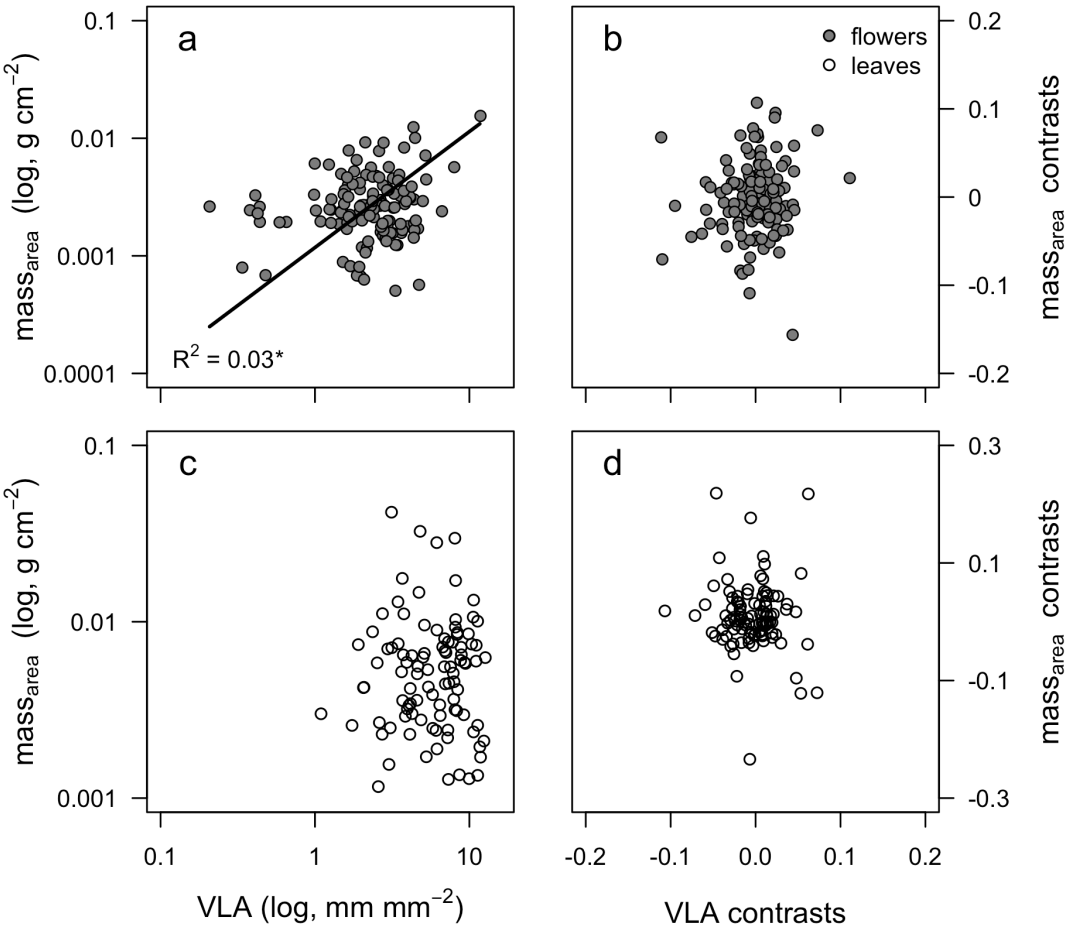

Figure 7. Relationships between H_2O_{area}, g_{min} and $mass_{area}$ and their independent contrasts for flowers (a-b, e-f) and leaves (c-d, g-h). Significant relationships using standard major axis regression are shown by best fit lines and accompanying R^2 values. *P < 0.05, **P < 0.01

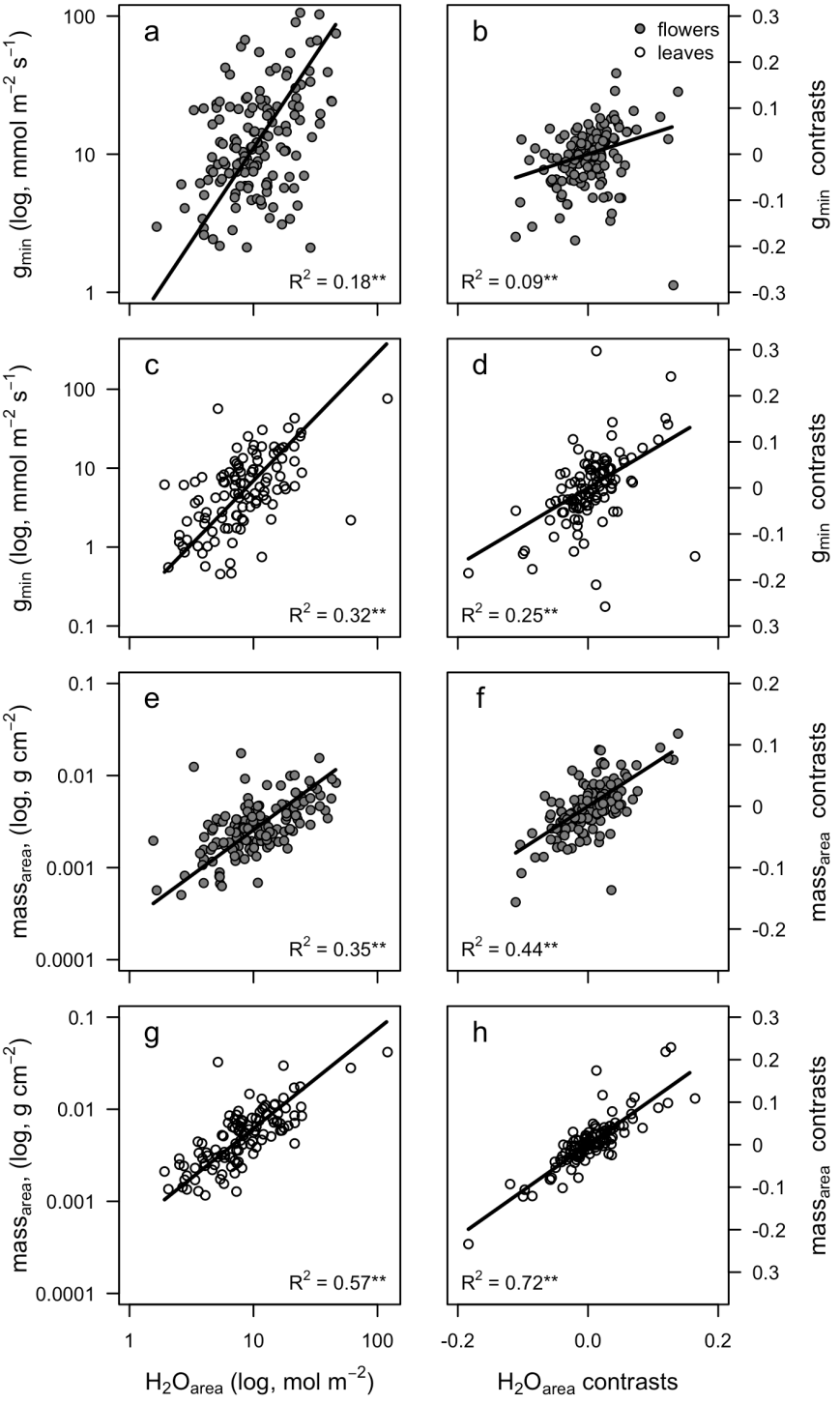

Table 1. List of physiological and morphological traits used in the present study, their descriptions, and their units.

Abbreviation	Description	Units
Physiological traits		
VLA	Vein length per area (vein density)	mm mm^{-2}
Huber	Huber ratio: ratio of cross-sectional xylem area to projected surface area	mm^2 cm^{-2}
g_{min}	minimum cuticular conductance under non-transpiring conditions	mmol m^{-2} s^{-1}
R_{des}	Desiccation rate: proportional rate of desiccation from full hydration	hr^{-1}
area	Projected surface area of display structures	cm^2
dry mass	Dry mass	g
$mass_{area}$	Dry mass per projected surface area	g cm^{-2}
H_2O_{area}	Absolute water content per projected surface area	mol m^{-2}
Morphological traits		
perianth cycly	0 = dichlamydeous 1 = mono-/achlamydeous	
corolla fusion	0 = polypetalous 1 = sympetalous	
flower symmetry	0 = actinomorphic 1 = zygomorphic	
stamen number	0 = polystemonous 1 = oligostemonous	
gynoecial/carpel fusion	0 = apocarpous 1 = syncarpous	

seeds per carpel/ovary chamber/locule	0 = more than 1 1 = one	
placentation	0 = axile 1 = non-axile	
perianth position	0 = hypo-/perigynous 1 = epigynous	

Table 2. First two principal component scores of flower traits and of phylogenetic independent contrasts of those traits. Separate PCAs were run on traits and on independent contrasts. Percentages after the PC axis labels represent the percentage of variation described by that principal component.

	Traits		Contrasts	
	PC1 (36%)	**PC2 (32%)**	**PC1 (39%)**	**PC2 (31%)**
VLA	-0.288	0.006	0.054	-0.018
g_{min}	-0.632	0.114	0.457	-0.480
R_{des}	-0.549	-0.369	0.619	-0.107
area	0.309	0.393	-0.520	0.053
$mass_{area}$	-0.324	0.523	-0.214	-0.621
H_2O_{area}	-0.124	0.650	-0.298	-0.607

Table 3. Results of canonical correlation analysis between morphological traits and physiological traits. The top section shows results of the significance test of each dimension. Only the first five dimensions were statistically significant. The bottom section of the table shows for each dimension the standardized canonical coefficients for each variable.

Tests of Canonical Dimensions					
Dimension	**Canonical Corr.**	**Multi. F**	**df1**	**df2**	**P**
1	0.71	4.45	48	560.1	**<0.0001**
2	0.54	3.22	35	482.0	**<0.0001**
3	0.47	2.83	24	402.4	**<0.0001**
4	0.38	2.44	15	320.6	**0.0022**
5	0.31	2.11	8	234.0	**0.0358**
6	0.19	1.44	3	118.0	0.2359
Standardized Canonical Coefficients					
	Dimension				
	1	**2**	**3**	**4**	**5**
Morphological variables					
perianth cycly	-0.86	-0.27	-0.08	0.18	0.38
corolla fusion	-0.42	-0.90	0.38	0.53	-0.42
flower symmetry	0.23	0.36	0.42	0.03	0.29
stamen number	0.39	-0.02	-0.55	0.47	0.06
gynoecial/carpel fusion	0.25	0.57	-0.05	0.53	0.82
seeds per carpel/ ovary chamber/ locule	0.25	-0.47	0.16	-0.36	0.67
placentation	0.61	-0.17	-0.65	0.86	0.15
perianth position	0.09	-0.58	0.28	0.34	0.34
Physiological variables					

VLA	0.50	-0.56	0.45	0.23	-0.61
g_{min}	-1.23	-18.78	10.41	-0.31	15.89
R_{des}	1.53	18.40	-10.68	-0.63	-15.54
area	-0.25	0.03	-0.24	-1.08	0.05
$mass_{area}$	0.41	0.29	-0.83	0.27	0.62
H_2O_{area}	0.41	12.94	-7.77	0.24	-12.31

Literature Cited

Ackerly D.D. and Donoghue M.J. 1998. Leaf size, sapling allometry, and Corner's rules: phylogeny and correlated evolution in maples (Acer). *The American Naturalist* 152:767-791.

Ackerly D.D. and Reich P.B. 1999. Convergence and correlations among leaf size and function in seed plants: a comparative test using independent contrasts. *American Journal of Botany* 86:1272-1281.

Armbruster W.S., Di Stilio V.S., Tuxill J.D., Flores T.C. and Runk J.L.V. 1999. Covariance and decoupling of floral and vegetative traits in nine neotropical plants: a re-evaluation of Berg's correlation-pleiades concept. *American Journal of Botany* 86:39-55.

Azad K., Sawa Y., Ishikawa T. and Shibata H. 2007. Temperature-dependent stomatal movement in tulip petals controls water transpiration during flower opening and closing. *Annals of Applied Biology* 150:81-87.

Barkman T.J., Bendiksby M., Lim S.H., Salleh K.M., Nais J., Madulid D. and Schumacher T. 2008. Accelerated rates of floral evolution at the upper size limit for flowers. *Current Biology* 18:1508-1513.

Bazzaz F.A., Carlson R.W. and Harper J.L. 1979. Contribution to reproductive effort by photosynthesis of flowers and fruits. *Nature* 279:554-555.

Bazzaz F.A., Chiariello N.R., Coley P.D. and Pitelka L.F. 1987. Allocating resources to reproduction and defense. *BioScience* 37:58-67.

Bazzaz F.A. and Carlson R.W. 1979. Photosynthetic contribution of flowers and seeds to reproductive effort of an annual colonizer. *New Phytologist* 82:223-232.

Bell C.D., Soltis D.E. and Soltis P.S. 2010. The age and diversification of the angiosperms re-revisited. *American Journal of Botany* 97:1296-1303.

Berg R.L. 1959. A general evolutionary principle underlying the origin of developmental homeostasis. *The American Naturalist* 93:103-105.

Berg R.L. 1960. The ecological significance of correlation pleiades. *Evolution* 14:171-180.

Bertsch A. 1983. Nectar production of *Epilobium angustifolium* L. at different air humidities; nectar sugar in individual flowers and the optimal foraging theory. *Oecologia* 59:40-48.

Blanke M.M. and Lovatt C.J. 1993. Anatomy and transpiration of the avocado inflorescence. *Annals of Botany* 71:543-547.

Blonder B., Violle C., Bentley L.P. and Enquist B.J. 2011. Venation networks and the origin of the leaf economics spectrum. *Ecology Letters* 14:91-100.

Blonder B., Violle C., Bentley L.P. and Enquist B.J. 2014. Inclusion of vein traits improves predictive power for the leaf economic spectrum: a response to Sack et al. (2013). *Journal of Experimental Botany* 65:5109-5114.

Blonder B., Violle C. and Enquist B.J. 2013. Assessing the causes and scales of the leaf economics spectrum using venation networks in *Populus tremuloides*. *Journal of Ecology* 101:981-989.

Bond W.J. and Midgley J. 1988. Allometry and sexual differences in leaf size. *The American Naturalist* 131:901-910.

Bowman J.L. 1997. Evolutionary conservation of angiosperm flower development at the molecular and genetic levels. *Journal of Biosciences* 22:515-527.

Boyce C.K., Brodribb T.J., Feild T.S. and Zwieniecki M.A. 2009. Angiosperm leaf vein evolution was physiologically and environmentally transformative. *Proceedings of the Royal Society B* 276:1771-1776.

Bradshaw H.D. and Schemske D.W. 2003. Allele substitution at a flower colour locus produces a pollinator shift in monkeyflowers. *Nature* 426:176-178.

Brenes-Arguedas T., Roddy A.B., Coley P.D. and Kursar T.A. 2011. Do differences in understory light contribute to species distributions along a tropical rainfall gradient? *Oecologia* 166:443-456.

Brenes-Arguedas T., Roddy A.B. and Kursar T.A. 2013. Plant traits in relation to the performance and distribution of woody species in wet and dry tropical forest types in Panama. *Functional Ecology* 27:392-402.

Brodribb T.J., Feild T.S. and Jordan G.J. 2007. Leaf maximum photosynthetic rate and venation are linked by hydraulics. *Plant Physiology* 144:1890-1898.

Brodribb T.J., Feild T.S. and Sack L. 2010. Viewing leaf structure and evolution from a hydraulic perspective. *Functional Plant Biology* 37:488.

Brodribb T.J., Holbrook N.M., Zwieniecki M.A. and Palma B. 2005. Leaf hydraulic capacity in ferns, conifers and angiosperms: impacts on photosynthetic maxima. *New Phytologist* 165:839-846.

Brodribb T.J., Jordan G.J. and Carpenter R.J. 2013. Unified changes in cell size permit coordinated leaf evolution. *New Phytologist* 199:559-570.

Brodribb T.J., McAdam S.A., Jordan G.J. and Martins S.C. 2014. Conifer species adapt to low-rainfall climates by following one of two divergent pathways. *Proceedings of the National Academy of Sciences* 111:14489-14493.

Brodribb T.J. and Feild T.S. 2010. Leaf hydraulic evolution led a surge in leaf photosynthetic capacity during early angiosperm diversification. *Ecology Letters* 13:175-183.

Brodribb T.J. and Jordan G.J. 2011. Water supply and demand remain balanced during leaf acclimation of *Nothofagus cunninghamii* trees. *New Phytologist* 192:437-448.

Brodribb T.J. and McAdam S.A. 2011. Passive origins of stomatal control in vascular plants. *Science* 331:582-585.

Bucci S.J., Scholz F.G., Campanello P.I., Montti L., Jimenez-Castillo M., Rockwell F.A., Manna L.L., Guerra P., Bernal P.L., et al. 2012. Hydraulic differences along the water transport system of South American *Nothofagus* species: do leaves protect the stem functionality? *Tree Physiology* 32:880-893.

Buck A.L. 1981. New equations for computing vapor pressure and enhancement factor. *Journal of Applied Meterology* 20:1527-1532.

Burgess S.S., Adams M.A., Turner N.C., Beverly C.R., Ong C.K., Khan A.A. and Bleby T.M. 2001. An improved heat pulse method to measure low and reverse rates of sap flow in woody plants. *Tree Physiology* 21:589-598.

Chapotin S.M., Holbrook N.M., Morse S.R. and Gutiérrez M.V. 2003. Water relations of tropical dry forest flowers: pathways for water entry and the role of extracellular polysaccharides. *Plant, Cell & Environment* 26:623-630.

Chartier M., Jabbour F., Gerber S., Mitteroecker P., Sauquet H., von Balthazar M., Staedler Y., Crane P.R. and Schönenberger J. 2014. The floral morphospace - a modern comparative approach to study angiosperm evolution. *New Phytologist* 204:841-853.

Choat B., Gambetta G.A., Shackel K.A. and Matthews M.A. 2009. Vascular function in grape berries across development and its relevance to apparent hydraulic isolation. *Plant Physiology* 151:1677-1687.

Clausen J.C., Keck D.D. and Hiesey W.M. 1940. *Experimental studies on the nature of species*. Washington: Carnegie Institute of Washington.

Clearwater M.J., Luo Z., Mazzeo M. and Dichio B. 2009. An external heat pulse method for measurement of sap flow through fruit pedicels, leaf petioles and other small-diameter stems. *Plant, Cell & Environment* 32:1652-1663.

Clearwater M.J., Luo Z., Ong S.E., Blattmann P. and Thorp T.G. 2012. Vascular functioning and the water balance of ripening kiwifruit (*Actinidia chinensis*) berries. *Journal of Experimental Botany* 63:1835-1847.

Clearwater M.J., Ong S.E.C. and Li K.T. 2013. Sap flow and vascular functioning during fruit development. *Acta Horticulturae* 991:385-392.

Corner E.J.H. 1949. The durian theory or the origin of the modern tree. *Annals of Botany* 13:367-414.
Crepet W.L. and Niklas K.J. 2009. Darwin's second 'abominable mystery': Why are there so many angiosperm species? *American Journal of Botany* 96:366-381.
Darwin C. 1859. *On the origin of species by means of natural selection*. London: John Murray.
Darwin C. 1888. *The various contrivances by which orchids are fertilised by insects*. London: John Murray.
Davis C.C., Latvis M., Nickrent D.L., Wurdack K.J. and Baum D.A. 2007. Floral gigantism in Rafflesiaceae. *Science* 315:1812.
Dichio B., Remorini D. and Lang S. 2002. Developmental changes in xylem functionality in kiwifruit fruit: implications for fruit calcium accumulation. *Acta Horticulturae* 610:191-195.
DiVittorio C.T. 2014. Mechanisms of adaptive radiation in *Encelia*. Berkeley, California: University of California Berkeley.
Dodd M.E., Silvertown J. and Chase M.W. 1999. Phylogenetic analysis of trait evolution and species diversity variation among angiosperm families. *Evolution* 53:732-744.
Endress P.K. 2011. Evolutionary diversification of the flowers in angiosperms. *American Journal of Botany* 98:370-396.
Endress P.K. and Doyle J.A. 2009. Reconstructing the ancestral angiosperm flower and its initial specializations. *American Journal of Botany* 96:22-66.
Feild T.S., Brodribb T.J., Iglesias A., Chatelet D.S., Baresch A., Upchurch G.R., Gomez B., Mohr B.A., Coiffard C., et al. 2011. Fossil evidence for Cretaceous escalation in angiosperm leaf vein evolution. *Proceedings of the National Academy of Sciences* 108:8363-8366.
Feild T.S., Chatelet D.S. and Brodribb T.J. 2009. Ancestral xerophobia: a hypothesis on the whole plant ecophysiology of early angiosperms. *Geobiology* 7:237-264.
Feild T.S., Chatelet D.S. and Brodribb T.J. 2009. Giant flowers of Southern magnolia are hydrated by the xylem. *Plant Physiology* 150:1587-1597.
Feild T.S., Upchurch Jr G.R., Chatelet D.S., Brodribb T.J., Grubbs K.C., Samain M.-S. and Wanke S. 2011. Fossil evidence for low gas exchange capacities for Early Cretaceous angiosperm leaves. *Paleobiology* 37:195-213.
Feild T.S. and Arens N.C. 2007. The ecophysiology of early angiosperms. *Plant, Cell & Environment* 30:291-309.
Feild T.S. and Brodribb T.J. 2013. Hydraulic tuning of vein cell microstructure in the evolution of angiosperm venation networks. *New Phytologist* 199:720-726.
Felsenstein J. 1985. Phylogenies and the comparative method. *American Naturalist* 125:1-15.
Fenster C.B., Armbruster W.S., Wilson P., Dudash M.R. and Thomson J.D. 2004. Pollination syndromes and floral specialization. *Annual Review of Ecology, Evolution, and Systematics* 35:375-403.
Galen C. 1999. Why do flowers vary? *BioScience* 49:631-640.
Galen C. 2000. High and dry: drought stress, sex-allocation trade-offs, and selection on flower size in the alpine wildflower *Polemonium viscosum* (Polemoniaceae). *The American Naturalist* 156:72-83.
Galen C., Dawson T.E. and Stanton M.L. 1993. Carpels as leaves: meeting the carbon cost of reproduction in an alpine buttercup. *Oecologia* 95:187-193.
Galen C., Sherry R.A. and Carroll A.B. 1999. Are flowers physiological sinks or faucets? Costs and correlates of water use by flowers of *Polemonium viscosum*. *Oecologia* 118:461-470.
Gottsberger G. 1999. Pollination and evolution in neotropical Annonaceae. *Plant Species Biology* 14:143-152.
Grant V. 1950. The pollination of *Calycanthus occidentalis*. *American Journal of Botany* 37:294-297.

Greenspan M.D., Shackel K.A. and Matthews M.A. 1994. Developmental changes in the diurnal water budget of the grape berry exposed to water deficits. *Plant, Cell & Environment* 17:811-820.
Gullo M.A.L., Nardini A., Trifilò P. and Salleo S. 2005. Diurnal and seasonal variations in leaf hydraulic conductance in evergreen and deciduous trees. *Tree Physiology* 25:505-512.
Hansen T.F., Pélabon C. and Armbruster W.S. 2007. Comparing variational properties of homologous floral and vegetative characters in *Dalechampia scandens*: testing the Berg hypothesis. *Evolutionary Biology* 34:86-98.
Harris M.S. and Pannell J.R. 2010. Canopy seed storage is associated with sexual dimorphism in the woody dioecious genus *Leucadendron*. *Journal of Ecology* 98:509-515.
Herrera C.M. 1996. Floral traits and plant adaptation to insect pollinators: a devil's advocate approach. In *Floral Biology: Studies on Floral Evolution in Animal-Pollinated Plants*. ed. Lloyd D.G. and Barrett S.C.H., pp. 65-87. New York: Chapman & Hall.
Hew C.S., Lee G.L. and Wong S.C. 1980. Occurrence of non-functional stomata in the flowers of tropical orchids. *Annals of Botany* 46:195-201.
Higuchi H. and Sakuratani T. 2005. The sap flow in the peduncle of the mango (*Mangifera indica* L.) inflorescence as measured by the stem heat balance method. *Journal of the Japanese Society of Horticultural Science* 74:109-114.
Higuchi H. and Sakuratani T. 2006. Water dynamics in mango (*Mangifera indica* L.) fruit during the young and mature fruit seasons as measured by the stem heat balance method. *Journal of the Japanese Society for Horticultural Science* 75:11-19.
Ho L.C., Grange R.I. and Picken A.J. 1987. An analysis of the accumulation of water and dry matter in tomato fruit. *Plant, Cell & Environment* 10:157-162.
Hopkins R. and Rausher M.D. 2011. Identification of two genes causing reinforcement in the Texas wildflower *Phlox drummondii*. *Nature* 469:411-414.
Hopkins R. and Rausher M.D. 2012. Pollinator-mediated selection on flower color allele drives reinforcement. *Science* 335:1090-1092.
Hu S., Dilcher D.L., Jarzen D.M. and Taylor D.W. 2008. Early steps of angiosperm-pollinator coevolution. *Proceedings of the National Academy of Sciences* 105:240-245.
Irish V.F. 2009. Evolution of petal identity. *Journal of Experimental Botany* 60:2517-2527.
Irish V.F. and Litt A. 2005. Flower development and evolution: gene duplication, diversification and redeployment. *Current Opinion in Genetics & Development* 15:454-460.
Jepson Flora Project. 2014. Jepson Flora Project.<http://ucjeps.berkeley.edu/IJM.html>.
Johnson D.M., McCulloh K.A., Meinzer F.C., Woodruff D.R. and Eissenstat D.M. 2011. Hydraulic patterns and safety margins, from stem to stomata, in three eastern U.S. tree species. *Tree Physiology* 31:659-668.
Johnson R.W., Dixon M.A. and Lee D.R. 1992. Water relations of the tomato during fruit growth. *Plant, Cell & Environment* 15:947-953.
Judd W.S., Campbell C.S., Kellogg E.A., Stevens P.F. and Donoghue M.J. 2007. *Plant Systematics: A Phylogenetic Approach*. Sunderland, MA: Sinauer Associated.
Juenger T., Pérez-Pérez J.M., Bernal S. and Micol J.L. 2005. Quantitative trait loci mapping of floral and leaf morphology traits in *Arabidopsis thaliana*: evidence for modular genetic architecture. *Evolution & Development* 7:259-271.
Jürgens A. 2009. The hidden language of flowering plants: floral odours as a key for understanding angiosperm evolution? *New Phytologist* 183:240-243.
Kerstiens G. 1996. Cuticular water permeability and its physiological significance. *Journal of Experimental Botany* 47:1813-1832.
Kevan P.G. 1975. Sun-tracking solar furnaces in high arctic flowers: significance for pollination and insects. *Science* 189:723-726.

Kolb K.J., Sperry J.S. and Lamont B.B. 1996. A method for measuring xylem hydraulic conductance and embolism in entire root and shoot systems. *Journal of Experimental Botany* 47:1805-1810.
De la Barrera E. and Nobel P.S. 2004. Nectar: properties, floral aspects, and speculations on origin. *Trends in Plant Science* 9:65-69.
Lambrecht S.C. 2013. Floral water costs and size variation in the highly selfing *Leptosiphon bicolor* (Polemoniaceae). *International Journal of Plant Sciences* 174:74-84.
Lambrecht S.C., Santiago L.S., Devan C.M., Cervera J.C., Stripe C.M., Buckingham L.A. and Pasquini S.C. 2011. Plant water status and hydraulic conductance during flowering in the southern California coastal sage shrub *Salvia mellifera* (Lamiaceae). *American Journal of Botany* 98:1286-1292.
Lambrecht S.C. and Dawson T.E. 2007. Correlated variation of floral and leaf traits along a moisture availability gradient. *Oecologia* 151:574-583.
Lang A. 1990. Xylem, phloem and transpiration flows in developing apple fruits. *Journal of Experimental Botany* 41:645-651.
Marshall D.C. 1958. Measurement of sap flow in conifers by heat transport. *Plant Physiology* 33:385-396.
Mathews S. and Kramer E.M. 2012. The evolution of reproductive structures in seed plants: a re-examination based on insights from developmental genetics. *New Phytologist* 194:910-923.
McAdam S.A.M. and Brodribb T.J. 2012. Stomatal innovation and the rise of seed plants. *Ecology Letters* 15:1-8.
McCulloh K.A., Johnson D.M., Meinzer F.C. and Woodruff D.R. 2014. The dynamic pipeline: hydraulic capacitance and xylem hydraulic safety in four tall conifer species. *Plant, Cell & Environment* 37:1171-1183.
Meinzer F.C., James S.A., Goldstein G. and Woodruff D. 2003. Whole-tree water transport scales with sapwood capacitance in tropical forest canopy trees. *Plant, Cell & Environment* 26:1147-1155.
Meinzer F.C., Johnson D.M., Lachenbruch B., McCulloh K.A. and Woodruff D.R. 2009. Xylem hydraulic safety margins in woody plants: coordination of stomatal control of xylem tension with hydraulic capacitance. *Functional Ecology* 23:922-930.
Meinzer F.C., Woodruff D.R., Domec J.C., Goldstein G., Campanello P.I., Gatti M.G. and Villalobos-Vega R. 2008. Coordination of leaf and stem water transport properties in tropical forest trees. *Oecologia* 156:31-41.
Melville R. 1960. A new theory of the angiosperm flower. *Nature* 188:14-18.
Melville R. 1969. Leaf venation patterns and the origin of the angiosperms. *Nature* 224:121-125.
Midgley J. and Bond W. 1989. Leaf size and inflorescence size may be allometrically related traits. *Oecologia* 78:427-429.
Moles A.T., Perkins S.E., Laffan S.W., Flores-Moreno H., Awasthy M., Tindall M.L., Sack L., Pitman A., Kattge J., et al. 2014. Which is a better predictor of plant traits: temperature or precipitation? *Journal of Vegetation Science* 25:1167-1180.
Münch E. 1930. *Die Stoffbewegungen in der Pflanze*. Jena, Germany: Gustav Fischer.
Nardini A., Gortan E. and Salleo S. 2005. Hydraulic efficiency of the leaf venation system in sun- and shade-adapted species. *Functional Plant Biology* 32:953.
Nardini A. and Salleo S. 2000. Limitation of stomatal conductance by hydraulic traits: sensing or preventing xylem cavitation? *Trees* 15:14-24.
Nobel P.S. 1977. Water relations of flowering of *Agave deserti*. *Botanical Gazette* 138:1-6.
Nobel P.S. 1983. *Biophysical Plant Physiology and Ecology*. San Francisco: W.H. Freeman.
Patiño S., Jeffree C. and Grace J. 2002. The ecological role of orientation in tropical convolvulaceous flowers. *Oecologia* 130:373-379.

Patiño S. and Grace J. 2002. The cooling of convolvulaceous flowers in a tropical environment. *Plant, Cell & Environment* 25:41-51.
Pélabon C., Armbruster W.S. and Hansen T.F. 2011. Experimental evidence for the Berg hypothesis: vegetative traits are more sensitive than pollination traits to environmental variation. *Functional Ecology* 25:247-257.
Pittermann J. 2010. The evolution of water transport in plants: an integrated approach. *Geobiology* 8:112-139.
Pittermann J., Sperry J.S., Wheeler J.K., Hacke U.G. and Sikkema E.H. 2006. Mechanical reinforcement of tracheids compromises the hydraulic efficiency of conifer xylem. *Plant, Cell and Environment* 29:1618-1628.
PRISM Climate Group. 2014. <http://prism.oregonstate.edu>.
Rasband W.S. 2012. <http://imagej.nih.gov/ij/> Bethesda, MD, USA: National Institutes of Health.
R Core Team. 2012. <http://www.R-project.org/> Vienna, Austria: R Foundation for Statistical Computing.
Reekie E.G. and Bazzaz F.A. 1987. Reproductive effort in plants. 1. Carbon allocation to reproduction. *American Naturalist* 129:876-896.
Reekie E.G. and Bazzaz F.A. 1987. Reproductive effort in plants. 2. Does carbon reflect the allocation of other resources? *American Naturalist* 129:897-906.
Reekie E.G. and Bazzaz F.A. 1987. Reproductive effort in plants. 3. Effect of reproduction on vegetative activity. *American Naturalist* 129:907-919.
Reich P.B. 2014. The world-wide 'fast-slow' plant economics spectrum: a traits manifesto. *Journal of Ecology* 102:275-301.
Reich P.B., Walters M.B. and Ellsworth D.S. 1997. From tropics to tundra: global convergence in plant functioning. *Proceedings of the National Academy of Sciences* 94:13730-13734.
Roddy A.B., Guilliams C.M., Lilittham T., Farmer J., Wormser V., Pham T., Fine P.V.A., Feild T.S. and Dawson T.E. 2013. Uncorrelated evolution of leaf and petal venation patterns across the angiosperm phylogeny. *Journal of Experimental Botany* 64:4081-4088.
Roddy A.B. and Dawson T.E. 2012. Determining the water dynamics of flowering using miniature sap flow sensors. *Acta Horticulturae* 951:47-53.
Sack L., Cowan P.D., Jaikumar N. and Holbrook N.M. 2003. The hydrology of leaves: co-ordination of structure and function in temperate woody species. *Plant, Cell & Environment* 26:1343-1356.
Sack L., Melcher P.J., Zwieniecki M.A. and Holbrook N.M. 2002. The hydraulic conductance of the angiosperm leaf lamina: a comparison of three measurement methods. *Journal of Experimental Botany* 53:2177-2184.
Sack L., Scoffoni C., John G.P., Poorter H., Mason C.M., Mendez-Alonzo R. and Donovan L.A. 2013. How do leaf veins influence the worldwide leaf economic spectrum? Review and synthesis. *Journal of Experimental Botany* 64:4053-4080.
Sack L., Scoffoni C., John G.P., Poorter H., Mason C.M., Mendez-Alonzo R. and Donovan L.A. 2014. Leaf mass per area is independent of vein length per area: avoiding pitfalls when modelling phenotypic integration (reply to Blonder et al. 2014). *Journal of Experimental Botany* 65:5115-5123.
Sack L. and Frole K. 2006. Leaf structural diversity is related to hydraulic capacity in tropical rain forest trees. *Ecology* 87:483-491.
Sargent R.D. 2004. Floral symmetry affects speciation rates in angiosperms. *Proceedings of the Royal Society B* 271:603-608.

Sauret-Güeto K.S., Schiessl K., Bangham A., Sablowski R. and Coen E. 2013. JAGGED controls *Arabidopsis* petal growth and shape by interacting with a divergent polarity field. *PLoS Biology* 11:e1001550.

Scheper J., Reemer M., Kats R.V., Ozinga W.A., Linden G.T.J.V.D., Schaminée J.H.J., Siepel H. and Kleijn D. 2014. Museum specimens reveal loss of pollen host plants as key factor driving wild bee decline in The Netherlands. *Proceedings of the National Academy of Sciences* 111:17552-17557.

Scoffoni C., Pou A., Aasamaa K. and Sack L. 2008. The rapid light response of leaf hydraulic conductance: new evidence from two experimental methods. *Plant, Cell & Environment* 31:1803-1812.

Simonin K.A., Burns E., Choat B., Barbour M.M., Dawson T.E. and Franks P.J. *In press.* Increasing leaf hydraulic conductance with transpiration rate minimizes the water potential drawdown from stem to leaf. *Journal of Experimental Botany*.

Simonin K.A., Limm E.B. and Dawson T.E. 2012. Hydraulic conductance of leaves correlates with leaf lifespan: implications for lifetime carbon gain. *New Phytologist* 193:939-947.

Simpson M.G. 2010. *Plant Systematics*. Burlington, MA: Academic Press.

Soltis D.E., Chanderbali A.S., Kim S., Buzgo M. and Soltis P.S. 2007. The ABC model and its applicability to basal angiosperms. *Annals of Botany* 100:155-163.

Specht C.D. and Bartlett M.E. 2009. Flower evolution: the origin and subsequent diversification of the angiosperm flower. *Annual Review of Ecology, Evolution, and Systematics* 40:217-243.

Sprengel C.K. 1793. *Das entdeckte Geheimnis der Natur im Bau und in der Befruchtung der Blumen*. Berlin: Friedrich Vieweg dem Aeltern.

Sprengel C.K. 1996. Discovery of the secret of nature in the structure and fertilization of flowers. In *Floral Biology: Studies on Floral Evolution in Animal-pollinated Plants*. ed. Lloyd D.G. and Barrett S.C.H., pp. 3-43. New York: Chapman & Hall.

Stebbins G.L. 1951. Natural selection and the differentiation of angiosperm families. *Evolution* 299-324.

Stebbins G.L. 1970. Adaptive radiation of reproductive characteristics in angiosperms, I: pollination mechanisms. *Annual Review of Ecology and Systematics* 307-326.

Strauss S.Y. and Whittall J.B. 2006. Non-pollinator agents of selection on floral traits. In *Ecology and Evolution of Flowers.*, pp. 120-138. Oxford: Oxford University Press.

Teixido A.L. and Valladares F. 2014. Disproportionate carbon and water maintenance costs of large corollas in hot Mediterranean ecosystems. *Perspectives in Plant Ecology, Evolution and Systematics* 16:83-92.

Thien L.B., Azuma H. and Kawano S. 2000. New perspectives on the pollination biology of basal angiosperms. *International Journal of Plant Sciences* 161:S225-S235.

Thien L.B., Bernhardt P., Devall M.S., Chen Z.D., Luo Y.B., Fan J.H., Yuan L.C. and Williams J.H. 2009. Pollination biology of basal angiosperms (ANITA grade). *American Journal of Botany* 96:166-182.

Trolinder N.L., McMichael B.L. and Upchurch D.R. 1993. Water relations of cotton flower petals and fruit. *Plant, Cell & Environment* 16:755-760.

Tyree M.T. and Hammel H.T. 1972. The measurement of the turgor pressure and the water relations of plants by the pressure-bomb technique. *Journal of Experimental Botany* 23:267-282.

van Schaik C.P., Terborgh J.W. and Wright S.J. 1993. The phenology of tropical forests: adaptive significance and consequences for primary consumers. *Annual Review of Ecology and Systematics* 353-377.

von Arx M., Goyret J., Davidowitz G. and Raguso R.A. 2012. Floral humidity as a reliable sensory cue for profitability assessment by nectar-foraging hawkmoths. *Proceedings of the National Academy of Sciences* 109:9471-9476.

Warton D.I., Duursma R.A., Falster D.S. and Taskinen S. 2012. smatr 3 - an R package for estimation and inference about allometric lines. *Methods in Ecology and Evolution* 3:257-259.
Webb C.O., Ackerly D.D. and Kembel S.W. 2008. Phylocom: software for the analysis of phylogenetic community structure and trait evolution. *Bioinformatics* 24:2098-2100.
Webb C.O. and Donoghue M.J. 2005. Phylomatic: tree assembly for applied phylogenetics. *Molecular Ecology Notes* 5:181-183.
Westoby M. and Wright I.J. 2006. Land-plant ecology on the basis of functional traits. *Trends in Ecology and Evolution* 21:261-268.
Whitney H.M., Bennett K.M., Dorling M., Sandbach L., Prince D., Chittka L. and Glover B.J. 2011. Why do so many petals have conical epidermal cells? *Annals of Botany* 108:609-616.
Whittall J.B. and Hodges S.A. 2007. Pollinator shifts drive increasingly long nectar spurs in columbine flowers. *Nature* 447:706-709.
Windt C.W., Gerkema E. and Van As H. 2009. Most water in the tomato truss is imported through the xylem, not the phloem: a nuclear magnetic resonance flow imaging study. *Plant Physiology* 151:830-842.
Wright I.J., Reich P.B., Westoby M., Ackerly D.D., Baruch Z., Bongers F., Cavender-Bares J., Chapin T., Cornelissen J.H., et al. 2004. The worldwide leaf economics spectrum. *Nature* 428:821-827.
Zanis M.J., Soltis P.S., Qiu Y.L., Zimmer E. and Soltis D.E. 2003. Phylogenetic analyses and perianth evolution in basal angiosperms. *Annals of the Missouri Botanical Garden* 90:129-150.
Zhang W., Kramer E.M. and Davis C.C. 2012. Similar genetic mechanisms underlie the parallel evolution of floral phenotypes. *PLoS One* 7:e36033.
Zhou S., Renner S.S. and Wen J. 2006. Molecular phylogeny and intra- and intercontinental biogeography of Calycanthaceae. *Moecular Phylogenetics and Evolution* 39:1-15.